

APPENDIX F

TIER 2 VAPOR MODELING RESULTS

<u>Section</u>	<u>Page</u>
F.1 INTRODUCTION	F-1
F.1.1 Approach.....	F-1
F.2 SITE-SPECIFIC MODEL DEVELOPMENT	F-2
F.2.1 Model Selection	F-2
F.2.2 Model Assumptions	F-4
F.2.3 Model Calibration	F-4
F.2.3.1 The Waste Pit Area	F-5
F.2.3.2 The MW-20 NAPL Area	F-6
F.2.3.3 The Benzene Pipeline Area in the Southeastern Former Butadiene Plant Area.....	F-6
F.2.3.4 Model Calibration Summary.....	F-7
F.2.4 Comparison of Vapor Migration of Biodegradable and Recalcitrant Contaminants	F-7
F.2.4.1 Locations of Potential Soil Gas Profile Data	F-7
F.2.4.2 Selection of Clusters for Evaluation	F-8
F.2.4.3 Modeling and Data Evaluation	F-8
F.3 TIER 2 EVALUATION TO SUPPORT RISK ASSESSMENT	F-9
F.3.1 Attenuation Factors	F-9
F.3.2 Exposure Point Concentrations.....	F-9
F.4 REFERENCES	F-10

Table F-1	Input Parameters for Modeled Locations in the Waste Pit Area
Table F-2	Input Parameters for Modeled Locations in the MW-20 NAPL Area
Table F-3	Input Parameters for Modeled Locations in the Benzene Pipeline Area
Table F-4	Summary of Dominant Layer Model Biodegradation Parameters
Table F-5	Benzene, PCE, and TCE Soil Gas Data Summary for Vapor Transport Modeling
Table F-6	Tier 2 Model Input Parameters
Table F-7	Tier 2 Modeling Attenuation Factors
Table F-8	Tier 2 Indoor Air EPCs, Shallow Soil/Soil Gas
Table F-9	Tier 2 Indoor Air EPCs, Deep Soil/Soil Gas
Table F-10	Soil Vapor Data Adequacy Evaluation
Table F-11	Tier 2 Indoor Air EPCs, Groundwater-to-Indoor Air Pathway

- Figure F-1 EAPCs and Tier 2 Vapor Modeling Areas
- Figure F-2 Literature Values of BTEX Vadose Zone Biodegradation Rate Constants
- Figure F-3 Model Conceptualization
- Figure F-4 Waste Pits Area CPT-7 DLM and JEM Results
- Figure F-5 Waste Pit Area CPT-8 DLM and JEM Results
- Figure F-6 Waste Pit Area CPT-15 DLM and JEM Results
- Figure F-7 Waste Pit Area CPT-16 DLM and JEM Results
- Figure F-8 MW-20 NAPL Area, SGL0028 DLM and JEM Results
- Figure F-9 MW-20 NAPL Area, SGL0033 DLM and JEM Results
- Figure F-10 MW-20 NAPL Area, SGL0035 DLM and JEM Results
- Figure F-11 MW-20 Area NAPL, SGL0044 DLM and JEM Results
- Figure F-12 Benzene Pipeline Area, SG-01 DLM and JEM Results
- Figure F-13 Benzene Pipeline Area, SG-02 DLM and JEM Results
- Figure F-14 Benzene Pipeline Area, SG-04 DLM and JEM Results
- Figure F-15 Benzene Pipeline Area, SG-022 DLM and JEM Results
- Figure F-16 BTEX Degradation Rate Constants from Site Data Evaluation
- Figure F-17 TCE and PCE Soil Gas Sampling Locations
- Figure F-18 Sampling Point Clusters
- Figure F-19 Waste Pits Area CPT-7 Benzene and PCE Comparison
- Figure F-20 Waste Pit Area CPT-15 Benzene and PCE Comparison
- Figure F-21 MW-20 NAPL Area, SGL0044 Benzene and PCE Comparison

LIST OF ATTACHMENTS

- Attachment F-1 Example DLM Spreadsheet Calculations
- Attachment F-2 Comments and Response to Comments on Dominant Layer Model

F.1 INTRODUCTION

A Tier 2 evaluation of potential migration of vapor-phase benzene, toluene, ethylbenzene, and xylene (BTEX) transport through the vadose zone was conducted for the Del Amo Site. A site map showing the parcels evaluated in the Baseline Risk Assessment is provided in **Figure F-1**. The purpose of the evaluation was to estimate indoor air concentrations using a site-specific vapor transport model that considers the impact of aerobic biodegradation of BTEX on the vapor intrusion pathway. These predicted indoor air concentrations were used as input into the risk calculations, as described in Section 4 of the Baseline Risk Assessment.

This appendix describes the approach used for Tier 2 modeling at the site, site-specific model development, and Tier 2 evaluation results to support the Baseline Risk Assessment.

F.1.1 Approach

The Tier 2 evaluation was performed using the Dominant Layer Model (DLM) developed by Johnson et al. (1999). The development of the methodology using the DLM for analyzing the vapor transport from a groundwater source or shallow soil source was documented in the Draft Vapor Transport Modeling Report (Dames & Moore, 1999).

It has been recognized that biodegradation plays an important role in the reduction of contaminant concentrations of petroleum compounds in the vadose zone (Ostendorf and Kampbell, 1991; Fisher et al., 1996; Fitzpatrick and Fitzgerald, 1997; Lahvis, et al., 1999; Hers et al., 2000; DeVauil et al., 2002; Hohener, et al., 2003; DTSC, 2004). Some of these studies compared measured and modeled indoor air concentrations while others examined biological activity indicators (O_2 and CO_2) compared to volatile organic compound (VOC) concentrations. Additionally, conditional criteria for aerobic biodegradation of aromatic hydrocarbons have been identified and a literature review of BTEX biodegradation rate constants has been presented (DeVauil, et al., 1997). A summary of the BTEX biodegradation rate constants reported by DeVauil, et al. (1997) is shown in **Figure F-2**. Johnson et al. (1999) presented an analytical model that includes vadose zone biodegradation in estimating the migration of VOCs to indoor air. These findings can be used to simulate the migration of VOCs from subsurface sources to indoor air while incorporating biodegradation mechanisms.

Site soil gas data have been reviewed to assess the significance of vadose zone biodegradation at the site. Benzene soil vapor concentration profile data are compared to model predictions with and without biodegradation to evaluate which modeling scenarios provide a better match to site conditions. Additionally, comparisons of benzene soil gas concentration data to the concentration data for a non-degradable compound (PCE) are used to support the impact of vadose zone biodegradation on contaminant vapor migration. This review of site data is also used to select the most appropriate input parameters for the implementation of the DLM. Both the location of the biodegradation zone and the biodegradation rate constant are determined by model calibration to benzene soil gas concentration data.

The calibrated DLM is utilized to evaluate the vapor intrusion pathway for shallow soil/soil gas, deep soil/soil gas, and groundwater to indoor air exposure pathways for BTEX constituents. The calibrated DLM is implemented to calculate soil gas to indoor air attenuation factors which are used to predict indoor air concentrations for the calculation of exposure point concentrations for the risk assessment.

F.2 SITE-SPECIFIC MODEL DEVELOPMENT

F.2.1 Model Selection

Contaminant vapor migration of BTEX was evaluated in this study using the DLM (Johnson et al., 1999). This refined vapor intrusion model was developed in a similar manner to the Johnson and Ettinger (1991) model (JEM), but incorporated vadose zone biodegradation.

The JEM is a one-dimensional (1-D) analytical solution that describes the relationship between indoor air concentrations and subsurface vapor concentrations. The model considers 1-D VOC diffusion in soil vapor and soil moisture through the vadose zone, vapor convection due to indoor-outdoor pressure difference, and mixing of the contaminants migrating from the subsurface within the ventilated building. The model requires input of chemical properties of the contaminant, soil properties of the unsaturated soils and structural properties of the building. The JEM calculates a vapor intrusion attenuation factor, α :

$$\alpha = \frac{C_{indoor}}{C_{vs}} = \frac{\left[\frac{D_T^{eff} A_B}{Q_B L_T} \right] \exp\left(\frac{Q_{soil} L_{crack}}{D_{crack}^{eff} \eta A_B} \right)}{\exp\left(\frac{Q_{soil} L_{crack}}{D_{crack}^{eff} \eta A_B} \right) + \left[\frac{D_T^{eff} A_B}{Q_B L_T} \right] + \left[\frac{D_T^{eff} A_B}{Q_{soil} L_T} \right] \left(\exp\left(\frac{Q_{soil} L_{crack}}{D_{crack}^{eff} \eta A_B} \right) - 1 \right)}$$

where:

- D_T^{eff} = “overall” effective diffusion coefficient [cm^2/s]
- D_{crack}^{eff} = effective diffusion coefficient through cracks in foundation [cm^2/s]
- C_{vs} = vapor concentration at the source [g/cm^3]
- C_{indoor} = indoor air concentration [g/cm^3]
- L_T = distance from source to basement [cm]
- A_B = cross-sectional area of foundation available for vapor flux [cm^2]
- Q_{soil} = volumetric flow rate of soil gas into the building [cm^3/s]
- L_{crack} = thickness of the foundation [cm]
- A_{crack} = area of cracks or openings through which vapors enter building [cm^2]
- Q_B = building ventilation rate [m^3/s]
- η = the “crack factor” = A_{crack}/A_B

The DLM is also a 1-D analytical solution describing the vapor intrusion pathway. In addition to the transport mechanisms considered in the JEM (diffusion, convection, and mixing due to building ventilation), vadose zone biodegradation is also considered. As

illustrated in **Figure F-3**, in the DLM the vadose zone is conceptualized as a three-region, 1-D soil column in which biodegradation is assumed to occur within a specified layer between the source of contamination and building foundation or ground surface. The layer where biodegradation is assumed to occur is referenced as the biodegradation zone or dominant layer. The DLM was refined for this site-specific evaluation to permit multiple soil layers (e.g., multiple soil properties) below the biodegradation zone and to consider vapor migration to outdoor air. Using the DLM, the attenuation factor is calculated by:

$$\alpha = \frac{C_{indoor}}{C_{vs}} = \frac{1 - \beta}{(1 - \beta) \left(\frac{Q_B}{2\phi\gamma\psi} \right) + \left(\beta \left(\frac{Q_B}{Q_{soil}} \right) - 1 \right) \left(\frac{1 + \gamma\psi - \phi\psi^2}{2\gamma\psi^2} \right)}$$

where:

$$\beta = 1 - \text{Exp} \left(\frac{Q_{soil} L_{crack}}{D_{crack}^{eff} \eta A_B} \right)$$

$$\gamma = \left(\frac{D_1^{eff}}{D_2^{eff}} \right) \frac{(e^{-\delta} - e^{\delta})(L_2 - L_1)}{\delta L_1}$$

$$\sigma = \left(\frac{D_3^{eff}}{D_2^{eff}} \right) \frac{(e^{-\delta} - e^{\delta})(L_2 - L_1)}{\delta (L_3 - L_2)}$$

$$\psi = \frac{1}{e^{-\delta} + e^{\delta} - \gamma}$$

$$\phi = \left(\frac{A_B D_3^{eff}}{L_3 - L_2} \right) \frac{1}{\sigma - (1/\psi) - \gamma + 4\psi}$$

$$\delta = \sqrt{\frac{\lambda \theta_w (L_2 - L_1)^2}{H D_2^{eff}}}$$

and where

- λ = first order biodegradation rate constant [1/s];
- θ_w = soil moisture content of dominant layer [dimensionless];
- H = dimensionless Henry's Law coefficient;
- D_i^{eff} = effective diffusion coefficient for layer i [cm²/s]; and
- L_i = distance above the source for layer i [cm]

F.2.2 Model Assumptions

Key assumptions used in this evaluation include the following:

- Significant biodegradation of aromatic hydrocarbons takes place in the vadose zone. The biodegradation of BTEX can be modeled assuming first order kinetics. The biodegradation zone is assumed to occur in shallow soils, near the ground surface where adequate oxygen for aerobic biodegradation is expected. The estimated biodegradation rate and depth of the biodegradation interval will be determined by comparing modeled results with measured benzene concentrations.
- The analysis assumes steady-state transport conditions. The source terms are assumed to remain constant over time. Model-predicted concentration at any given depth is also assumed to be constant over time. No source depletion is considered. These assumptions will yield conservative predicted indoor air concentrations resulting from subsurface releases.
- It was assumed that vapors originate from either a contaminated groundwater source or a shallower source in the vadose zone. No contaminant sources above the assumed model source depth are considered.
- The influences of individual source areas have not overlapped laterally so that the sources can be considered separately by the vapor transport model (i.e., 1-D transport).
- The calibration of the DLM was performed for benzene only; fate and transport of ethylbenzene, toluene, and xylene in the Tier 2 analysis was evaluated assuming the same degradation rate constant determined for benzene based on expected similarity in their degradation mechanisms. This approach was necessary because sufficient soil gas concentration profile data are not available for ethylbenzene, toluene, and xylene to assess chemical-specific biodegradation rate constants.

F.2.3 Model Calibration

The DLM was evaluated for the following three selected areas with the Del Amo Site: (1) the Waste Pit Area, (2) the MW-20 NAPL area on the former styrene plant, and (3) the benzene pipeline area near the corner of the former butadiene plant (see **Figure F-1**). At selected boring locations within these areas, the first order degradation rate constant and biodegradation interval were adjusted to match measured and modeled results.

No building structures existed in the sample locations selected for model calibration. Therefore, model parameters related to building and ventilation characteristics were adjusted to reflect the open ground-surface conditions in this area for the calibration analysis. Under these conditions, subsurface vapor transport is controlled by diffusion.

- The vapor transport is evaluated over a 15m x 15m source area (note that the model results are not sensitive to this parameter);

- The air ventilation rate is set to $1.3 \times 10^4 \text{ day}^{-1}$ (equivalent to a wind speed of 2.25 m/s over the 15m x 15m area);
- The indoor-outdoor pressure difference and Q_{soil} are assumed to be very small to simulate the open-space conditions in the sampling areas; and
- The “foundation” crack ratio was set to 1 in the Waste Pit Area (where the soil gas samples were taken from the open field) and the “foundation” crack ratio was set to 0.01 in the other two areas (where the samples were taken from soil borings drilled through asphalt in areas surrounding building with planter boxes and green strips).

Data used for model calibration include the measured soil gas concentrations from field gas chromatography (GC) analysis (with detection limit of 1 ppmv) and Summa canister confirmation samples analyzed by EPA Method TO-14 (with detection limit of less than 0.0005 ppmv). All available measurements performed at or near the same depth within a 50-ft radius from the boring locations were selected as calibration targets.

To assist in the evaluation, the DLM and JEM results are compared to soil gas profile data collected at 12 locations across the site. The JEM analysis does not consider biodegradation and can be used to assess the significance of biodegradation.

F.2.3.1 The Waste Pit Area

The Waste Pit Area, located on the southern boundary of the site, includes six small rectangular pits designated as the 2-series pits and four large rectangular impoundments or evaporation known as the 1-series pits (**Figure F-1**)

Vapor migration modeling results are presented for four boring locations evaluated for the Waste Pit Area: CPT-7 and CPT-8 located near the 1-series pits and CPT-15 and CPT-16 located near the 2-series pits. The details of sampling data including depth, soil vapor concentrations, and distance to the modeled point are provided in Dames & Moore, 1999). The modeling input parameters for the Waste Pit Area are summarized in **Table F-1**. The model calculations and comparison with measured concentrations are shown in **Figures F-4 through F-7**.

These figures indicate a reasonable match of measured and modeled concentration data can be obtained assuming a biodegradation zone from 1 – 10 ft bgs and a first order biodegradation constant of $0.25 - 0.5 \text{ day}^{-1}$. Review of the vapor transport analysis conducted for the Waste Pit Area clearly demonstrates that the JEM, which does not consider biodegradation, does not match the observed soil gas concentration profiles. Rather, the DLM, which incorporates biodegradation, results in an improved match with the observed soil gas concentrations. This indicates that biodegradation is occurring in the Waste Pit Area and that this mechanism can be simulated using the DLM.

F.2.3.2 The MW-20 NAPL Area

The MW-20 NAPL area for which Tier 2 modeling was completed is located at parcel 7351-34-57, along the western portion of the former styrene plant (**Figure F-1**). Benzene light non-aqueous phase liquid (LNAPL) was detected in monitoring well MW-20 and nearby monitoring wells within this area.

Vapor fate and transport modeling are presented for four boring locations in this area: SGL0028, SGL0033, SGL0035, and SGL0044. The source of subsurface vapor impacts at the locations modeled was assumed to be from contaminated groundwater. The benzene source vapor concentrations, based on measured vapor concentrations in samples collected immediately above the capillary fringe, varied from 10,100 ppmv at SGL0033 to 25,900 ppmv at SGL0044.

In this area, soil gas concentration data for model calibration were available immediately above the capillary fringe (~50 – 60 ft bgs) and shallower than 10 ft bgs. No soil gas data at intermediate depths were collected. The details of the sampling data are provided in Dames & Moore, 1999. The modeling input parameters for the MW-20 NAPL Area are summarized in **Table F-2**. The model calculations and comparison with measured concentrations are shown in **Figures F-8 through F-11**.

These figures indicate a reasonable match of measured and modeled concentration data can be obtained assuming a biodegradation zone from 1 – 6 ft bgs and a first order biodegradation constant of 0.048 – 0.1 day⁻¹. Review of the vapor transport analysis conducted for the MW-20 NAPL Area also demonstrates that the JEM does not match the observed soil gas concentration profiles, while the DLM results in an improved match with the observed soil gas concentrations. This indicates that biodegradation is occurring in the MW-20 NAPL Area and that this mechanism can be simulated using the DLM.

F.2.3.3 The Benzene Pipeline Area in the Southeastern Former Butadiene Plant Area

This area refers to the area comprising parcels 7351-33-22, -27, and -26, and the surrounding area located in the southern portion of the former butadiene plant (**Figure F-1**). This area is also in proximity to a former underground hydrocarbon product pipeline which served the plant site. Groundwater sampling indicates that LNAPL is likely present in the area (Dames & Moore, 1998a). In addition, results of field investigations indicate hydrocarbon contamination and detection of benzene vapor in shallow soils within this area (Dames & Moore, 1998b).

Vapor fate and transport modeling are presented for four boring locations in this area: SG-01, SG-02, SG-04, and SG-022. Soil vapor concentrations were measured at two depths for each of these locations; 5 ft and 13 ft bgs. The modeling input parameters for this area are summarized in **Table F-3**. The model calculations and comparison with measured concentrations are shown in **Figures F-12 through F-15**.

These figures indicate a reasonable match of measured and modeled concentration data can be obtained assuming a biodegradation zone from 1 – 10 ft bgs and a first order biodegradation constant of 0.2 – 0.6 day⁻¹. Review of the vapor transport analysis conducted for the Benzene Pipeline Area also demonstrates that the JEM does not match the observed soil gas concentration profiles, while the DLM results in an improved match with the observed soil gas concentrations. This indicates that biodegradation is occurring in the Benzene Pipeline Area and that this mechanism can be simulated using the DLM.

F.2.3.4 Model Calibration Summary

The DLM provides a technically defensible approach to modeling the vapor migration pathway for BTEX at the Del Amo site. The methodology used in this model calibration follows the approach previously documented to evaluate vadose zone biodegradation for the Del Amo Site (Dames & Moore, 1999). The only update from the earlier modeling approach is that the current model application assumes the biodegradation zone is present in the uppermost portion of the vadose zone. **Table F-4** summarizes the range of biodegradation parameters (first order biodegradation rate constant and interval of the biodegradation zone) used in the calibration of the model. Also, a comparison of estimated biodegradation rate constants to other literature reported values is illustrated in **Figure F-16**. The estimated degradation rate constants determined in this evaluation are lower (i.e., more conservative) than the range of values reported by others. This may be a result of the cautious approach was used to estimate degradation rate constants in this evaluation and/or limitations to oxygen transport to the subsurface leading to anaerobic conditions and a lower degradation rate.

F.2.4 Comparison of Vapor Migration of Biodegradable and Recalcitrant Contaminants

To further support the use of the DLM for the BTEX vapor migration modeling to be included in the risk assessment, a comparison between the measured and modeled concentration profiles for biodegradable and recalcitrant constituents was conducted. The objective of this comparison is to evaluate the applicability of the two tiers of modeling for the Del Amo site.

Since the JEM does not consider the biodegradation of constituents in the vadose zone, the JEM predictions should simulate the measured concentrations for recalcitrant compounds such as the chlorinated VOCs. However, if biodegradation is occurring, measured concentrations of degradable compounds such as BTEX are expected to be lower than the JEM predictions. Conversely, the DLM, which includes vadose zone degradation, will simulate the measured BTEX concentrations and under-predict the concentrations for the chlorinated VOCs.

F.2.4.1 Locations of Potential Soil Gas Profile Data

The evaluation of the vapor migration models requires biodegradable and recalcitrant soil gas results at (or near) one location from multiple depths. These data will be used to determine measured soil gas profiles that will be compared with modeled estimates. Benzene was

analyzed in all of the samples reviewed and will be used to characterize the biodegradable compounds. For the recalcitrant compounds, the trichloroethene (TCE) and tetrachloroethene (PCE) results were reviewed. Note that these constituents were analyzed less frequently than benzene at this site.

To determine potential locations with sufficient soil gas concentration data for the evaluation of the vapor migration models, all site data were reviewed to identify both the locations where soil gas samples were collected at multiple depths and where analyses for TCE and/or PCE were conducted. **Figure F-17** summarizes the locations and depths for soil gas samples collected at the Del Amo site for TCE and/or PCE analysis. This figure illustrates that samples collected in the Waste Pit Area and MW-20 NAPL Area on the former styrene plant are potential locations for the vapor migration modeling analysis. Eight clusters of sample points (nearby sample points at multiple depths) for potential evaluation were identified and are shown on **Figure F-18**.

F.2.4.2 Selection of Clusters for Evaluation

The analytical results for benzene, TCE and PCE for the clusters identified for potential evaluation are summarized in **Table F-5**. Note that limited data is available for TCE at the site. TCE was detected at 2 or more depths only in Clusters SGL0033 and SGL0034. Also, TCE was not analyzed in any of the samples collected in the Waste Pit Area (Clusters CPT-7, CPT-15, and CPT-16). Consequently, this vapor migration evaluation focuses on benzene and PCE.

The data in **Table F-5** indicates that there is limited PCE data available for the vapor migration evaluation. PCE was not detected in any of the samples in Clusters SGL0034 or CPT-16 and was only detected in one sample in Cluster SGL0035. Additionally, PCE was not detected in the groundwater monitoring point closest to SGL0028 and SGL0033. Consequently, these clusters are not considered for the vapor migration evaluation. The soil gas data from the three remaining clusters (SGL0044, CPT-7, and CPT-15) are compared with the JEM and DLM models.

F.2.4.3 Modeling and Data Evaluation

Vapor concentrations profiles for the locations identified in the previous section were calculated for no vadose zone biodegradation (JEM) and vadose zone biodegradation (DLM) scenarios. At each cluster, the only difference between the JEM and DLM input parameters is the characterization of the biodegradation zone of the DLM. All other input parameters (i.e., vadose zone soil characterization parameters) are identical in both models. The source concentration for the vapor migration modeling was estimated from measured groundwater concentrations. At each of the clusters, the source concentrations for benzene and PCE differ by orders of magnitude. Consequently, the reported soil gas concentrations have been normalized by the source concentration.

Figures F-19 through F-21 show the results for the JEM and DLM models as well as the normalized concentrations for the measured benzene and PCE in soil gas for the selected

clusters. In these figures, the calibrated model results and benzene concentrations are the same as those reported earlier in Section 2.3. The source concentrations and inputs to characterize the biodegradation zone for the DLM are also shown on these figures. Although there is limited data available to compare measured and modeled soil gas concentration profiles, these figures do illustrate that the benzene concentrations are more accurately represented by the DLM and the PCE concentrations are better represented by the JEM. The concentration profiles for the biodegradable compound examined (benzene) are clearly different from the profiles for the recalcitrant compound (PCE). This supports the proposed two-tiered modeling approach for calculating risks attributable to BTEX due to the vapor intrusion pathway at the Del Amo site.

F.3 TIER 2 EVALUATION TO SUPPORT RISK ASSESSMENT

F.3.1 Attenuation Factors

Using the calibrated model as discussed in the previous section, a Tier 2 evaluation was conducted. Tier 2 vapor intrusion attenuation factors for BTEX were calculated for shallow soil/soil gas sources, deep soil/soil gas sources, and groundwater sources. Printouts of example spreadsheet calculations are provided in Attachment F-1. Both commercial and residential scenarios were considered. These attenuation factors are then multiplied by the soil gas concentration to calculate the indoor air concentration for each source considered. Conservative biodegradation parameters were used in the Tier 2 Evaluation. The minimum first order degradation rate constant determined from the calibration evaluation, 0.048 day^{-1} , and the smaller biodegradation zone (from 1 to 6 ft bgs) was used in the Tier 2 calculations for all parcels considered. No attempt was made to use different degradation parameters for different parcels. Key input parameters for the Tier 2 analysis are summarized in **Table F-6**.

Table F-7 lists the calculated Tier 2 attenuation factors for BTEX to be used in the risk assessment. For comparison, the Tier 1 attenuation factors are also shown.

F.3.2 Exposure Point Concentrations

For the soil/soil gas concentrations, a Tier 2 vapor analysis was conducted for parcels with a calculated Tier 1 cumulative risk greater than 1×10^{-6} . For each of these parcels, the indoor air EPC for the Tier 2 evaluation was calculated by multiplying the representative soil gas concentration by the Tier 2 attenuation factor. **Tables F-8 and F-9** summarize the Tier 2 indoor air EPCs. Risks are then calculated from these indoor air EPCs as described in Section 6 of the risk assessment.

For the groundwater sources, a Tier 2 evaluation was conducted only for parcels with limited shallow soil gas measurements. If sufficient shallow soil gas measurements are available for a parcel, there is less uncertainty in the risk estimates for the vapor intrusion pathway from the soil gas concentrations than from the deeper groundwater concentrations. The available soil gas data for each Parcel was reviewed to determine whether sufficient soil gas data was available to justify using predicted indoor air concentrations from soil vapor data over those from groundwater concentrations. The number of soil vapor samples, the distribution of the soil vapor sample locations, and the historical use of the parcel were considered in the

evaluation. **Table F-10** summarizes the number of soil vapor samples and the determination of the soil vapor data adequacy for each parcel. Following this evaluation, 13 parcels were selected to evaluate the groundwater to indoor air pathway.

The Tier 2 attenuation factors were utilized to calculate predicted indoor air concentrations due to vapor intrusion from groundwater for the parcels identified above. Calculations were made for both the commercial and residential scenarios. The calculated indoor air concentration is the product of the estimated groundwater concentration, the Henry's Law Coefficient, and the Tier 2 attenuation factor. The predicted Tier 2 indoor air EPCs are shown in **Table F-11**. Risks are then calculated from these indoor air EPCs as described in Section 6 of the risk assessment.

F.4 REFERENCES

- California Department of Toxic Substances Control (DTSC), 2004. Interim Final Guidance for the Evaluation and Mitigation of Subsurface Vapor Intrusion to Indoor Air, December 15, 2004.
- Dames & Moore. 1999. Vapor Transport Modeling Report. Del Study Area, Los Angeles, California. November 4, 1999.
- Dames & Moore. 1998a. Final Groundwater Remedial Investigation Report. Del Amo Study Area. May, 1998.
- Dames & Moore. 1998b. Summary of NAPL Screening Investigations, Source Areas 6, 11, and 12, May 19, 1998.
- DeVaull, G. E., R. A. Ettinger, and J. B. Gustafson, 2002. Chemical Vapor Intrusion from Soil or Groundwater to Indoor Air: Significance of Unsaturated Zone Biodegradation of Aromatic Hydrocarbons, Soil and Sediment Contamination, Vol. 11, No. 4, pp. 625-641.
- DeVaull, G. E., R. A. Ettinger, J. P. Salinitro, and J. B. Gustafson. 1997. "Benzene, Toluene, Ethylbenzene and Xylenes (BTEX) Degradation in Vadose Zone Soils During Vapor Transport: First Order Rate Constants." Proceedings of the API/NGWA Petroleum Hydrocarbons and Organic Chemicals in Groundwater: Prevention, Detection and Remediation Conference. Houston, TX. November 12-14. 365-379.
- Fischer, M.L., A.J. Bentley, K.A. Dunkin, A.T. Hodgson, W.W. Nazaroff, R.G. Sextro, and J.M. Daisey. 1996. *Factors Affecting Indoor Air Concentrations of Volatile Organic Compounds at a Site of Subsurface Gasoline Contamination*. Environ. Sci. Technol., 30(10): 2948-2957.
- Fitzpatrick, N.A., and J.J. Fitzgerald. 1996. *An Evaluation of Vapor Intrusion Into Buildings Through a Study of Field Data*. Presented at the 11th Annual Conference on Contaminated Soils, University of Massachusetts at Amherst, October 1996. pp 1-15

- Hers, I., Atwater, J., Li, L., and Zapf-Gilje, R., 2000: Evaluation of vadose zone biodegradation of BTX vapors, *Journal of Contaminant Hydrology*, 46, 233-264.
- Hohener, P., C. Duwig, G. Pasteris, K. Kaufmann, N. Dakhel, and H. Harms, 2003: Biodegradation of Petroleum Hydrocarbon Vapors: Laboratory Studies on rates and Kinetics in Unsaturated Alluvial Sand, *Journal of Contaminant Hydrology*, 66, 93-115.
- Johnson, P.C. and R.A. Ettinger, 1991. Heuristic Model for Predicting the Intrusion Rate of Contaminant Vapors into Buildings: *Environmental Science & Technology*, Vol. 25, p. 1445-1452.
- Johnson, P.C., M.W. Kemblowski, and R.L. Johnson. 1999. Assessing the Significance of Subsurface Contaminant Vapor Migration to Enclosed Spaces: Site-Specific Alternatives to Generic Estimates, *Journal of Soil Contamination*, 8(3) 389-421.
- Lahvis, M. A., A. L. Baehr, and R. J. Baker, 1999: Quantification of aerobic biodegradation and volatilization rates of gasoline hydrocarbons near the water table under natural attenuation conditions, *Water Resources Research*, 35, 3, 753-765. March.

TABLE F-1
Input Parameters for Modeled Locations in the Waste Pit Area

Parameter	Value	Units	Reference
CAS No.	71432		
Chemical Name	Benzene		Selected
Chemical Properties			
Dair	8.80E-02	cm ² /s	USEPA, 2003
	7.60E-01	m ² /d	Calculated
Dwater	9.80E-06	cm ² /s	USEPA, 2003
	8.47E-05	m ² /d	Calculated
Hi	2.28E-01	-	USEPA, 2003
MW	7.81E+01	g/mol	
Ambient Air Calculation Parameters			
W	15	m	Estimated
δ _{amb}	2	m	ASTM, 1995
U	2.25	m/s	ASTM, 1995
	194400	m/d	Calculated
Building Parameters			
AB	225	m ²	Assume 15 m x 15 m source area
η	1	-	Open Field
ER	1.30E+04	1/d	Equivalent to 2.25 m/s wind over 15 m x 15 m area
Lb	3	m	Estimated for commercial building, not critical for calibration
Qb	8.75E+06	m ³ /d	Calculated
Lcrk	0.15	m	Estimated for commercial building, not critical for calibration
Dcrk	0.1	m ² /d	Estimated for commercial building, not critical for calibration
Constant Soil Parameters			
Qsoil	1.00E-10	m ³ /s	Estimated for no scenario with no building. Assumes limited convection at surface
Qsoil	8.64E-06	m ³ /d	Calculated
Dimensionless Groups			
QsLcrk/DcrkAcrk	5.76E-08	-	Calculated
Qs/Qb	9.88E-13	-	Calculated

USEPA, 2003. User's Guide for the Johnson and Ettinger (1991) Model for Subsurface Vapor Intrusion into Buildings, USEPA Office of Emergency and Remedial Response.

TABLE F-1
Input Parameters for Modeled Locations in the Waste Pit Area

Soil Properties

CPT-7 Depth bgs (ft)	Porosity	Soil Moisture Content
0-15	0.396	0.211
15-20	0.376	0.249
20-25	0.457	0.383
25-30	0.386	0.269
30-35	0.465	0.315
35-40	0.452	0.353
45-47	0.413	0.361

CPT-8 Depth bgs (ft)	Porosity	Soil Moisture Content
0-10	0.396	0.211
10-15	0.383	0.178
15-20	0.376	0.249
20-25	0.457	0.383
25-30	0.386	0.269
30-35	0.465	0.315
35-40	0.452	0.353
40-45	0.429	0.283

CPT-15 Depth bgs (ft)	Porosity	Soil Moisture Content
0-10	0.491	0.197
10-15	0.437	0.199
15-20	0.422	0.358
20-25	0.370	0.314
25-30	0.372	0.270
30-35	0.433	0.413
35-40	0.434	0.122
40-43	0.458	0.070
43-48	0.550	0.490
48-52	0.522	0.145
52-53	0.437	0.133

CPT-16 Depth bgs (ft)	Porosity	Soil Moisture Content
0-10	0.491	0.293
10-15	0.437	0.199
15-20	0.442	0.358
20-25	0.370	0.314
25-30	0.372	0.270
30-35	0.433	0.413
35-40	0.434	0.122
40-43	0.458	0.070
43-48	0.550	0.490
48-52	0.522	0.145
52-53	0.437	0.133

Dames & Moore, 1999. Vapor Transport Modeling Report, Del Amo Study Area

Table F-2
Input Parameters for Modeled Locations in the MW-20 NAPL Area

Parameter	Value	Units	Reference
CAS No.	71432		
Chemical Name	Benzene		Selected
Chemical Properties			
Dair	8.80E-02	cm ² /s	USEPA, 2003
	7.60E-01	m ² /d	Calculated
Dwater	9.80E-06	cm ² /s	USEPA, 2003
	8.47E-05	m ² /d	Calculated
Hi	2.28E-01	-	USEPA, 2003
MW	7.81E+01	g/mol	
Ambient Air Calculation Parameters			
W	15	m	Estimated
δ _{amb}	2	m	ASTM, 1995
U	2.25	m/s	ASTM, 1995
	194400	m/d	Calculated
Building Parameters			
AB	225	m ²	Assume 15 m x 15 m source area
η	0.01	-	Assumed for asphalt cover
ER	1.30E+04	1/d	Equivalent to 2.25 m/s wind over 15 m x 15 m area
Lb	3	m	Estimated for commercial building, not critical for calibration
Qb	8.75E+06	m ³ /d	Calculated
Lcrk	0.15	m	Estimated for commercial building, not critical for calibration
Dcrk	0.1	m ² /d	Estimated for commercial building, not critical for calibration
Constant Soil Parameters			
Qsoil	1.00E-10	m ³ /s	Estimated for no scenario with no building. Assumes limited convection at surface
Qsoil	8.64E-06	m ³ /d	Calculated
Dimensionless Groups			
QsLcrk/DcrkAcrk	5.76E-06	-	Calculated
Qs/Qb	9.88E-13	-	Calculated

USEPA, 2003. User's Guide for the Johnson and Ettinger (1991) Model for Subsurface Vapor Intrusion into Buildings, USEPA Office of Emergency and Remedial Response.

Table F-2
 Input Parameters for Modeled Locations in the MW-20 NAPL Area

Soil Properties

SGL0028 Depth bgs (ft)	Porosity	Soil Moisture Content
0-15	0.448	0.380
15-30	0.500	0.300
30-40	0.425	0.399
40-44	0.459	0.404
44-54	0.474	0.410
54-55	0.455	0.381
55-60	0.474	0.368

SGL0033 Depth bgs (ft)	Porosity	Soil Moisture Content
0-15	0.448	0.380
15-30	0.500	0.300
30-40	0.425	0.399
40-44	0.459	0.404
44-54	0.474	0.410
54-55	0.455	0.381
55-60	0.474	0.368

SGL0035 Depth bgs (ft)	Porosity	Soil Moisture Content
0-15	0.448	0.380
15-30	0.500	0.300
30-40	0.425	0.399
40-44	0.459	0.404
44-49	0.474	0.410

SGL0044 Depth bgs (ft)	Porosity	Soil Moisture Content
0-15	0.448	0.380
15-30	0.500	0.300
30-40	0.425	0.399
40-44	0.459	0.404
44-54	0.474	0.410
54-55	0.455	0.381
55-60	0.474	0.368

Dames & Moore, 1999. Vapor Transport Modeling Report, Del Amo Study Area

Table F-3
Input Parameters for Modeled Locations in the Benzene Pipeline Area

Parameter	Value	Units	Reference
CAS No.	71432		
Chemical Name	Benzene		Selected
Chemical Properties			
Dair	8.80E-02	cm ² /s	USEPA, 2003
	7.60E-01	m ² /d	Calculated
Dwater	9.80E-06	cm ² /s	USEPA, 2003
	8.47E-05	m ² /d	Calculated
Hi	2.28E-01	-	USEPA, 2003
MW	7.81E+01	g/mol	
Ambient Air Calculation Parameters			
W	15	m	Estimated
δ _{amb}	2	m	ASTM, 1995
U	2.25	m/s	ASTM, 1995
	194400	m/d	Calculated
Building Parameters			
AB	225	m ²	Assume 15 m x 15 m source area
η	0.01	-	Assumed for asphalt cover
ER	1.30E+04	1/d	Equivalent to 2.25 m/s wind over 15 m x 15 m area
Lb	3	m	Estimated for commercial building, not critical for calibration
Qb	8.75E+06	m ³ /d	Calculated
Lcrk	0.15	m	Estimated for commercial building, not critical for calibration
Dcrk	0.1	m ² /d	Estimated for commercial building, not critical for calibration
Constant Soil Parameters			
Qsoil	1.00E-10	m ³ /s	Estimated for no scenario with no building. Assumes limited convection at surface
Qsoil	8.64E-06	m ³ /d	Calculated
Dimensionless Groups			
QsLcrk/DcrkAcrk	5.76E-06	-	Calculated
Qs/Qb	9.88E-13	-	Calculated

USEPA, 2003. User's Guide for the Johnson and Ettinger (1991) Model for Subsurface Vapor Intrusion into Buildings, USEPA Office of Emergency and Remedial Response.

Table F-3
 Input Parameters for Modeled Locations in the Benzene Pipeline Area

Soil Properties

SG-01	Porosity	Soil Moisture Content
Depth bgs (ft)		
0-13	0.362	0.164

Dames & Moore, 1999

SG-02	Porosity	Soil Moisture Content
Depth bgs (ft)		
0-13	0.362	0.164

Dames & Moore, 1999

SG-04	Porosity	Soil Moisture Content
Depth bgs (ft)		
0-13	0.362	0.164

Dames & Moore, 1999

SG-022	Porosity	Soil Moisture Content
Depth bgs (ft)		
0-13	0.362	0.164

Dames & Moore, 1999

Dames & Moore, 1999. Vapor Transport Modeling Report, Del Amo Study Area

Table F-4
 Summary of Dominant Layer Model Biodegradation Parameters

Area	Boring ID	Deg Rate Constant (1/day)	Dominant Layer Interval (ft)
Waste Pit Area	CPT-7	0.25	1-10
	CPT-8	0.5	1-10
	CPT-15	0.5	1-10
	CPT-16	0.5	1-10
MW-20 Area	SGL0028	0.05	1-6
	SGL0033	0.048	1-6
	SGL0035	0.05	1-6
	SGL0044	0.1	1-6
Benzene P/L Area	SG-01	0.59	1-8
	SG-02	0.59	1-8
	SG-04	0.29	1-8
	SG-22	0.17	1-4

Table F-5
Benzene, PCE and TCE Soil Gas Data Summary for Vapor Transport Modeling

Cluster ID	Sample ID	Sample Depth (ft)	Benzene (ppmV)	PCE (ppmV)	TCE (ppmV)
SGL0028	SGL0046	3.00	<0.3	0.119	<0.06
	SGL0046	6.00	<0.3	<0.06	<0.06
	SGL0133	8.00	<0.012	0.25	<0.01
	SGL0132	10.00	0.019	<0.0120	<0.0120
	SGL0134	10.00	<0.0300	<0.0120	<0.0120
	SGL0028	59.00	12700	<0.6	0.086
SGL0033	SGL0040	1.00	<0.3	15.50	0.022
	SGL0041	2.00	<0.3	<0.06	<0.06
	SGL0040	3.00	<0.3	10.30	0.110
	SGL0041	5.00	<0.3	<0.06	<0.06
	SGL0042	5.00	<0.3	<0.06	<0.06
	SGL0040	6.00	3.19	2.86	0.026
	SGL0033	59.00	10100	<0.06	0.058
SGL0034	SGL0036	3.00	150	<0.0600	<0.06
	SGL0036	6.00	2120	<0.06	0.015
	SGL0242	6.00	2.3	<0.300	<0.250
	SGL0048	10.00	480	<0.005	<0.005
	SGL0048	9.80	0.016	<0.06	0.015
	SGL0125	10.00	<0.0300	<0.0120	<0.0120
	SGL0034	59.00	15600	<0.06	<0.06
SGL0035	SGL0013	6.00	0.037	0.012	<0.005
	SGL0087	6.00	<0.300	<0.0600	<0.0600
	SGL0035	48.00	15300	<0.06	0.017
SGL0044	SGL0053	10.00	<0.3	2.54	<0.06
	SGL0054	10.00	23.2	0.305	<0.0600
	SGL0056	10.00	31.0	2.64	<0.0600
	SGL0057	10.00	5.60	0.162	<0.0600
	SGL0058	10.00	<0.3	0.165	<0.06
	SGL0060	10.00	<0.3	<0.06	<0.06
	SGL0125	10.00	<0.0300	<0.0120	<0.0120
	SGL0126	10.00	0.027	<0.0120	<0.0120
	SGL0044	57.00	25900	<0.06	<0.06
CPT-7	SGL0836	6.00	<0.10	NA	NA
	SGL0849	6.50	0.028	0.0014	NA
	SGL0835	7.00	<0.00043	0.001	NA
	SGL0837	7.00	<0.10	NA	NA
	SGL0837	12.00	<0.10	NA	NA
	SGL0849	13.00	0.0067	0.014	NA
	SGL0836	14.00	<0.10	NA	NA
	SGL0835	14.00	0.0036	0.0023	NA

Table F-5
Benzene, PCE and TCE Soil Gas Data Summary for Vapor Transport Modeling

Cluster ID	Sample ID	Sample Depth (ft)	Benzene (ppmV)	PCE (ppmV)	TCE (ppmV)
CPT-15	SGL0822	7.00	<0.00042	0.00075	NA
	SGL0823	7.00	<0.10	NA	NA
	SGL0824	7.00	<0.10	NA	NA
	SGL0825	7.00	0.01	0.00035	NA
	SGL0842	7.00	<0.00042	<0.00042	NA
	SGL0843	7.00	<0.00044	0.0009	NA
	SGL0823	12.00	<0.10	NA	NA
	SGL0844	12.80	0.0092	0.0017	NA
	SGL0822	14.00	0.0035	0.00065	NA
	SGL0824	14.00	<0.10	NA	NA
	SGL0825	14.00	<0.10	NA	NA
CPT-16	SGL0841	6.00	0.00063	<0.00045	NA
	SGL0816	7.00	0.0005	<0.00039	NA
	SGL0817	7.00	<0.10	NA	NA
	SGL0818	7.00	<0.10	NA	NA
	SGL0819	7.00	0.00041	<0.00041	NA
	SGL0840	7.00	0.0026	<0.00042	NA
	SGL0816	14.00	<0.10	NA	NA
	SGL0817	11.50	<0.00041	<0.00041	NA
	SGL0818	14.00	<0.10	NA	NA
	SGL0819	14.00	<0.10	NA	NA

NA - Not Analyzed

Shaded values are not detected

Bolded values are detected

Table F-6
Tier 2 Model Input Parameters

Model Input Parameter	Value Used	Rationale
Soil Properties		
Average Soil / Groundwater Temperature (Ts), °C	18	Area-Specific Value
Depth below grade to bottom of enclosed space floor (L _F), cm	15	Slab construction
Depth below grade to top of shallow contamination (Lt), cm	228	Shallow, assumes infinite source impacts start at 7.5 ft bgs
Depth below grade to top of deep contamination (Lt), cm	914	Deep, assumes infinite source impacts start at 30 ft bgs
Depth below grade to bottom of contamination (Lb), cm	0	Assume infinite source
Depth below grade to water table (Lwt), cm	1435	Site-Specific, 47 feet bgs
Thickness of soil stratum A (h _A), cm	458	Site-Specific Value, 15 feet bgs
Thickness of soil stratum B (h _B), cm	458	Site-Specific Value, 15-30 feet bgs
Thickness of soil stratum C (h _C), cm	519	Site-Specific Value, 30-47 feet bgs
Soil stratum A SCS soil type	SCL	Site-Specific based on boring logs
Soil stratum directly above water table	C	Site-Specific based on boring logs
SCS soil type directly above water table	SL	Sandy-Loam based on USCS soil classification for Stratum C
Stratum A soil dry bulk density, gm/cm ³	1.6317	Geomean, Site-Specific Value based on soil physical property testing - 0 to 458 cm bgs
Stratum A soil total porosity, unitless	0.3794	Geomean, Site-Specific Value based on soil physical property testing - 0 to 458 cm bgs
Stratum A soil water-filled porosity, cm ³ /cm ³	0.2526	Geomean, Site-Specific Value based on soil physical property testing - 0 to 458 cm bgs
Stratum A soil organic carbon fraction (f _{oc} ^A), unitless	0.006	Default Assumption
Stratum B soil dry bulk density, gm/cm ³	1.5388	Geomean, Site-Specific Value based on soil physical property testing - >458 to 916 cm bgs
Stratum B soil total porosity, unitless	0.4136	Geomean, Site-Specific Value based on soil physical property testing - >458 to 916 cm bgs
Stratum B soil water-filled porosity, cm ³ /cm ³	0.1760	Geomean, Site-Specific Value based on soil physical property testing - >458 to 916 cm bgs
Stratum B soil organic carbon fraction (f _{oc} ^B), unitless	0.006	Default Assumption
Stratum C soil dry bulk density, gm/cm ³	1.5614	Geomean, Site-Specific Value based on soil physical property testing - >916 to 1435 cm bgs
Stratum C soil total porosity, unitless	0.3995	Geomean, Site-Specific Value based on soil physical property testing - >916 to 1435 cm bgs
Stratum C soil water-filled porosity, cm ³ /cm ³	0.2193	Geomean, Site-Specific Value based on soil physical property testing - >916 to 1435 cm bgs
Stratum C soil organic carbon fraction (f _{oc} ^C), unitless	0.006	Default Assumption
Biodegradation Properties		
First order degradation rate constant, day ⁻¹	0.048	Site-specific value, based on minimum of calibration evaluation
Top of biodegradation zone, cm	30.5	Site-specific value, assumed 1 ft bgs
Bottom of biodegradation zone, cm	183	Site-specific value, based on minimum of calibration evaluation
Residential Building Parameters		
Enclosed space floor thickness (L _{crack}), cm	10	Default assumption
Soil-building pressure differential, g/cm-sec ²	40	Default assumption
Enclosed space floor length (L _B), cm	1000	Default residential building dimension
Enclosed space floor width (W _B), cm	1000	Default residential building dimension
Enclosed space height (H _B), cm	244	Default residential building dimension for slab-on-grade, 8 feet
Floor-wall seam crack width (w), cm	0.1	Default assumption
Indoor air exchange rate (ER), hour ⁻¹	0.5	50th percentile from a comprehensive US study (USPEA 2003)
Average vapor flow rate into building (Q _{soil}), L/m	5	Default residential assumption
Commercial Building Parameters		
Enclosed space floor thickness (L _{crack}), cm	10	Default assumption
Soil-building pressure differential, g/cm-sec ²	40	Default assumption
Enclosed space floor length (L _B), cm	5400	Assume commercial building length ~ 180 feet
Enclosed space floor width (W _B), cm	3000	Site-specific commercial building width ~ 98 feet
Enclosed space height (H _B), cm	305	Assume commercial building ceiling height = 10 feet
Floor-wall seam crack width (w), cm	0.1	Default assumption
Indoor air exchange rate (ER), hour ⁻¹	0.9	0.15 cfm/ft ² (California Energy Commission, 2001)
Average vapor flow rate into building (Q _{soil}), L/m	80	Calculated based on site-specific building dimensions

Table F-7
Tier 2 Modeling Attenuation Factors

Tier 2 Modeling Summary

Compound	Scenario	α JEM	α DLM	FRF
Benzene	Commercial Deep	1.53E-05	4.04E-08	3.79E+02
	Commercial Shallow	3.76E-05	4.82E-07	7.80E+01
	Commercial Groundwater	1.02E-05	1.79E-08	5.70E+02
	Residential Deep	3.43E-05	8.82E-08	3.88E+02
	Residential Shallow	8.42E-05	1.06E-06	7.95E+01
	Residential Groundwater	2.30E-05	4.04E-08	5.68E+02
Toluene	Commercial Deep	1.50E-05	5.96E-08	2.52E+02
	Commercial Shallow	3.69E-05	6.57E-07	5.63E+01
	Residential Deep	3.38E-05	1.34E-07	2.52E+02
	Residential Shallow	8.31E-05	1.48E-06	5.62E+01
Ethylbenzene	Commercial Deep	1.30E-05	4.95E-08	2.62E+02
	Commercial Shallow	3.20E-05	5.52E-07	5.80E+01
	Residential Deep	2.92E-05	1.10E-07	2.65E+02
	Residential Shallow	7.19E-05	1.23E-06	5.85E+01
Xylene	Commercial Deep	1.33E-05	4.95E-08	2.69E+02
	Commercial Shallow	3.28E-05	5.53E-07	5.92E+01
	Residential Deep	3.00E-05	1.11E-07	2.69E+02
	Residential Shallow	7.38E-05	1.25E-06	5.92E+01

α JEM = Attenuation factor calculated using Johnson and Ettinger (1991) model

α DLM = Attenuation factor calculated using Dominant Layer Model (Johnson et al., 1999)

FRF = Flux Reduction Factor: Reduction in estimated flux using Tier 2 analysis

TABLE F-8
TIER 2 INDOOR AIR EPCs
SHALLOW SOIL/SOIL GAS
Baseline Risk Assessment
Del Amo Site

Analyte	Residential Scenario				Commercial Scenario			
	Max Soil EPC mg/kg	Converted SG* ug/m ³	Resident Alpha	Resident IA EPC mg/m ³	UCL95 Soil EPC mg/kg	Converted SG* ug/m ³	Worker Alpha	Worker IA EPC mg/m ³
Parcel: 7351-33-17; EAPC No. 5								
Benzene	5.9	2.60E+06	1.06E-06	2.75E-03	0.728	3.20E+05	4.82E-07	1.54E-04
Ethylbenzene	17	2.29E+06	1.23E-06	2.81E-03	0.899	1.21E+05	5.52E-07	6.67E-05
Toluene	18	3.81E+06	1.48E-06	5.64E-03	0.931	1.97E+05	6.57E-07	1.29E-04
Xylenes (Total)	22	2.56E+06	1.25E-06	3.20E-03	10.1	1.18E+06	5.53E-07	6.50E-04
Parcel: 7351-33-22; EAPC No. 6								
Benzene	29.5	1.30E+07	1.06E-06	1.38E-02	3.29	1.45E+06	4.82E-07	6.98E-04
Parcel: 7351-33-24; EAPC No. 7								
Benzene	2.7	1.19E+06	1.06E-06	1.26E-03	0.44	1.94E+05	4.82E-07	9.33E-05
Ethylbenzene	55	7.40E+06	1.23E-06	9.10E-03	10.6	1.43E+06	5.52E-07	7.87E-04
Xylenes (Total)	72	8.38E+06	1.25E-06	1.05E-02	32.7	3.81E+06	5.53E-07	2.10E-03
Parcel: 7351-33-26; EAPC No. 8								
Benzene	0.89	3.92E+05	1.06E-06	4.15E-04	0.248	1.09E+05	4.82E-07	5.26E-05
Xylenes (Total)	0.38	4.42E+04	1.25E-06	5.53E-05	0.262	3.05E+04	5.53E-07	1.69E-05
Parcel: 7351-33-27; EAPC No. 9								
Benzene	4	1.76E+06	1.06E-06	1.87E-03	1.26	5.54E+05	4.82E-07	2.67E-04
Xylenes (Total)	0.025	2.91E+03	1.25E-06	3.64E-06	0.0149	1.73E+03	5.53E-07	9.59E-07
Parcel: 7351-33-34; EAPC No. 11								
Benzene	14.2	6.25E+06	1.06E-06	6.62E-03	6.26	2.75E+06	4.82E-07	1.33E-03
Toluene	0.102	2.16E+04	1.48E-06	3.19E-05	0.0427	9.04E+03	6.57E-07	5.94E-06
Parcel: 7351-33-900; EAPC No. 15								
Benzene	3.5	1.54E+06	1.06E-06	1.63E-03	3.5	1.54E+06	4.82E-07	7.42E-04
Ethylbenzene	0.008	1.08E+03	1.23E-06	1.32E-06	0.008	1.08E+03	5.52E-07	5.94E-07
Toluene	0.004	8.47E+02	1.48E-06	1.25E-06	0.004	8.47E+02	6.57E-07	5.56E-07
Parcel: 7351-34-15,-50,-56; EAPC No. 16								
Benzene	200	8.80E+07	1.06E-06	9.33E-02	11.2	4.93E+06	4.82E-07	2.38E-03
Ethylbenzene	12000	1.61E+09	1.23E-06	1.98E+00	703	9.45E+07	5.52E-07	5.22E-02
Toluene	200	4.23E+07	1.48E-06	6.26E-02	11.2	2.37E+06	6.57E-07	1.56E-03
Xylenes (Total)	200	2.33E+07	1.25E-06	2.91E-02	32.4	3.77E+06	5.53E-07	2.08E-03
Parcel: 7351-34-39; EAPC No. 17								
Benzene	1.52	6.69E+05	1.06E-06	7.09E-04	0.532	2.34E+05	4.82E-07	1.13E-04
Ethylbenzene	20	2.69E+06	1.23E-06	3.31E-03	6.93	9.32E+05	5.52E-07	5.14E-04
Toluene	1.05	2.22E+05	1.48E-06	3.29E-04	0.368	7.79E+04	6.57E-07	5.12E-05
Xylenes (Total)	1.6	1.86E+05	1.25E-06	2.33E-04	1.6	1.86E+05	5.53E-07	1.03E-04
Parcel: 7351-34-41; EAPC No. 18								
Benzene	0.0522	2.30E+04	1.06E-06	2.43E-05	0.0172	7.57E+03	4.82E-07	3.65E-06
Ethylbenzene	1.04	1.40E+05	1.23E-06	1.72E-04	0.339	4.56E+04	5.52E-07	2.52E-05
Toluene	0.165	3.49E+04	1.48E-06	5.17E-05	0.0538	1.14E+04	6.57E-07	7.48E-06
Xylenes (Total)	0.00643	7.48E+02	1.25E-06	9.35E-07	0.00643	7.48E+02	5.53E-07	4.14E-07
Parcel: 7351-34-47; EAPC No. 21								
Benzene	0.0355	1.56E+04	1.06E-06	1.66E-05	0.0152	6.69E+03	4.82E-07	3.22E-06
Ethylbenzene	2.06	2.77E+05	1.23E-06	3.41E-04	0.871	1.17E+05	5.52E-07	6.47E-05
Toluene	0.00805	1.70E+03	1.48E-06	2.52E-06	0.00398	8.42E+02	6.57E-07	5.53E-07

TABLE F-8
TIER 2 INDOOR AIR EPCs
SHALLOW SOIL/SOIL GAS
Baseline Risk Assessment
Del Amo Site

Analyte	Residential Scenario				Commercial Scenario			
	Max Soil EPC mg/kg	Converted SG* ug/m ³	Resident Alpha	Resident IA EPC mg/m ³	UCL95 Soil EPC mg/kg	Converted SG* ug/m ³	Worker Alpha	Worker IA EPC mg/m ³
Parcel: 7351-34-57; EAPC No. 23								
Benzene	300	1.32E+08	1.06E-06	1.40E-01	13.5	5.94E+06	4.82E-07	2.86E-03
Ethylbenzene	12000	1.61E+09	1.23E-06	1.98E+00	577	7.76E+07	5.52E-07	4.28E-02
Toluene	50	1.06E+07	1.48E-06	1.57E-02	2.38	5.04E+05	6.57E-07	3.31E-04
Xylenes (Total)	150	1.75E+07	1.25E-06	2.18E-02	23.8	2.77E+06	5.53E-07	1.53E-03
Parcel: 7351-34-58; EAPC No. 24								
Benzene	5	2.20E+06	1.06E-06	2.33E-03	1.19	5.24E+05	4.82E-07	2.52E-04
Ethylbenzene	82	1.10E+07	1.23E-06	1.36E-02	19.5	2.62E+06	5.52E-07	1.45E-03
Xylenes (Total)	15	1.75E+06	1.25E-06	2.18E-03	4.83	5.62E+05	5.53E-07	3.11E-04
Parcel: 7351-34-69; EAPC No. 28								
Benzene	0.17	7.48E+04	1.06E-06	7.93E-05	0.0219	9.64E+03	4.82E-07	4.64E-06
Ethylbenzene	2.45	3.29E+05	1.23E-06	4.05E-04	0.288	3.87E+04	5.52E-07	2.14E-05
Toluene	0.397	8.40E+04	1.48E-06	1.24E-04	0.0434	9.18E+03	6.57E-07	6.03E-06
Xylenes (Total)	1.1	1.26E+05	1.25E-06	1.58E-04	0.118	1.36E+04	5.53E-07	7.50E-06
Parcel: 7351-34-73; EAPC No. 31								
Benzene	0.00819	3.60E+03	1.06E-06	3.82E-06	0.00819	3.60E+03	4.82E-07	1.74E-06
Ethylbenzene	0.0223	3.00E+03	1.23E-06	3.69E-06	0.0223	3.00E+03	5.52E-07	1.66E-06
Toluene	0.00751	1.59E+03	1.48E-06	2.35E-06	0.00751	1.59E+03	6.57E-07	1.04E-06
Xylenes (Total)	0.00857	9.97E+02	1.25E-06	1.25E-06	0.00857	9.97E+02	5.53E-07	5.51E-07
Parcel: Magellan Dr; EAPC No. 35								
Benzene	6.4	2.82E+06	1.06E-06	2.99E-03	1.71	7.52E+05	4.82E-07	3.63E-04
Ethylbenzene	170	2.29E+07	1.23E-06	2.81E-02	45	6.05E+06	5.52E-07	3.34E-03
Toluene	34	7.20E+06	1.48E-06	1.06E-02	8.87	1.88E+06	6.57E-07	1.23E-03
Parcel: Pacific Gateway (S); EAPC No. 37								
Benzene	0.0025	1.10E+03	1.06E-06	1.17E-06	0.0022	9.68E+02	4.82E-07	4.67E-07
Ethylbenzene	0.477	6.41E+04	1.23E-06	7.89E-05	0.477	6.41E+04	5.52E-07	3.54E-05
Toluene	0.00822	1.74E+03	1.48E-06	2.57E-06	0.00772	1.63E+03	6.57E-07	1.07E-06
Xylenes (Total)	0.005	5.82E+02	1.25E-06	7.27E-07	0.005	5.82E+02	5.53E-07	3.22E-07

Notes:

EAPC: Exposure area of potential concern, EPC: exposure point concentration; IA: indoor air; SG: soil gas

* To convert mg/kg to ug/m³, take soil EPC ÷ CF: conversion factor: CF

Benzene	2.3E-06
Ethylbenzene	7.4E-06
Toluene	4.7E-06
Xylenes (Total)	8.6E-06

TABLE F-9
TIER 2 INDOOR AIR EPCs
DEEP SOIL/SOIL GAS
Baseline Risk Assessment
Del Amo Site

Analyte	Residential Scenario				Commercial Scenario			
	Max Soil EPC mg/kg	Converted SG* ug/m ³	Resident Alpha	Resident IA EPC mg/m ³	UCL95 Soil EPC mg/kg	Converted SG* ug/m ³	Worker Alpha	Worker IA EPC mg/m ³
Parcel: 7351-33-17; EAPC No. 5								
Benzene	39	1.74E+07	8.82E-08	1.54E-03	39	1.74E+07	4.04E-08	7.04E-04
Ethylbenzene	14	1.89E+06	1.10E-07	2.07E-04	14	1.89E+06	4.95E-08	9.34E-05
Toluene	68	1.45E+07	1.34E-07	1.94E-03	68	1.45E+07	5.96E-08	8.62E-04
Xylenes (Total)	32	3.73E+06	1.11E-07	4.14E-04	32	3.73E+06	4.95E-08	1.85E-04
Parcel: 7351-33-22; EAPC No. 6								
Benzene	1.9	8.50E+05	8.82E-08	7.49E-05	1.8	8.05E+05	4.04E-08	3.25E-05
Ethylbenzene	13	1.75E+06	1.10E-07	1.93E-04	8.7	1.17E+06	4.95E-08	5.80E-05
Toluene	11	2.34E+06	1.34E-07	3.14E-04	7.4	1.57E+06	5.96E-08	9.38E-05
Xylenes (Total)	78	9.09E+06	1.11E-07	1.01E-03	52.2	6.09E+06	4.95E-08	3.01E-04
Parcel: 7351-33-26; EAPC No. 8								
Benzene	2.1	9.39E+05	8.82E-08	8.28E-05	0.883	3.95E+05	4.04E-08	1.60E-05
Parcel: 7351-33-27; EAPC No. 9								
Benzene	20	8.94E+06	8.82E-08	7.89E-04	8.32	3.72E+06	4.04E-08	1.50E-04
Parcel: 7351-33-900; EAPC No. 15								
Benzene	910	4.07E+08	8.82E-08	3.59E-02	312	1.40E+08	4.04E-08	5.64E-03
Toluene	5	1.06E+06	1.34E-07	1.43E-04	1.23	2.62E+05	5.96E-08	1.56E-05
Parcel: 7351-34-15,-50,-56; EAPC No. 16								
Benzene	12.6	5.63E+06	8.82E-08	4.97E-04	6.9	3.09E+06	4.04E-08	1.25E-04
Ethylbenzene	1.2	1.62E+05	1.10E-07	1.78E-05	0.611	8.23E+04	4.95E-08	4.07E-06
Parcel: 7351-34-57; EAPC No. 23								
Benzene	220	9.84E+07	8.82E-08	8.68E-03	81.8	3.66E+07	4.04E-08	1.48E-03
Ethylbenzene	9.97	1.34E+06	1.10E-07	1.48E-04	2.39	3.22E+05	4.95E-08	1.59E-05
Toluene	3.36	7.15E+05	1.34E-07	9.58E-05	1.1	2.34E+05	5.96E-08	1.39E-05
Parcel: 7351-34-58; EAPC No. 24								
Benzene	2500	1.12E+09	8.82E-08	9.86E-02	2500	1.12E+09	4.04E-08	4.52E-02
Toluene	160	3.40E+07	1.34E-07	4.56E-03	146	3.11E+07	5.96E-08	1.85E-03
Parcel: 7351-34-70; EAPC No. 29								
Benzene	0.93	4.16E+05	8.82E-08	3.67E-05	0.738	3.30E+05	4.04E-08	1.33E-05
Parcel: 7351-34-901; EAPC No. 34								
Benzene	0.26	1.16E+05	8.82E-08	1.03E-05	0.215	9.61E+04	4.04E-08	3.88E-06
Parcel: Magellan Dr; EAPC No. 35								
Benzene	6.1	2.73E+06	8.82E-08	2.41E-04	6.1	2.73E+06	4.04E-08	1.10E-04
Parcel: Pacific Gateway (S); EAPC No. 37								
Benzene	12.7	5.68E+06	8.82E-08	5.01E-04	12.7	5.68E+06	4.04E-08	2.29E-04
Ethylbenzene	8.98	1.21E+06	1.10E-07	1.33E-04	8.98	1.21E+06	4.95E-08	5.99E-05
Toluene	0.0821	1.75E+04	1.34E-07	2.34E-06	0.0821	1.75E+04	5.96E-08	1.04E-06

Notes:

EAPC: Exposure area of potential concern, EPC: exposure point concentration; IA: indoor air; SG: soil gas

* To convert mg/kg to ug/m³, take soil EPC ÷ CF: conversion factor: CF

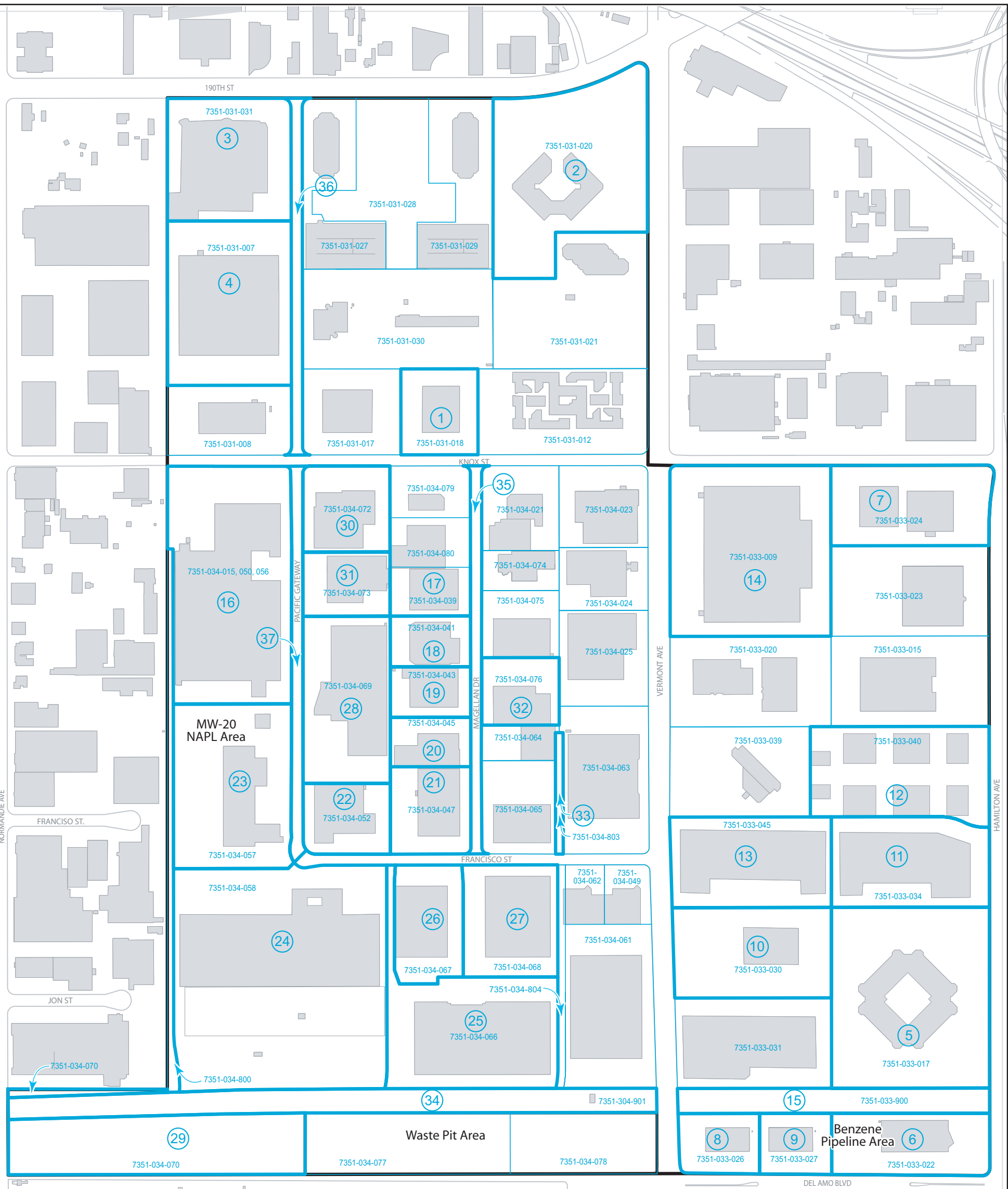
Benzene	2.2E-06
Ethylbenzene	7.4E-06
Toluene	4.7E-06
Xylenes (Total)	8.6E-06

Table F-10
Soil Vapor Data Adequacy Evaluation

EAPC	Parcel	Groundwater Data			Soil Gas Review		Notes
		Benzene	TCE	PCE	# of soil gas sampling locations	Soil Gas Data Adequate?	
1	31-18	43.00	<0.5	<0.5	21	yes	
2	31-20	<1	2.7	<1	3	no	soil gas and gw concs both low
3	31-31	1.20	2.9	3.9	8	yes	soil gas and gw concs both low
4	31-7	0.89	2	<1	3	no	soil gas and gw concs both low
5	33-17	Not provided			numerous	yes	soil gas and gw both elevated
6	33-22	860,000	5.8	8	numerous	yes	soil gas and gw both elevated
7	33-24	0.6	0.7	1.6	23	yes	soil gas and gw concs both low
8	33-26	10.00	11.3	6.5	13	yes	soil gas and gw concs both low
9	33-27	850,000	10	6.4	18	yes	soil gas and gw both elevated
10	33-30	21	<1	<1	1	no	gw low
11	33-34	40,000	<1000	<1000	14	yes	soil gas and gw both elevated
12	33-40	<1	<1	<1	2	no	gw low
13	33-45	<1	<1	2.4	18	yes	soil gas and gw concs both low
14	33-9	4.4	5	6	9	yes	soil gas and gw concs both low
15	33-900	860,000	<25	<25	0	no	GW high, but no buildings likely on this parcel because power line corridor.
16	34-15,50,56	340,000	2000	2100	numerous	yes	soil gas and gw both elevated
17	34-39	290	<10	<10	13	yes	soil gas elevated; gw moderate
18	34-41	10,000	<10	<10	19	yes	soil gas and gw both elevated; benzene in gw based on contours (no sampling location) -check detection limits at PZL0009 for TCE/PCE
19	34-43	10,000	3.9	4.8	5	YES	soil gas low, gw high; gw benzene based on contours - no location -TCE/PCE based on PZL0006. While # of samples is low, there is sufficient coverage of the potential sources
20	34-45	100,000	3.9	4.8	4	no	soil gas low, gw high; gw benzene based on contours - no location -TCE/PCE based on PZL0006
21	34-47	100,000	<500	<500	13	yes	soil gas and gw both elevated; gw benzene based on contours; TCE/PCE based on WPL0001
22	34-52	290,000	<3000	<3000	6	yes	soil gas low, gw elevated; gw B based on CWL0012
23	34-57	820,000	<10,000	<10,000	numerous	yes	soil gas and gw both elevated
24	34-58	420,000	39	<5	22	yes	soil gas low, gw elevated. 2000 gw DLs elevated; used max from historical values.
25	34-66	59,000	32	1.6	5	no	soil gas low, gw elevated; used MBFB for gw benzene because higher than WT; probable additional source area.
26	34-67	42,000	<500	<500	12	yes	soil gas low, gw elevated; source area nearby
27	34-68	3000	<100	<100	1	no	
28	34-69	140,000	<200	<200	numerous	yes	soil gas and gw both elevated
29	34-70	420,000	760	300	28	yes	soil gas low, gw elevated; gw TCE/PCE from XMW-13
30	34-72	43	<0.5	<0.5	20	yes	low soil gas, low gw; for gw used CWL0041
31	34-73	290	<10	<10	3	no	low soil gas, gw moderate. Few soil gas samples
32	34-76	11	3.9	4.8	4	no	low soil gas, low gw; gw TCE/PCE from PZL0006
33	34-803	7.5	<5	350	0	no	gw based on historical data at SWL0016
34	34-901	330,000	1.6	32	0	no	no buildings likely on this parcel due to utility corridor; B based on PZL0019; TCE/PCE based on XP-02
35	Magellan Dr	10,000	3.9	4.8	5	no	soil gas low, gw elevated; gw B based on contour; TCE/PCE based on PZL0006
36	Pac.Gateway (N)	<1	<1	<1	11	yes	soil gas low, gw low; gw based on PZL0014, PZL0015, SWL0038
37	Pac.Gateway (S)	140,000	<200	<200	9	yes	soil gas and gw elevated; gw B based on WPL0002; TCE/PCE

Table F-11
Tier 2 Indoor Air EPCs
Groundwater-to-Indoor Air Pathway

EAPC	Parcel	Benzene Groundwater Concentration (ug/L)	Tier 2 Calc. Air Concs. (Comm) (ug/m3)	Tier 2 Calc. Air Concs. (Res) (ug/m3)
2	31-20	< 1	< 2.99E-06	<6.75E-06
4	31-7	0.89	2.66E-06	6.00E-06
10	33-30	21	6.28E-05	1.42E-04
12	33-40	< 1	< 2.99E-06	<6.75E-06
15	33-900	860,000	2.57E+00	5.80E+00
20	34-45	100,000	2.99E-01	6.75E-01
25	34-66	59,000	1.76E-01	3.98E-01
27	34-68	3000	8.97E-03	2.02E-02
31	34-73	290	8.67E-04	1.96E-03
32	34-76	11	3.29E-05	7.42E-05
33	34-803	7.5	2.24E-05	5.06E-05
34	34-901	330,000	9.86E-01	2.23E+00
35	Magellan Dr	10,000	2.99E-02	6.75E-02



Legend



Exposure area of potential concern with exposure area number

7351-034-070

Assessor parcel number

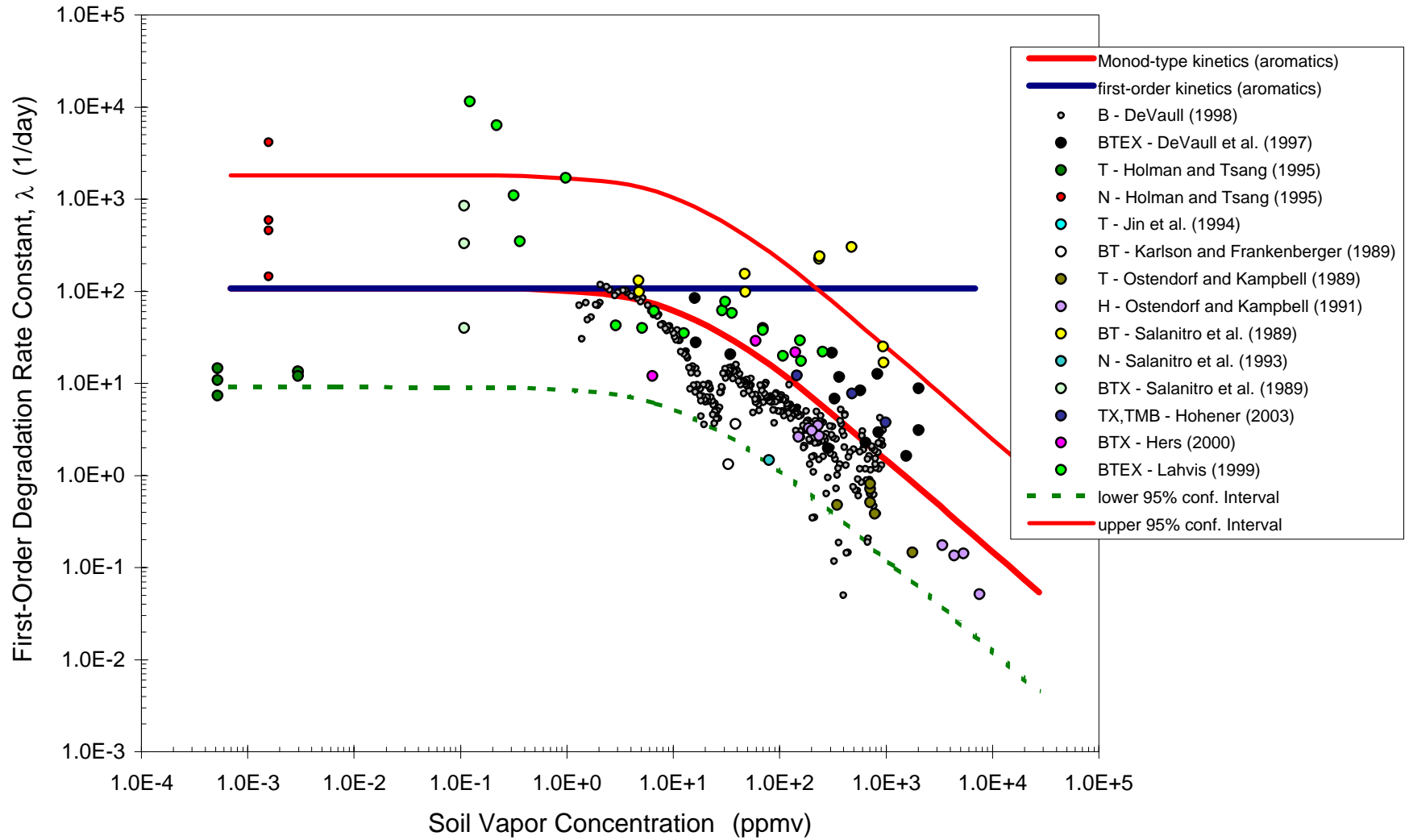
FIGURE F-1

EAPCs AND TIER 2 VAPOR MODELING AREAS

Baseline Risk Assessment
Del Amo Superfund Site



Figure F-2
Literature Values of BTEX Vados Zone Biodegradation Rate Constants
 (adapted from DeVaul et al., 1997)



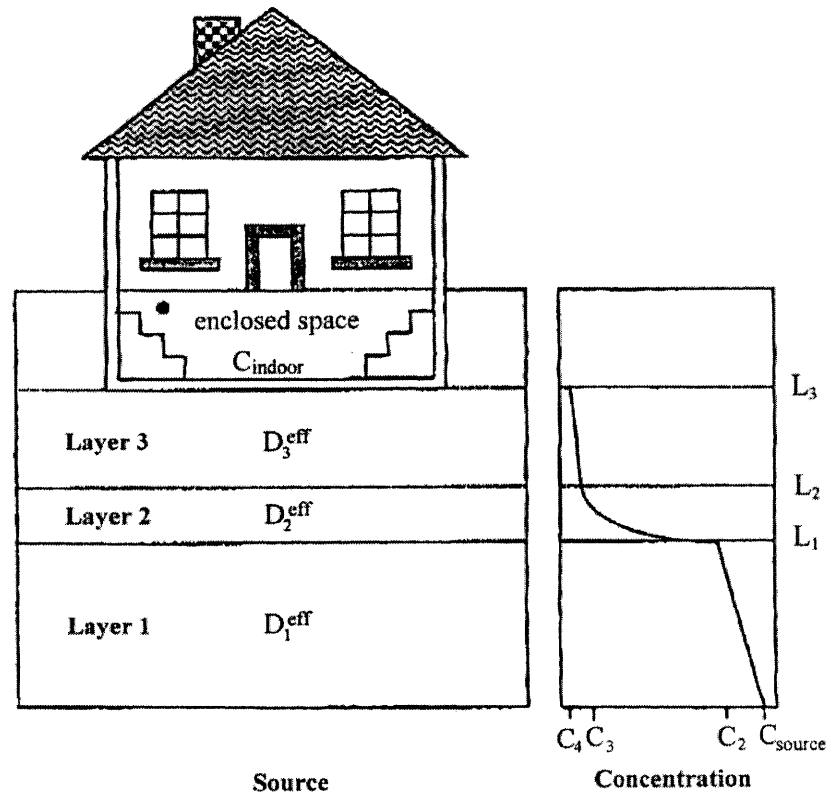


FIGURE F-3

Model Conceptualization

(from Johnson et al., 1999)

Figure F-4
Waste Pits Area CPT-7 DLM and JEM Results

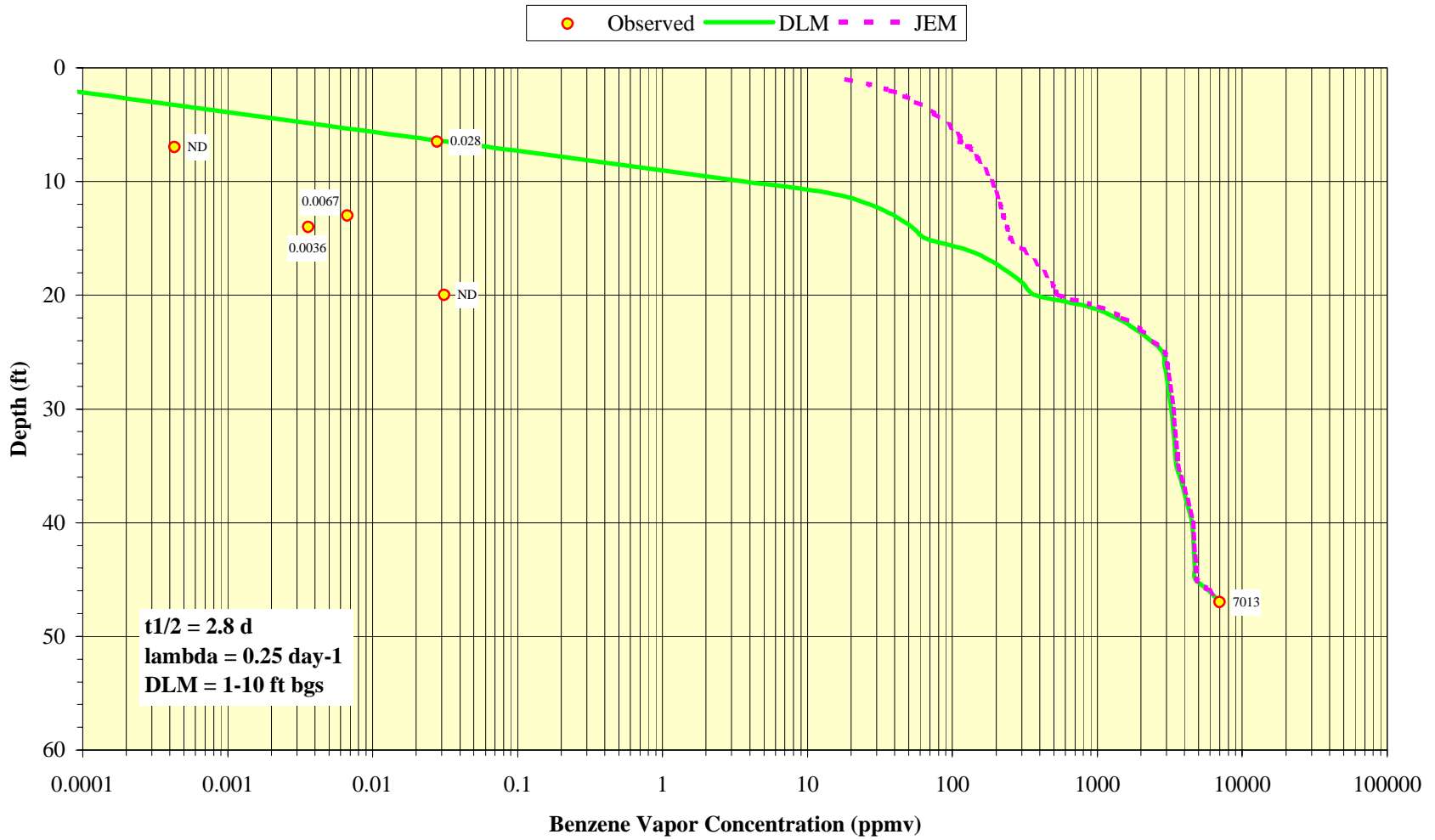


Figure F-5
Waste Pit Area CPT-8 DLM and JEM Results

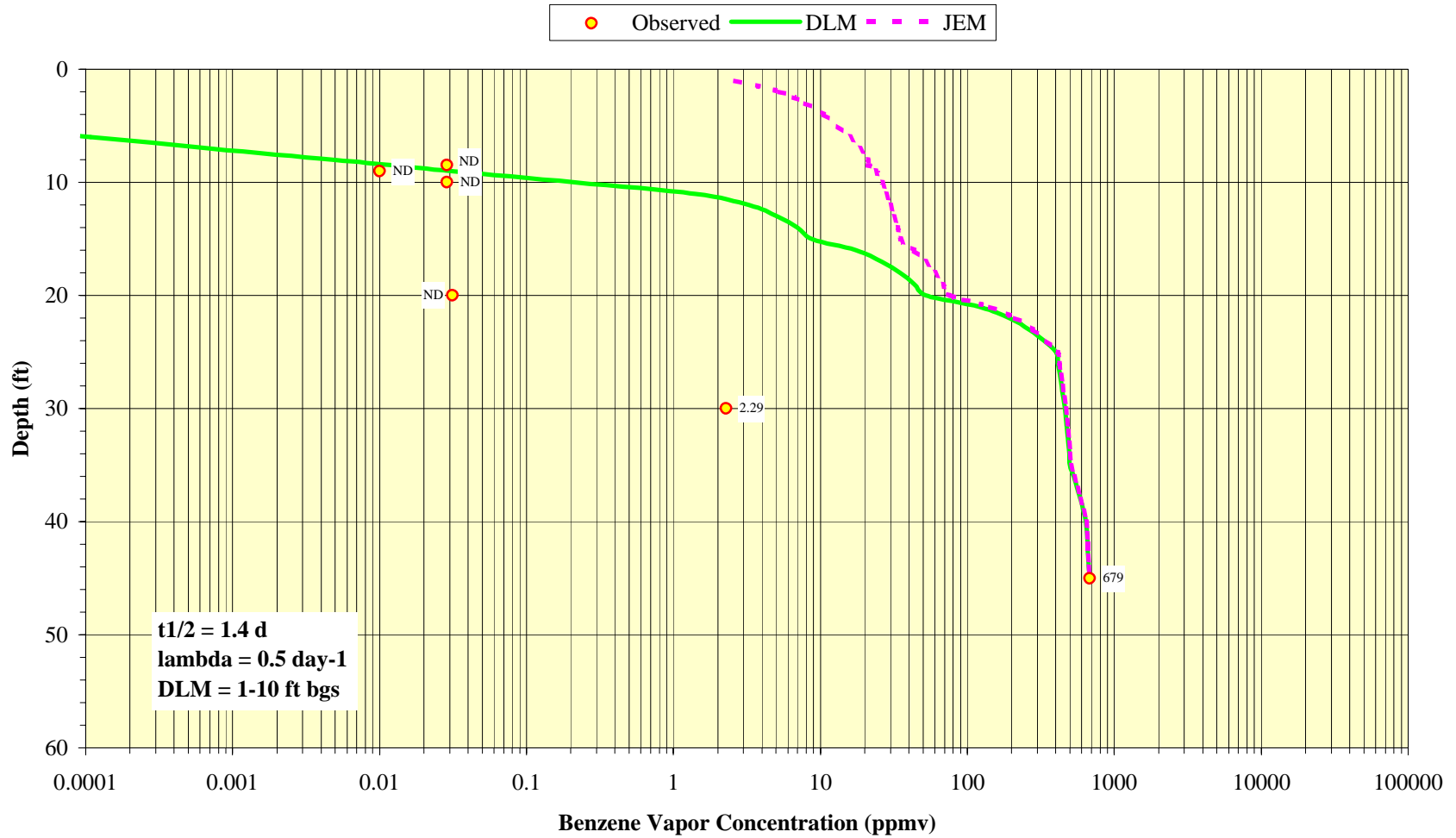


Figure F-6
Waste Pit Area CPT-15 DLM and JEM Results

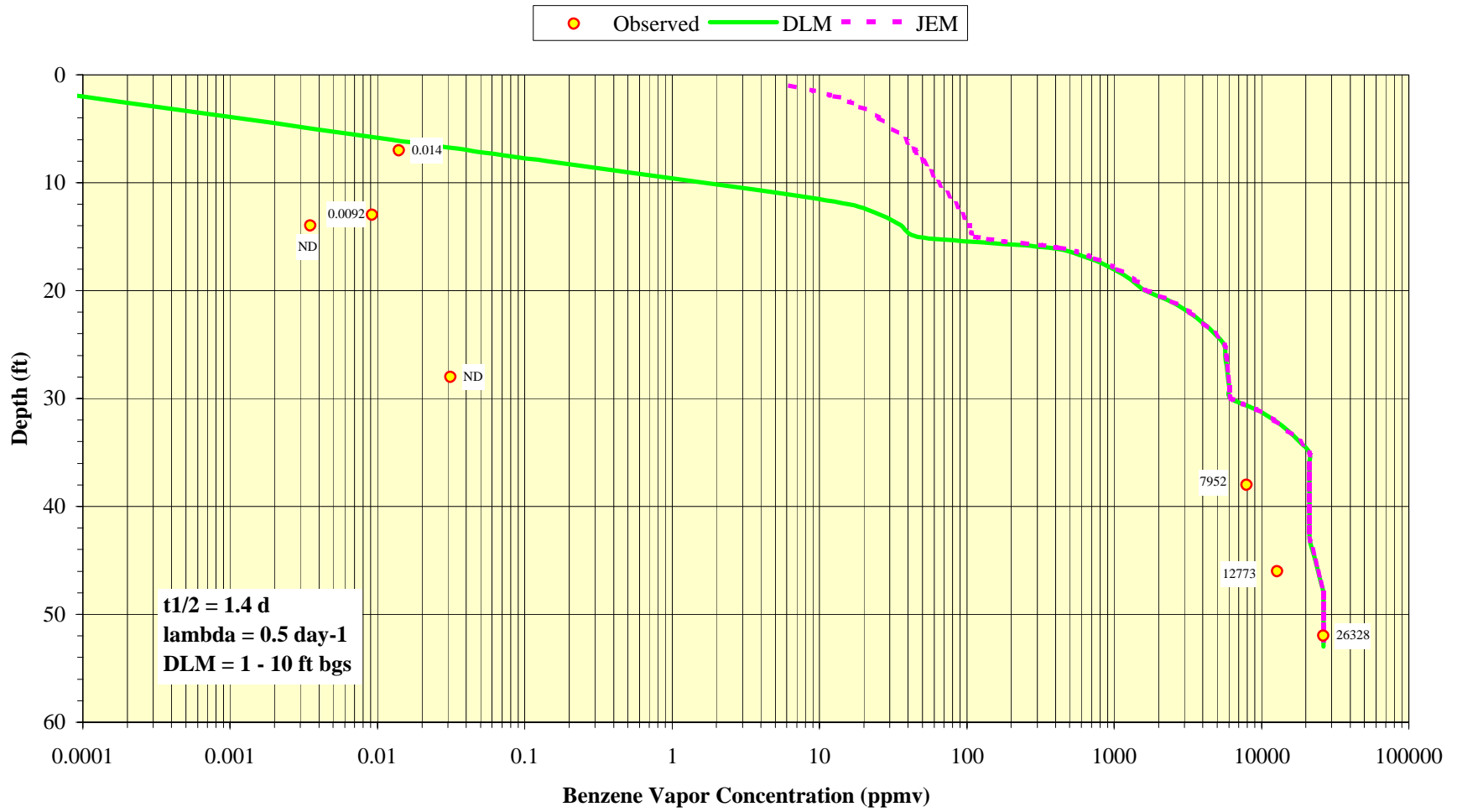


Figure F-7
Waste Pit Area CPT-16 DLM and JEM Results

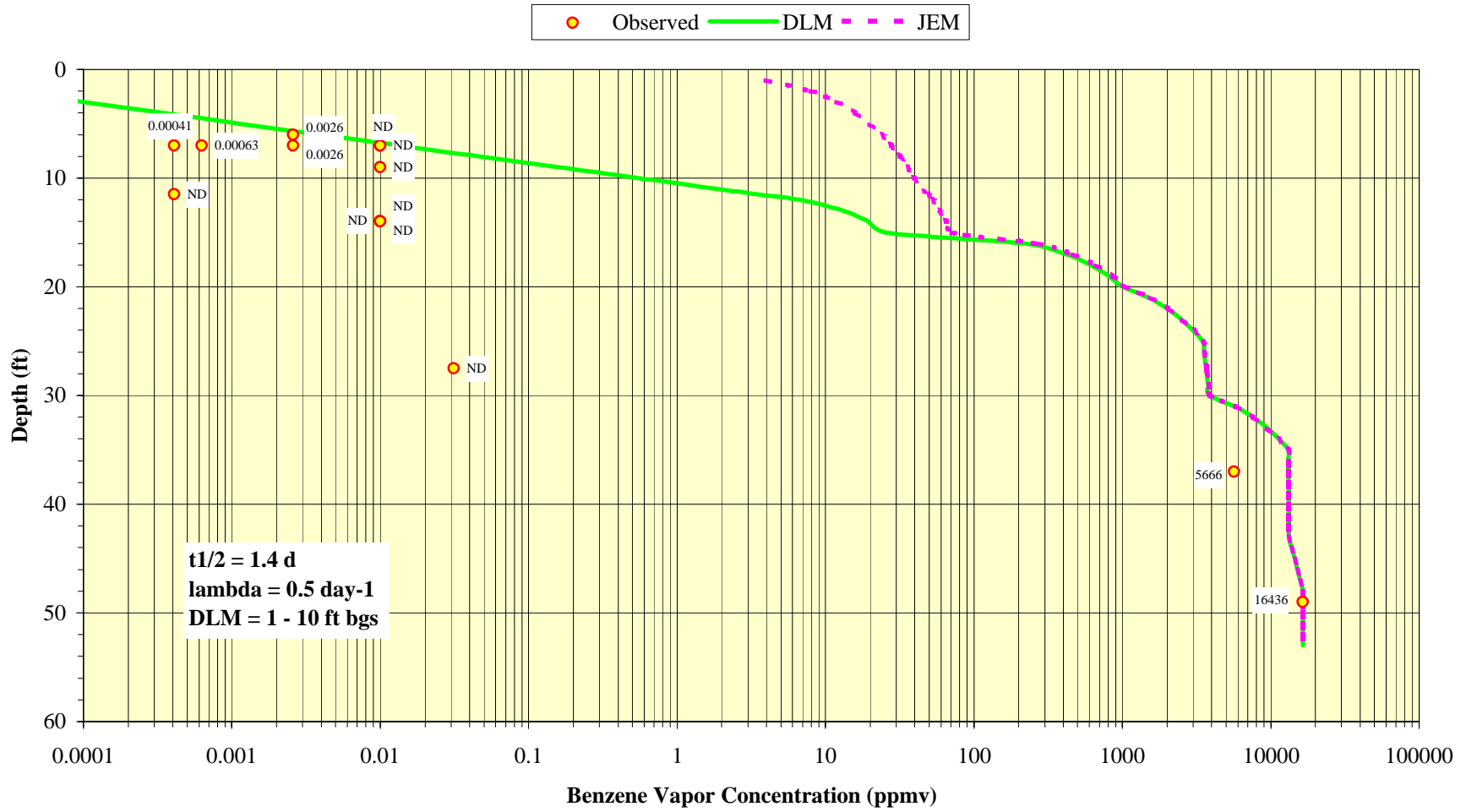


Figure F-8
MW-20 NAPL Area, SGL0028 DLM and JEM Results

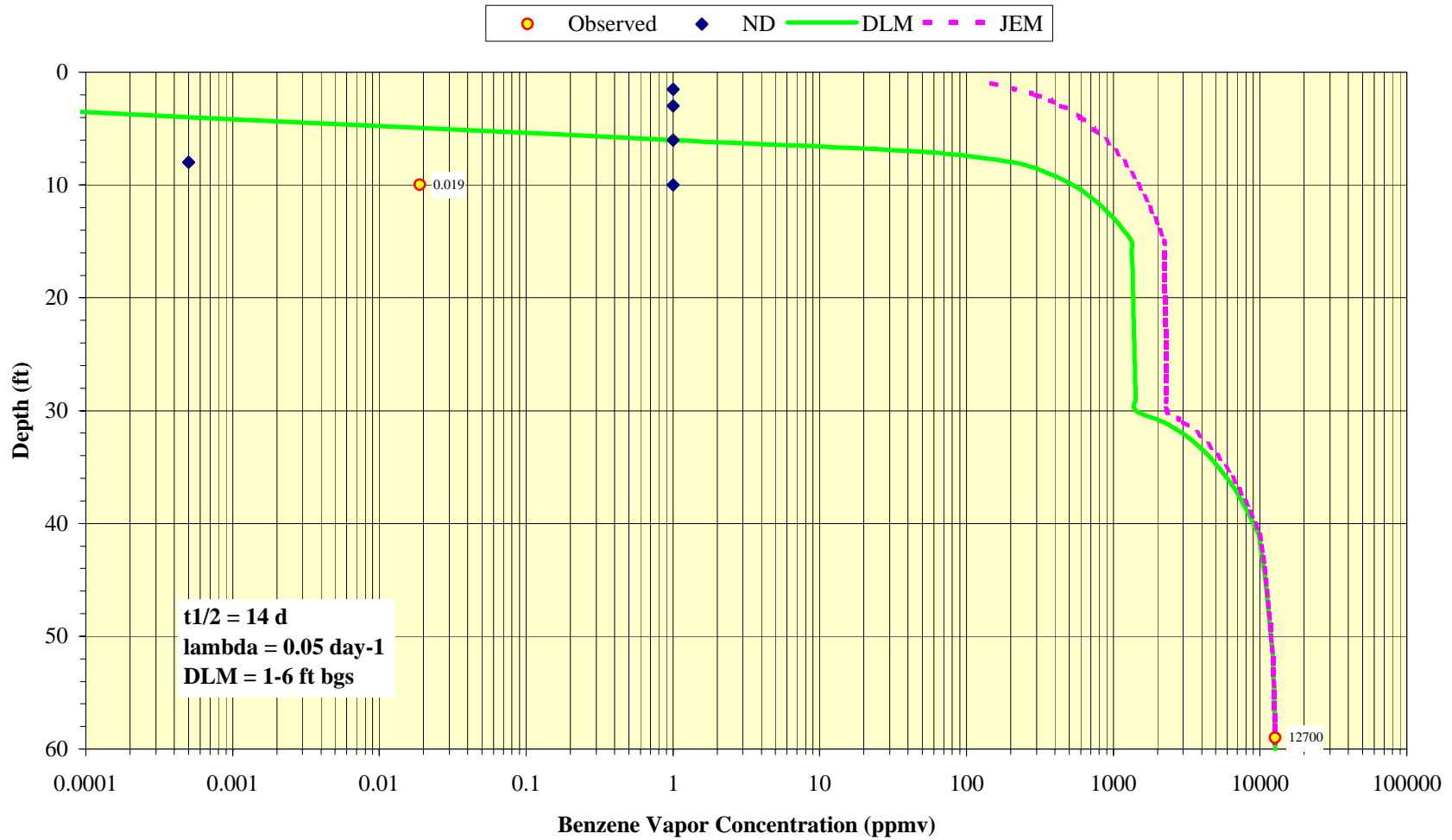


Figure F-9
MW-20 NAPL Area, SGL0033 DLM and JEM Results

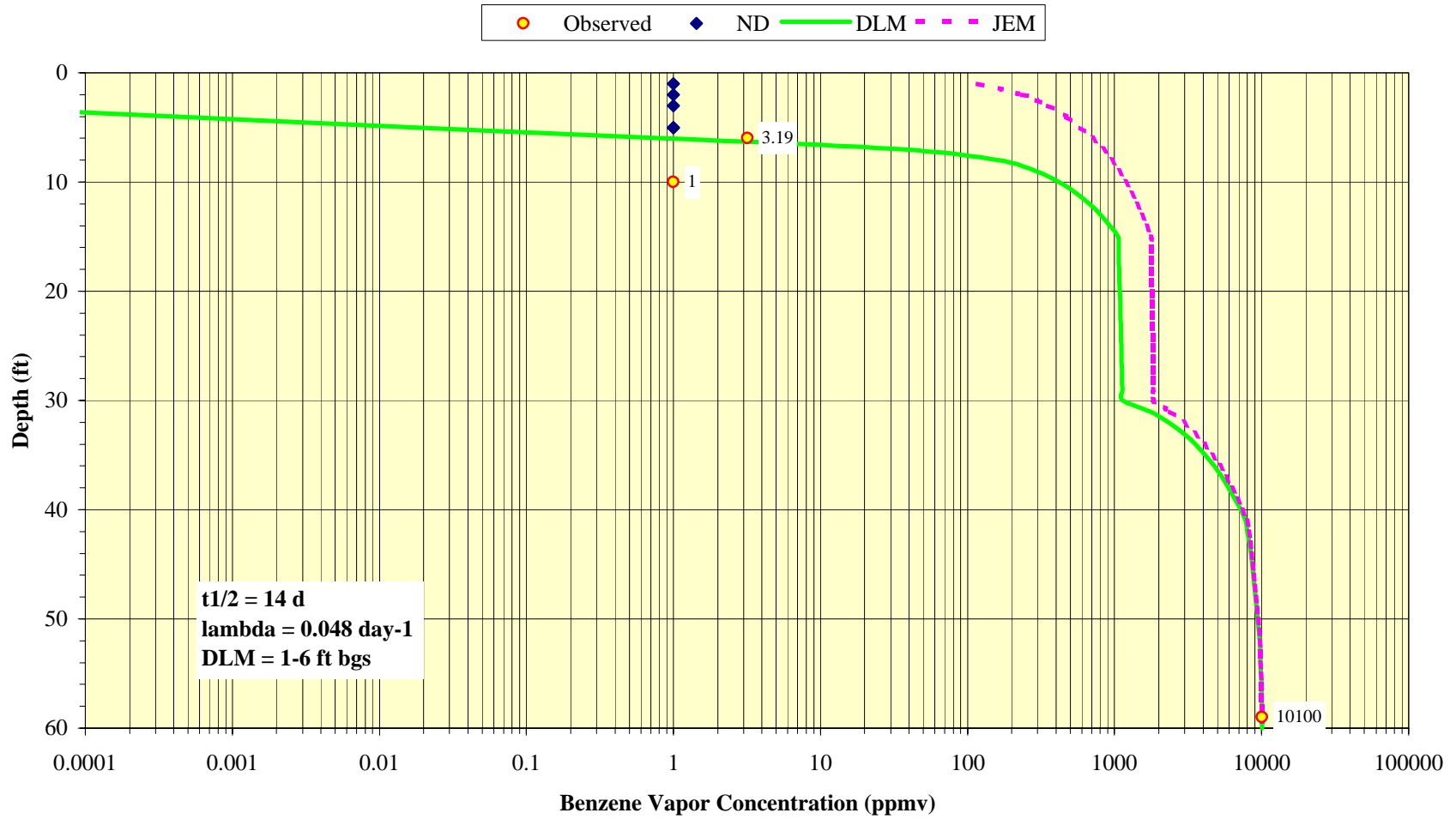


Figure F-10
MW-20 NAPL Area, SGL0035 DLM and JEM Results

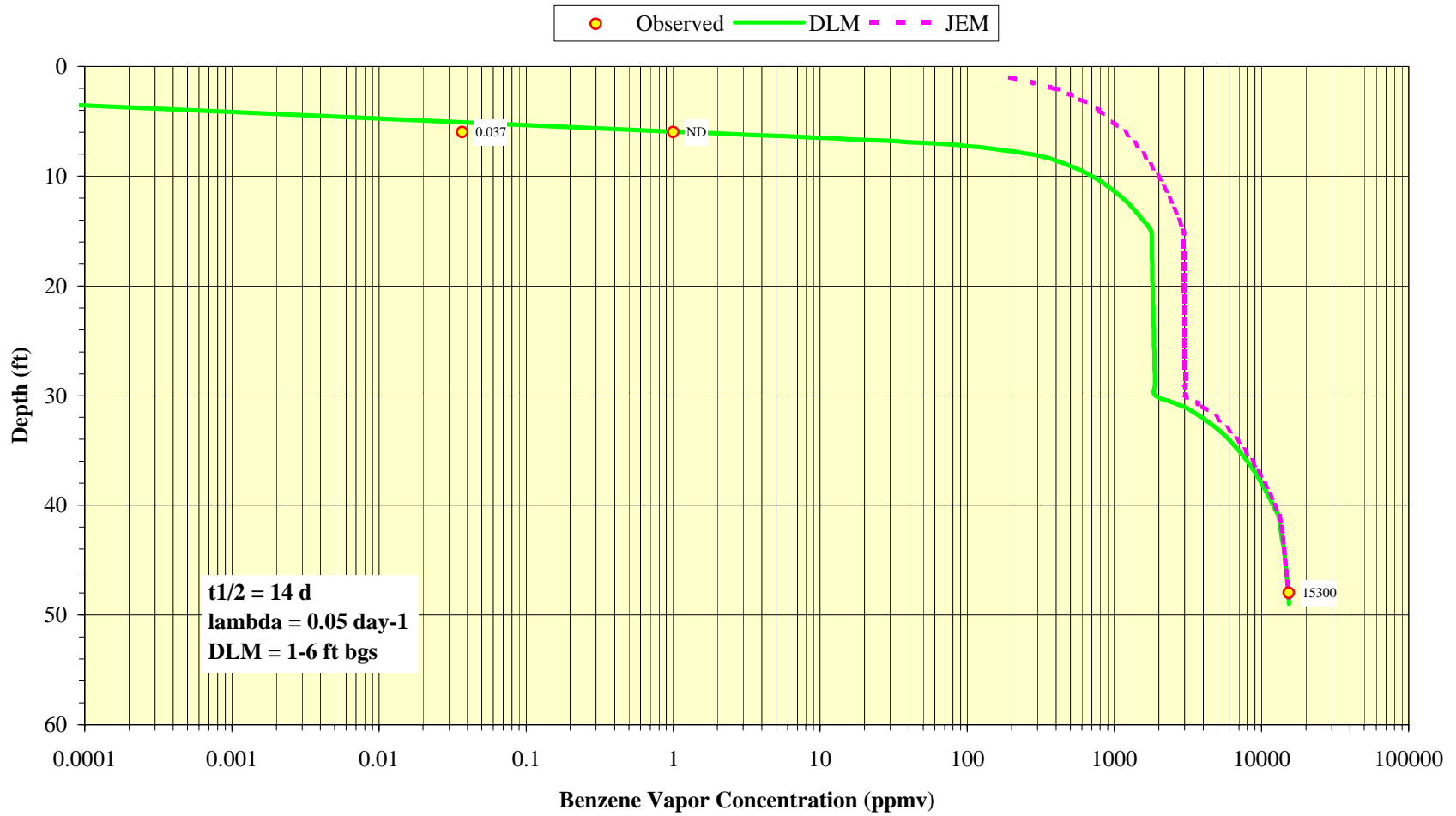


Figure F-11
MW-20 NAPL Area, SGL0044 DLM and JEM Results

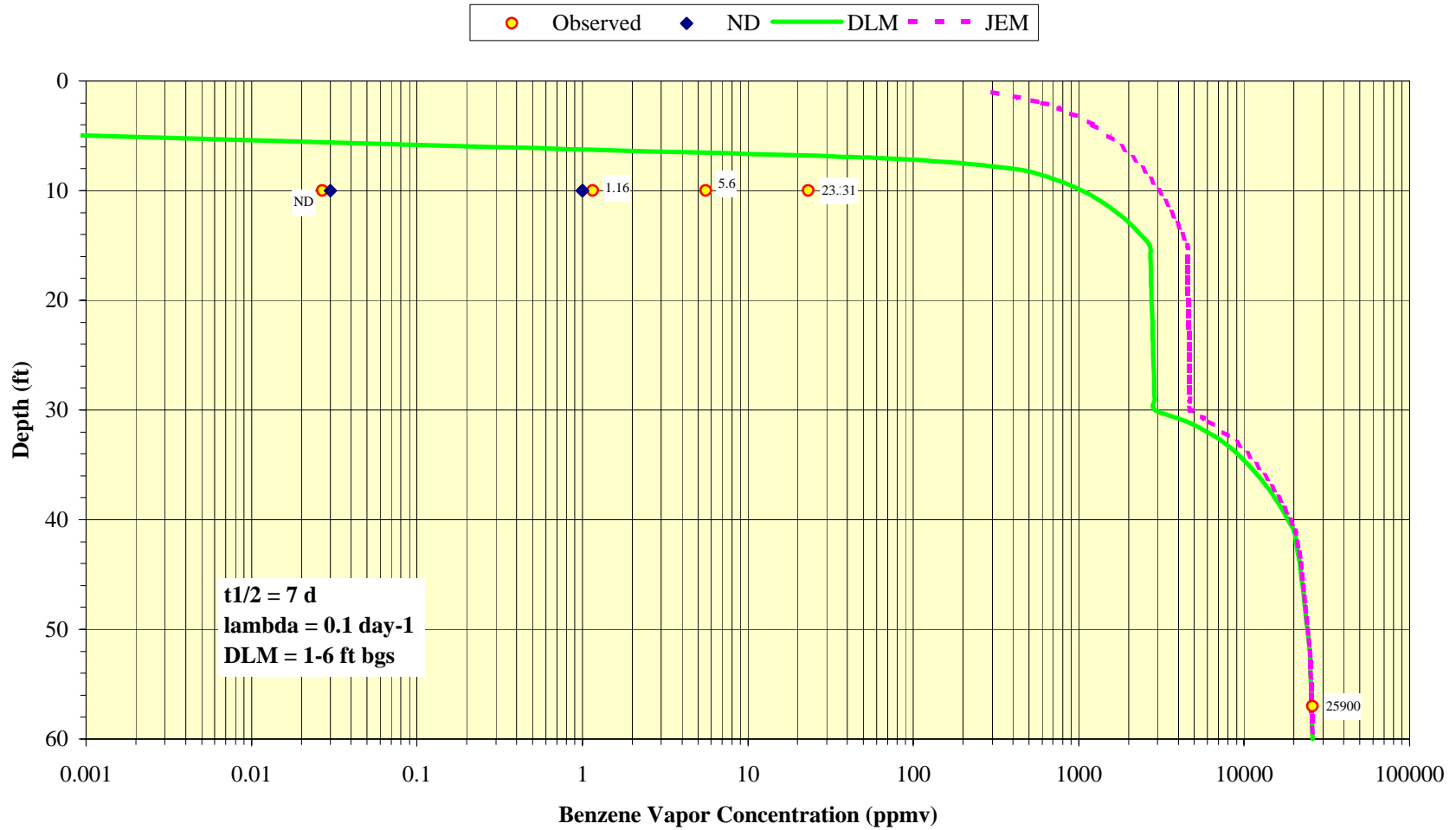


FIGURE F-12
Benzene Pipeline Area, SG-01 DLM and JEM Results

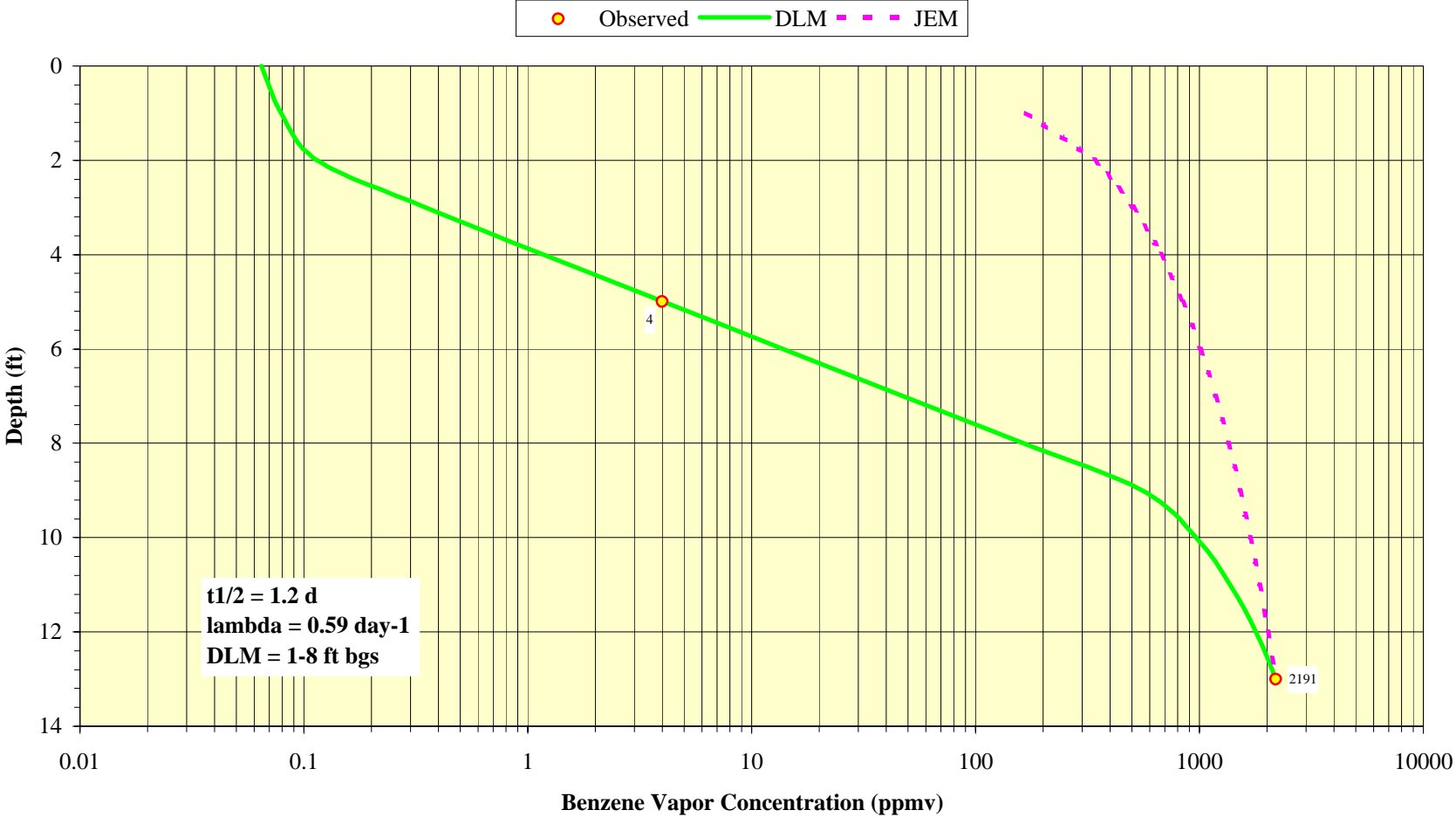


FIGURE F-13
Benzene Pipeline Area, SG-02 DLM and JEM Results

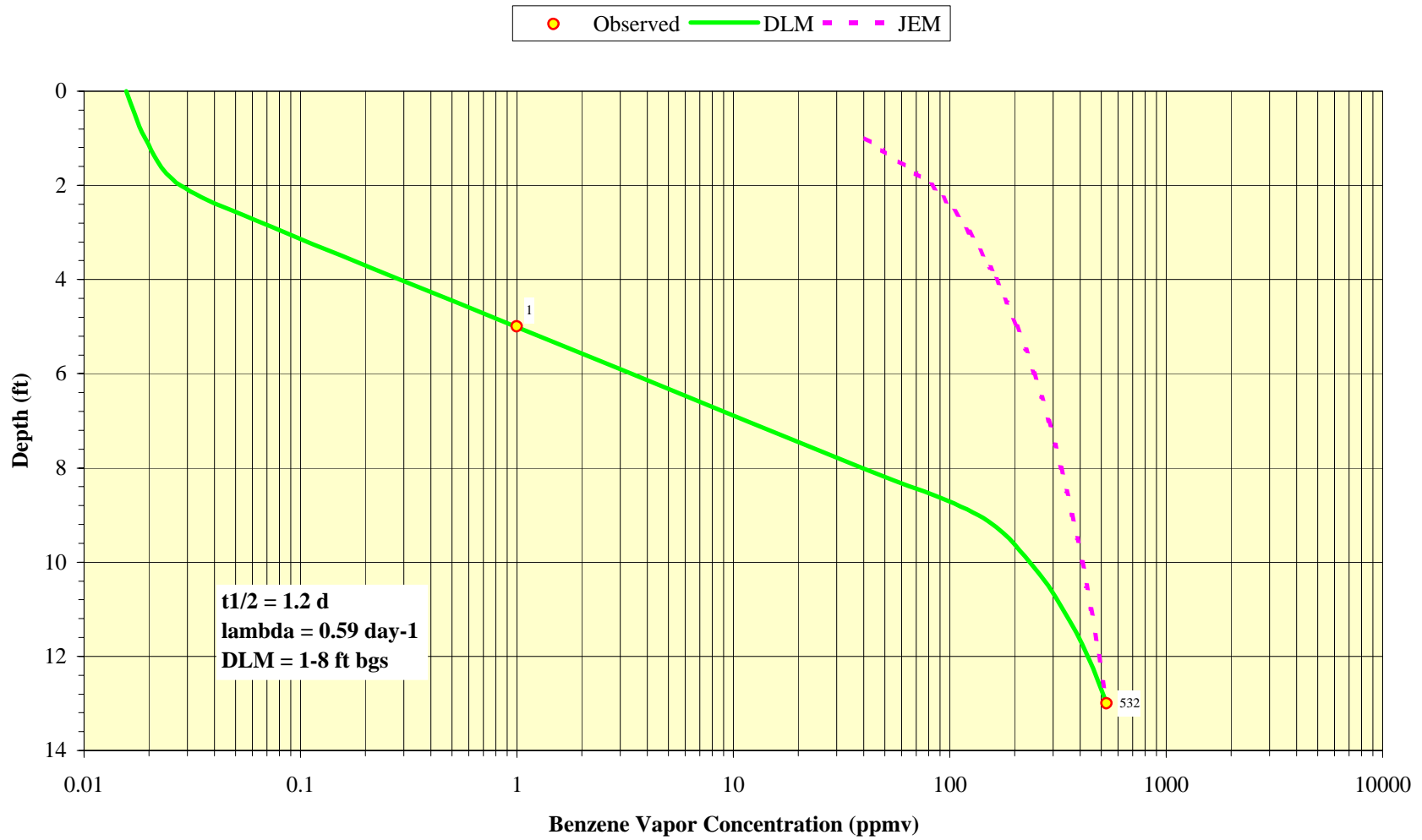


FIGURE F-14
Benzene Pipeline Area, SG-04 DLM and JEM Results

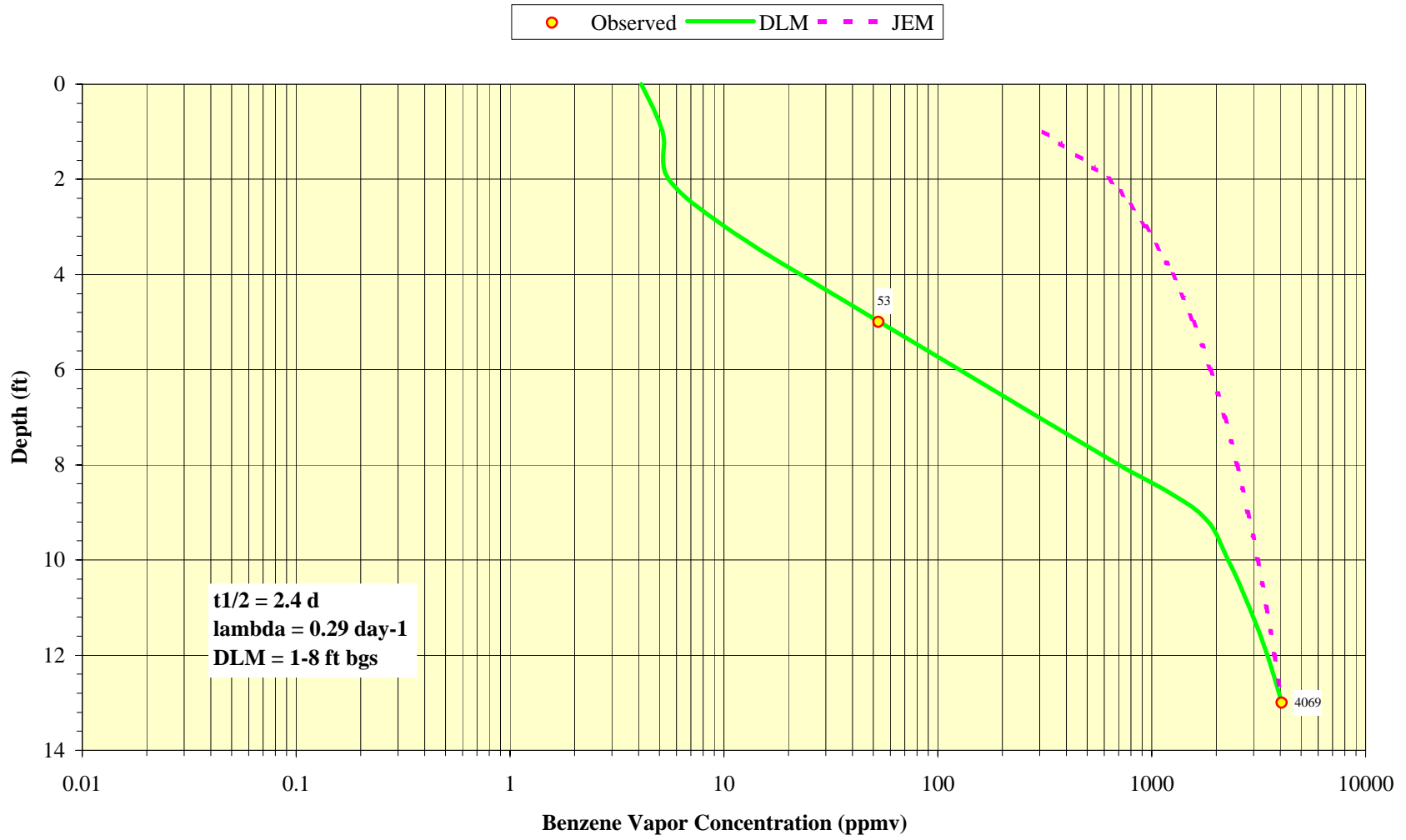


FIGURE F-15
Benzene Pipeline Area, SG-22 DLM and JEM Results

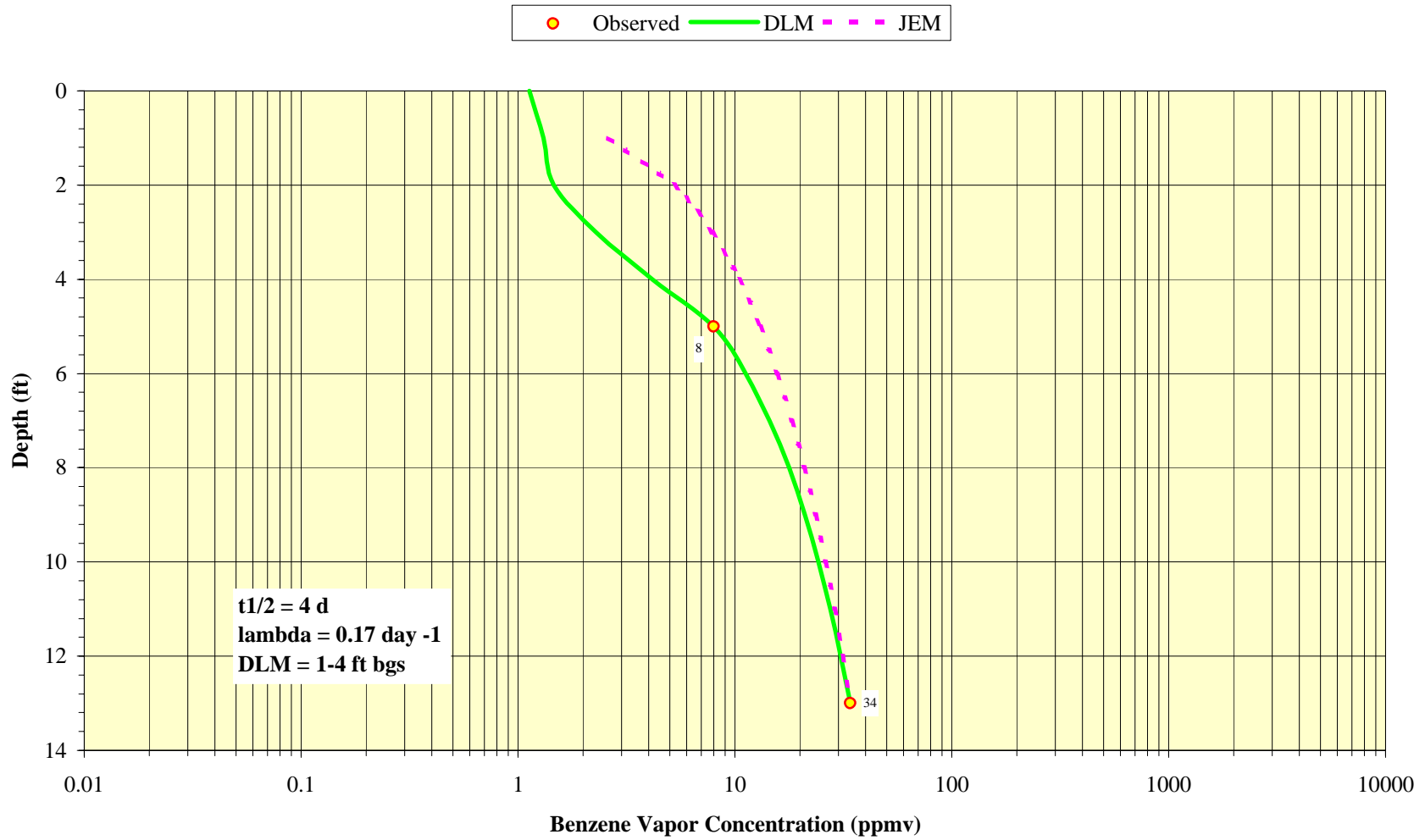
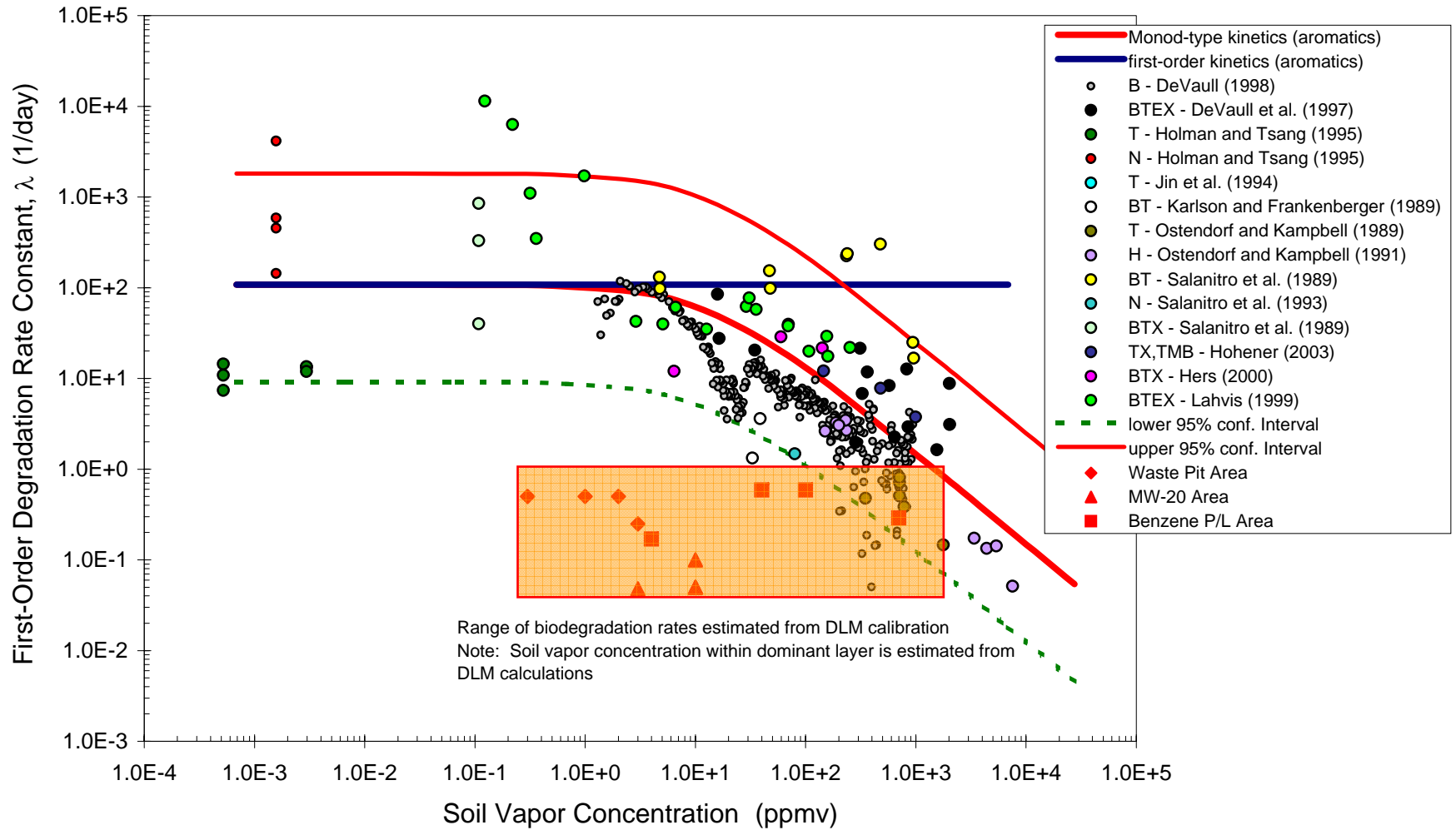


Figure F-16
BTEX Degradation Rate Constants from Site Data Evaluation





EXPLANATION

- Depth Ranges**
- => 0' and <= 10'
 - (blue) > 10' and <= 15'
 - (purple) > 15' and <= 45'
 - (pink) > 45'
-  Current building footprint.
-  Former rubber plant facilities and features evaluated as part of the RI.

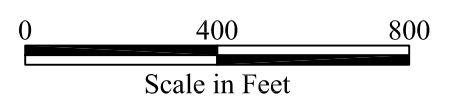
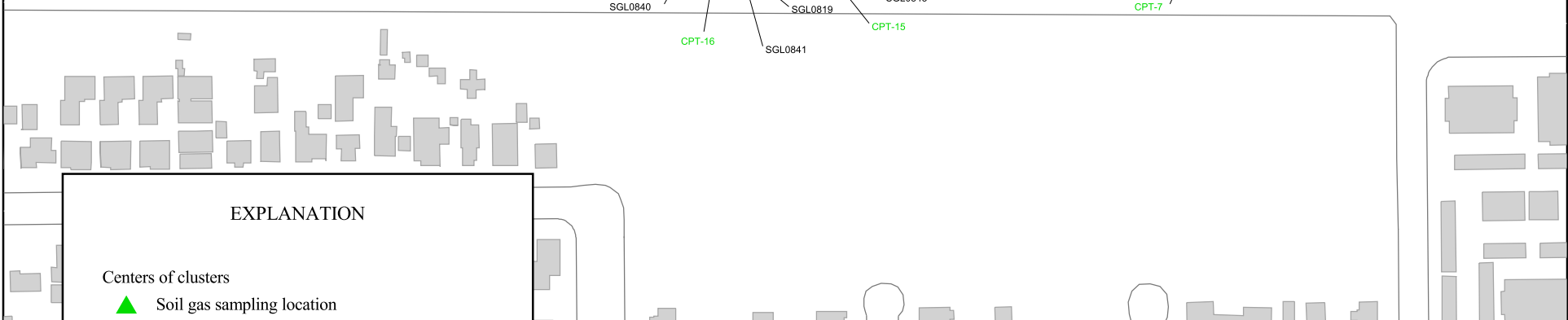
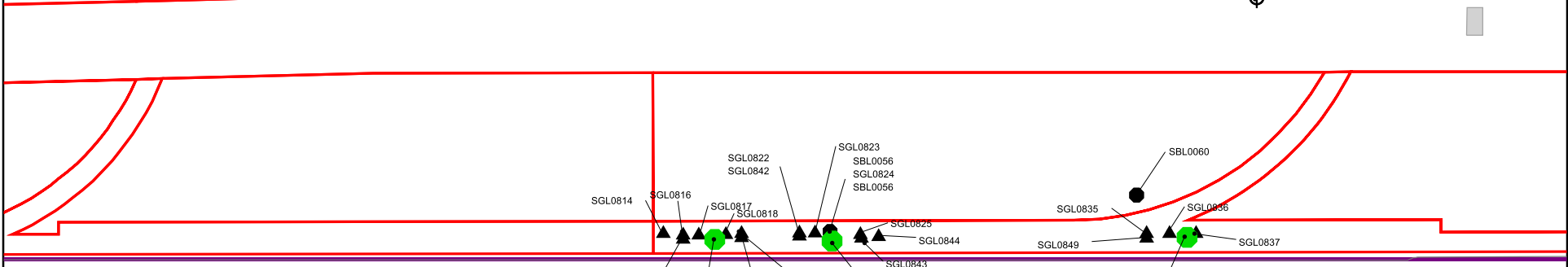
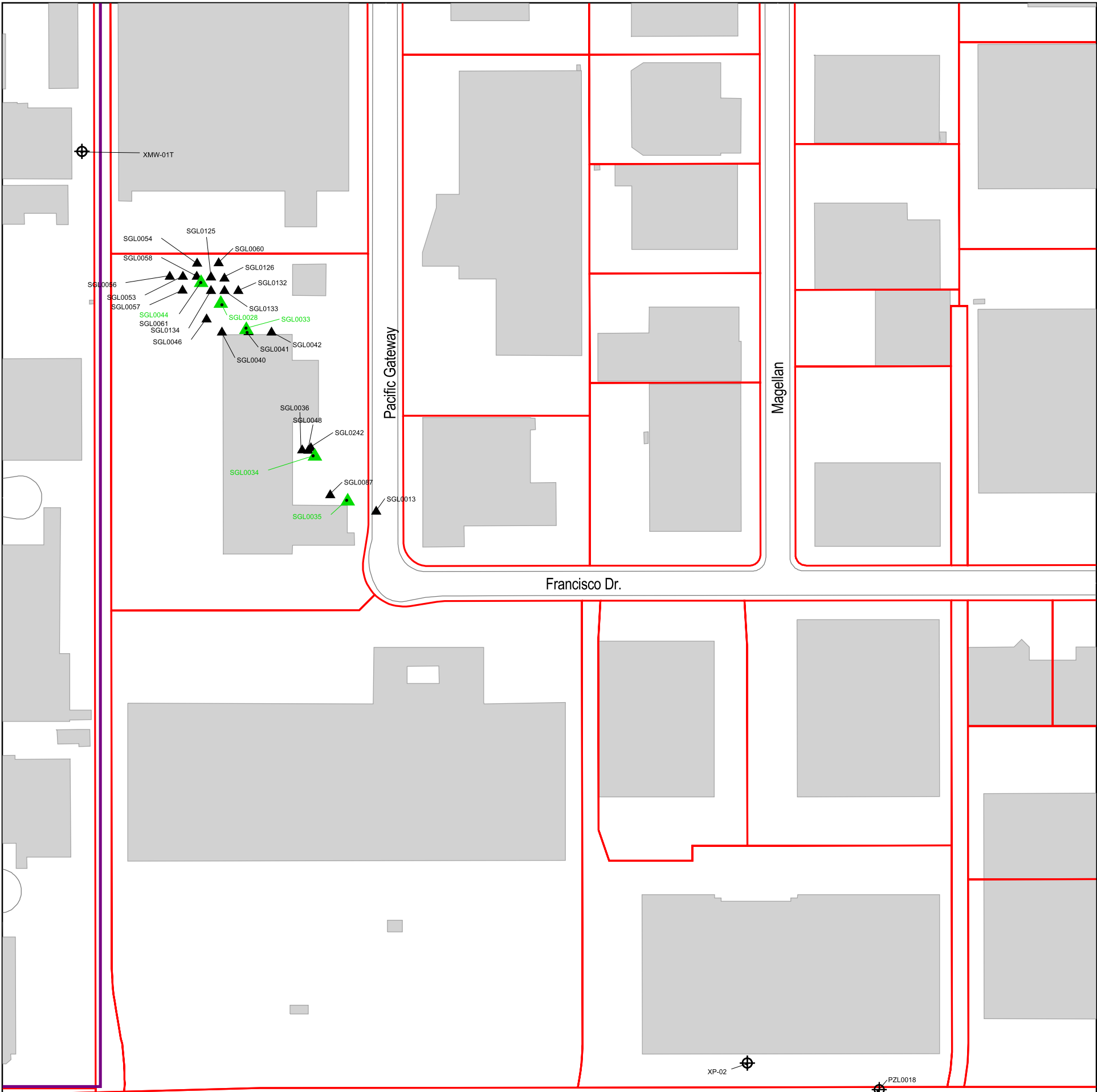


FIGURE F-17
TCE & PCE SOIL GAS SAMPLING LOCATIONS
 Baseline Risk Assessment
 Del Amo Superfund Site





EXPLANATION

- Centers of clusters
 - ▲ Soil gas sampling location
 - Boring location
- Sampling locations
 - ▲ Soil gas
 - boring
 - ⊕ well
- Streets
 - Streets
- Del Amo Site Area boundary
 - ▭ Del Amo Site Area boundary
- Parcel line
 - ▭ Parcel line
- Current building footprint
 - ▭ Current building footprint

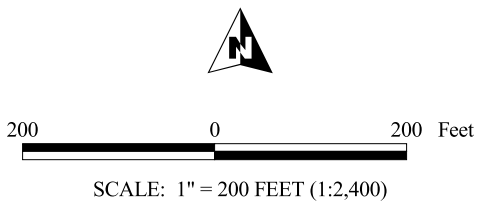


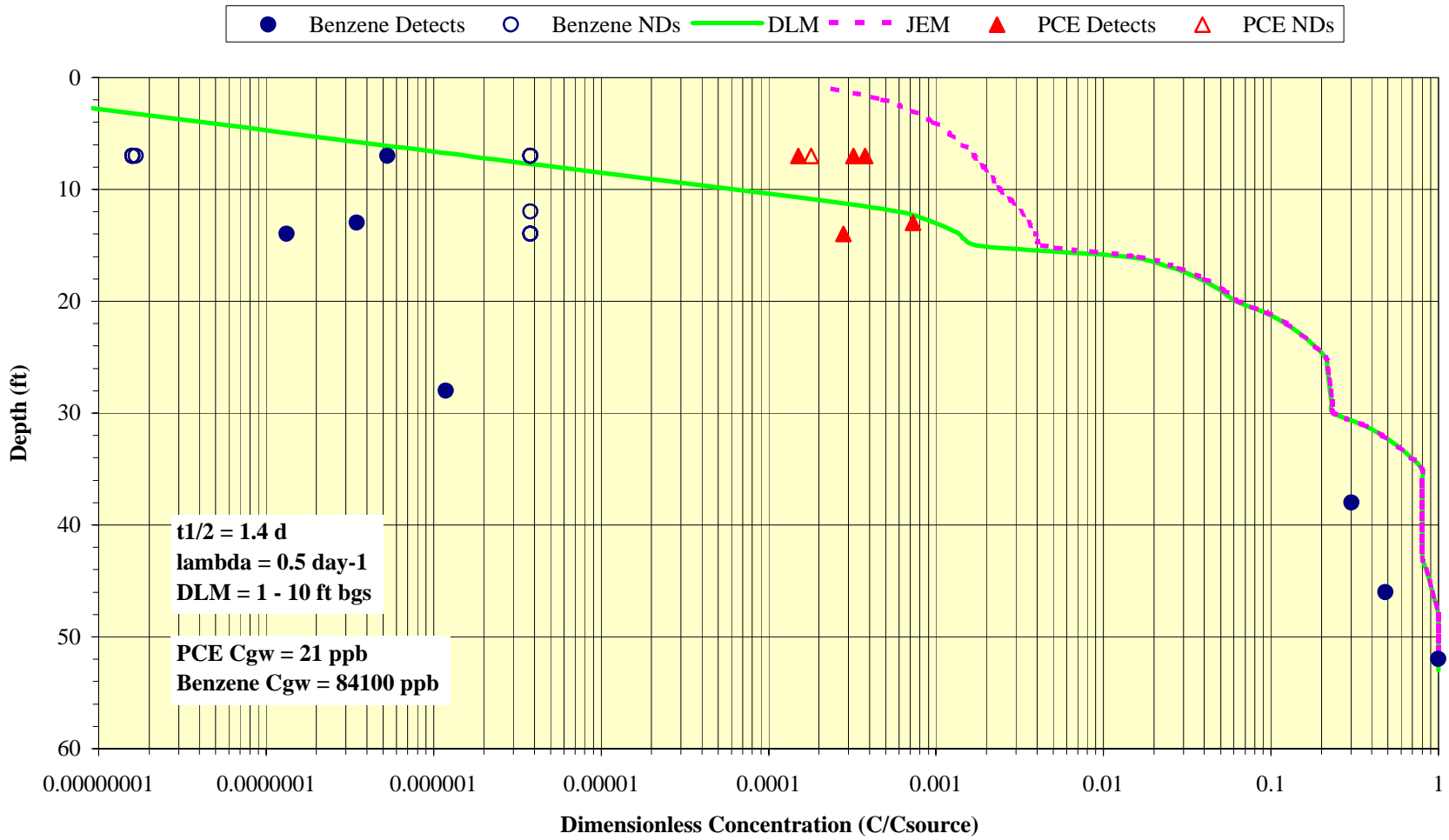
Figure F-18

SAMPLING POINT CLUSTERS

Baseline Risk Assessment
Del Amo Superfund Site



Figure F-20
Waste Pit Area CPT-15 Benzene and PCE Comparison



ATTACHMENT F-1

EXAMPLE DLM SPREADSHEET CALCULATIONS

Attachment F-1
Example DLM Spreadsheet Calculations

**Dominant Layer Model Input Parameters
Commercial Scenario**

Parameter	Value	Units	Note
CAS No.	71432		
Chemical Name	Benzene		
Chemical Properties			
Dair	8.80E-02	cm ² /s	
	7.60E-01	m ² /d	
Dwater	9.80E-06	cm ² /s	
	8.47E-05	m ² /d	
Hi	1.67E-01	-	Temp Corrected H'
MW	7.81E+01	g/mol	
Physical Properties			
μ	1.78E-04	g/cm/s	
Building Parameters			
ΔP	40	g/cm/s ²	
Zcrk	1.50E-01	m	
Xcrk	3.40E+01	m	
rcrk	0.005	m	
AB	1.65E+03	m ²	
η	1.02E-04	-	
ER	2.16E+01	1/d	
Lb	3.05	m	
Qb	1.08E+05	m ³ /d	
Lcrk	0.1	m	
Dcrk	5.48E-03	m ² /d	
Constant Soil Parameters			
kv	1.00E-12	m ²	
Qsoil	1.33E-03	m ³ /s	80 L/min
Qsoil	1.15E+02	m ³ /d	
Dimensionless Groups			
QsLcrk/DcrkAcrk	1.25E+04	-	
Qs/Qb	1.06E-03	-	

Attachment F-1
Example DLM Spreadsheet Calculations

Dominant Layer Model Simaiton
Commercial Scenario. Deep Source. Benzene

Parameter	Value	Units	Remark
λ	2.00E-03	hr-1	
	4.8E-02	day-1	
t1/2	3.47E+02	hr	
	1.44E+01	day	
L1	7.01	m	23.0 ft
L2	8.84	m	29.0 ft
L3	8.99	m	29.5 ft
Deff	9.21E-03	m ² /d	1.07E-03 cm ² /s
D1eff	1.47E-02	m ² /d	1.71E-03 cm ² /s
D2eff	5.48E-03	m ² /d	6.35E-04 cm ² /s
D3eff	5.48E-03	m ² /d	6.35E-04 cm ² /s
θ 2m	0.25	-	Region 2 Avg
η	6.66		API 4674 Eq. 15
α DLM	4.04E-08		Eq. 16 modified for high QsoilxLcrk/(DcrkxAcrk)
Bio atten fac	3.79E+02		(α JEM) / (α DLM)
β'	0.00E+00		Eq. 17 modified for high QsoilxLcrk/(DcrkxAcrk)
γ	-8.19E+01		Eq. 18
σ	-1.40E+03		Eq. 19
ψ	1.16E-03		Eq. 20
ϕ	-2.72E-02		Eq. 21
C1	1.00E+00		Csource - Set to 1 to show relative concentrations
C2	9.53E-02		Eq. 24
C3	1.12E-04		Eq. 23
C4 alternate	3.80E-05		Eq. 22 modified for high QsoilxLcrk/(DcrkxAcrk)

JEM Calcs	
Deff Ab/Qbldg/LT	1.55E-05
Qs Lc/Dc/Ac	1.25E+04
Qs/Qb	1.06E-03
α JEM	1.53E-05

Region	Depth (ft)	z (m)	n	θ v	θ m	Deff (m ² /d)	L(i) (m)	L(i)/D(i) (d/m)	DLM Update		JEM
									C/Csource	C/Csource	C/Csource
3	0.5	8.99	0.3794	0.127	0.253	5.48E-03	0.1524	2.78E+01	3.80E-05	0.00E+00	
2	1	8.84	0.379	0.127	0.253	5.48E-03	0.3048	5.56E+01	1.12E-04	2.85E-02	
2	2	8.53	0.379	0.127	0.253	5.48E-03	0.3048	5.56E+01	3.68E-04	8.54E-02	
2	3	8.23	0.379	0.127	0.253	5.48E-03	0.3048	5.56E+01	1.13E-03	1.42E-01	
2	4	7.92	0.379	0.127	0.253	5.48E-03	0.3048	5.56E+01	3.42E-03	1.99E-01	
2	5	7.62	0.379	0.127	0.253	5.48E-03	0.3048	5.56E+01	1.04E-02	2.56E-01	
2	6	7.32	0.379	0.127	0.253	5.48E-03	0.3048	5.56E+01	3.14E-02	3.13E-01	
1	7	7.01	0.379	0.127	0.253	5.48E-03	0.3048	5.56E+01	9.53E-02	3.70E-01	
1	8	6.71	0.379	0.127	0.253	5.48E-03	0.3048	5.56E+01	1.35E-01	4.27E-01	
1	9	6.40	0.379	0.127	0.253	5.48E-03	0.3048	5.56E+01	1.74E-01	4.84E-01	
1	10	6.10	0.379	0.127	0.253	5.48E-03	0.3048	5.56E+01	2.13E-01	5.41E-01	
1	11	5.79	0.379	0.127	0.253	5.48E-03	0.3048	5.56E+01	2.53E-01	5.98E-01	
1	12	5.49	0.379	0.127	0.253	5.48E-03	0.3048	5.56E+01	2.92E-01	6.55E-01	
1	13	5.18	0.379	0.127	0.253	5.48E-03	0.3048	5.56E+01	3.31E-01	7.11E-01	
1	14	4.88	0.379	0.127	0.253	5.48E-03	0.3048	5.56E+01	3.71E-01	7.68E-01	
1	15	4.57	0.379	0.127	0.253	5.48E-03	0.3048	5.56E+01	4.10E-01	8.25E-01	
1	16	4.27	0.414	0.238	0.176	3.71E-02	0.3048	8.21E+00	4.49E-01	8.82E-01	
1	17	3.96	0.414	0.238	0.176	3.71E-02	0.3048	8.21E+00	4.89E-01	8.91E-01	
1	18	3.66	0.414	0.238	0.176	3.71E-02	0.3048	8.21E+00	5.28E-01	8.99E-01	
1	19	3.35	0.414	0.238	0.176	3.71E-02	0.3048	8.21E+00	5.67E-01	9.07E-01	
1	20	3.05	0.414	0.238	0.176	3.71E-02	0.3048	8.21E+00	6.07E-01	9.16E-01	
1	21	2.74	0.414	0.238	0.176	3.71E-02	0.3048	8.21E+00	6.46E-01	9.24E-01	
1	22	2.44	0.414	0.238	0.176	3.71E-02	0.3048	8.21E+00	6.85E-01	9.33E-01	
1	23	2.13	0.414	0.238	0.176	3.71E-02	0.3048	8.21E+00	7.25E-01	9.41E-01	
1	24	1.83	0.414	0.238	0.176	3.71E-02	0.3048	8.21E+00	7.64E-01	9.50E-01	
1	25	1.52	0.414	0.238	0.176	3.71E-02	0.3048	8.21E+00	8.03E-01	9.58E-01	
1	26	1.22	0.414	0.238	0.176	3.71E-02	0.3048	8.21E+00	8.43E-01	9.66E-01	
1	27	0.91	0.414	0.238	0.176	3.71E-02	0.3048	8.21E+00	8.82E-01	9.75E-01	
1	28	0.61	0.414	0.238	0.176	3.71E-02	0.3048	8.21E+00	9.21E-01	9.83E-01	
1	29	0.30	0.414	0.238	0.176	3.71E-02	0.1524	4.11E+00	9.61E-01	9.92E-01	
1	29.5	0.15	0.414	0.238	0.176	3.71E-02	0.1524	4.11E+00	9.80E-01	9.96E-01	
1	30	0.00	0.414	0.238	0.176				1.00E+00	1.00E+00	

Attachment F-1
Example DLM Spreadsheet Calculations

Dominant Layer Model Simulaiton
Commercial Scenario. Shallow Source. Benzene

Parameter	Value	Units	Remark
λ	2.00E-03	hr-1	
	4.8E-02	day-1	
t1/2	3.47E+02	hr	
	1.44E+01	day	
L1	0.46	m	1.50 ft
L2	1.98	m	6.50 ft
L3	2.13	m	7.00 ft
Deff	5.48E-03	m^2/d	6.35E-04 6.35E-04
D1eff	5.48E-03	m^2/d	
D2eff	5.48E-03	m^2/d	
D3eff	5.48E-03	m^2/d	
θ_2m	0.25	-	Region 2 Avg
η	5.55		API 4674 Eq. 15
α DLM	4.82E-07		Eq. 16 modified for high QsoilxLcrk/(DcrkxAcrk)
Bio atten factor	7.80E+01		(α JEM) / (α DLM)
β'	0.00E+00		Eq. 17 modified for high QsoilxLcrk/(DcrkxAcrk)
γ	-1.54E+02		Eq. 18
σ	-4.62E+02		Eq. 19
ψ	2.44E-03		Eq. 20
ϕ	-8.24E-02		Eq. 21
C1	1.00E+00		Csource - Set to 1 to show relative concentrations
C2	3.75E-01		Eq. 24
C3	1.34E-03		Eq. 23
C4 alternate	4.54E-04		Eq. 22 modified for high QsoilxLcrk/(DcrkxAcrk)

JEM Calcs	
Deff Ab/Qbldg/LT	3.90E-05
Qs Lc/Dc/Ac	1.25E+04
Qs/Qb	1.06E-03
α JEM	3.76E-05

Region	Depth (ft)	z (m)	n	θ_v	θ_m	Deff (m^2/d)	L(i) (m)	L(i)/D(i) (d/m)	DLM Update		JEM	
									C/Csource	C/Csource	C/Csource	C/Csource
3	0.5	1.98	0.379	0.127	0.253	5.48E-03	0.03048	5.56E+00	1.34E-03	0.00E+00		
3	0.6	1.95	0.379	0.127	0.253	5.48E-03	0.03048	5.56E+00	1.51E-03	1.43E-02		
3	0.7	1.92	0.379	0.127	0.253	5.48E-03	0.01524	2.78E+00	1.69E-03	2.86E-02		
3	0.75	1.91	0.379	0.127	0.253	5.48E-03	0.0762	1.39E+01	1.84E-03	3.57E-02		
2	1	1.83	0.379	0.127	0.253	5.48E-03	0.0762	1.39E+01	2.48E-03	7.14E-02		
2	1.25	1.75	0.379	0.127	0.253	5.48E-03	0.0762	1.39E+01	3.31E-03	1.07E-01		
2	1.5	1.68	0.379	0.127	0.253	5.48E-03	0.0762	1.39E+01	4.40E-03	1.43E-01		
2	1.75	1.60	0.379	0.127	0.253	5.48E-03	0.0762	1.39E+01	5.83E-03	1.79E-01		
2	2	1.52	0.379	0.127	0.253	5.48E-03	0.0762	1.39E+01	7.71E-03	2.14E-01		
2	2.25	1.45	0.379	0.127	0.253	5.48E-03	0.0762	1.39E+01	1.02E-02	2.50E-01		
2	2.5	1.37	0.379	0.127	0.253	5.48E-03	0.0762	1.39E+01	1.35E-02	2.86E-01		
2	2.75	1.30	0.379	0.127	0.253	5.48E-03	0.0762	1.39E+01	1.78E-02	3.21E-01		
2	3	1.22	0.379	0.127	0.253	5.48E-03	0.0762	1.39E+01	2.34E-02	3.57E-01		
2	3.25	1.14	0.379	0.127	0.253	5.48E-03	0.0762	1.39E+01	3.09E-02	3.93E-01		
2	3.5	1.07	0.379	0.127	0.253	5.48E-03	0.0762	1.39E+01	4.08E-02	4.29E-01		
2	3.75	0.99	0.379	0.127	0.253	5.48E-03	0.0762	1.39E+01	5.39E-02	4.64E-01		
2	4	0.91	0.379	0.127	0.253	5.48E-03	0.0762	1.39E+01	7.11E-02	5.00E-01		
2	4.25	0.84	0.379	0.127	0.253	5.48E-03	0.0762	1.39E+01	9.38E-02	5.36E-01		
2	4.5	0.76	0.379	0.127	0.253	5.48E-03	0.0762	1.39E+01	1.24E-01	5.71E-01		
2	4.75	0.69	0.379	0.127	0.253	5.48E-03	0.0762	1.39E+01	1.63E-01	6.07E-01		
2	5	0.61	0.379	0.127	0.253	5.48E-03	0.0762	1.39E+01	2.16E-01	6.43E-01		
2	5.25	0.53	0.379	0.127	0.253	5.48E-03	0.0762	1.39E+01	2.84E-01	6.79E-01		
1	5.5	0.46	0.379	0.127	0.253	5.48E-03	0.0762	1.39E+01	3.75E-01	7.14E-01		
1	5.75	0.38	0.379	0.127	0.253	5.48E-03	0.0762	1.39E+01	4.79E-01	7.50E-01		
1	6	0.30	0.379	0.127	0.253	5.48E-03	0.0762	1.39E+01	5.84E-01	7.86E-01		
1	6.25	0.23	0.379	0.127	0.253	5.48E-03	0.0762	1.39E+01	6.88E-01	8.21E-01		
1	6.5	0.15	0.379	0.127	0.253	5.48E-03	0.0762	1.39E+01	7.92E-01	8.57E-01		
1	6.75	0.08	0.379	0.127	0.253	5.48E-03	0.0762	1.39E+01	8.96E-01	8.93E-01		
1	7	0.00	0.379	0.127	0.253	5.48E-03	0.06096	1.11E+01	1.00E+00	9.29E-01		
1	7.2	-0.06	0.379	0.127	0.253	5.48E-03	0.03048	5.56E+00	1.08E+00	9.57E-01		
1	7.3	-0.09	0.379	0.127	0.253	5.48E-03	0.06096	1.11E+01	1.12E+00	9.71E-01		
1	7.5	-0.15	0.379	0.127	0.253	5.48E-03	0.06096	1.11E+01	1.00E+00	1.00E+00		

Attachment F-1
Example DLM Spreadsheet Calculations

**Dominant Layer Model Input Parameters
Residential Scenario**

Parameter	Value	Units	Note
CAS No.	71432		
Chemical Name	Benzene		
Chemical Properties			
Dair	8.80E-02	cm ² /s	
	7.60E-01	m ² /d	
Dwater	9.80E-06	cm ² /s	
	8.47E-05	m ² /d	
Hi	1.67E-01	-	Temp Corrected H'
MW	7.81E+01	g/mol	
Physical Properties			
μ	1.80E-04	g/cm/s	
Building Parameters			
ΔP	40	g/cm/s ²	
Zcrk	1.50E-01	m	
Xcrk	3.40E+01	m	
rcrk	0.001	m	
AB	100	m ²	
η	3.77E-04	-	
ER	1.20E+01	1/d	
Lb	2.44	m	
Qb	2.93E+03	m ³ /d	
Lcrk	0.1	m	
Dcrk	5.45E-03	m ² /d	
Constant Soil Parameters			
kv	1.00E-12	m ²	
Qsoil	8.33E-05	m ³ /s	5 L/min
Qsoil	7.20E+00	m ³ /d	
Dimensionless Groups			
QsLcrk/DcrkAcrk	3.51E+03	-	
Qs/Qb	2.46E-03	-	

Attachment F-1
Example DLM Spreadsheet Calculations

**Dominant Layer Model Simulaiton
Residential Scenario. Deep Source. Benzene**

		Remark
λ	2.00E-03 hr-1	
	4.8E-02 day-1	
t1/2	3.47E+02 hr	
	1.44E+01 day	
L1	7.01 m	23.0 ft
L2	8.84 m	29.0 ft
L3	8.99 m	29.5 ft
Deff	9.15E-03 m ² /d	1.06E-03
D1eff	1.46E-02 m ² /d	1.70E-03
D2eff	5.45E-03 m ² /d	6.30E-04
D3eff	5.45E-03 m ² /d	6.30E-04
θ_2m	0.25 -	Region 2 Avg
η	6.68	API 4674 Eq. 15
α DLM	8.82E-08	Eq. 16 modified for high QsoilLcrk/(DcrkxAcrk)
Bio atten factor	3.88E+02	(α JEM) / (α DLM)
β'	0.00E+00	Eq. 17 modified for high QsoilLcrk/(DcrkxAcrk)
γ	-8.38E+01	Eq. 18
σ	-1.43E+03	Eq. 19
ψ	1.13E-03	Eq. 20
ϕ	-1.60E-03	Eq. 21
C1	1.00E+00	Csource - Set to 1 to show relative concentrations
C2	9.50E-02	Eq. 24
C3	8.68E-05	Eq. 23
C4 alternate	2.61E-06	Eq. 22 modified for high QsoilLcrk/(DcrkxAcrk)

JEM Calcs	
Deff Ab/Qbldg/LT	3.47E-05
Qs Lc/Dc/Ac	3.51E+03
Qs/Qb	2.46E-03
α JEM	3.43E-05

Region	Depth (ft)	z (m)	n	θ_v	θ_m	Deff (m ² /d)	L(i) (m)	L(i)/D(i) (d/m)	DLM Update		JEM
									C/Csource	C/Csource	
3	0.5	8.99	0.379	0.127	0.253	5.45E-03	0.1524	2.80E+01	2.61E-06	0.00E+00	
2	1	8.84	0.379	0.127	0.253	5.45E-03	0.3048	5.60E+01	8.68E-05	2.85E-02	
2	2	8.53	0.379	0.127	0.253	5.45E-03	0.3048	5.60E+01	3.52E-04	8.54E-02	
2	3	8.23	0.379	0.127	0.253	5.45E-03	0.3048	5.60E+01	1.10E-03	1.42E-01	
2	4	7.92	0.379	0.127	0.253	5.45E-03	0.3048	5.60E+01	3.36E-03	1.99E-01	
2	5	7.62	0.379	0.127	0.253	5.45E-03	0.3048	5.60E+01	1.02E-02	2.56E-01	
2	6	7.32	0.379	0.127	0.253	5.45E-03	0.3048	5.60E+01	3.12E-02	3.13E-01	
1	7	7.01	0.379	0.127	0.253	5.45E-03	0.3048	5.60E+01	9.50E-02	3.70E-01	
1	8	6.71	0.379	0.127	0.253	5.45E-03	0.3048	5.60E+01	1.34E-01	4.27E-01	
1	9	6.40	0.379	0.127	0.253	5.45E-03	0.3048	5.60E+01	1.74E-01	4.84E-01	
1	10	6.10	0.379	0.127	0.253	5.45E-03	0.3048	5.60E+01	2.13E-01	5.41E-01	
1	11	5.79	0.379	0.127	0.253	5.45E-03	0.3048	5.60E+01	2.52E-01	5.98E-01	
1	12	5.49	0.379	0.127	0.253	5.45E-03	0.3048	5.60E+01	2.92E-01	6.55E-01	
1	13	5.18	0.379	0.127	0.253	5.45E-03	0.3048	5.60E+01	3.31E-01	7.12E-01	
1	14	4.88	0.379	0.127	0.253	5.45E-03	0.3048	5.60E+01	3.70E-01	7.69E-01	
1	15	4.57	0.379	0.127	0.253	5.45E-03	0.3048	5.60E+01	4.10E-01	8.26E-01	
1	16	4.27	0.414	0.238	0.176	3.69E-02	0.3048	8.25E+00	4.49E-01	8.82E-01	
1	17	3.96	0.414	0.238	0.176	3.69E-02	0.3048	8.25E+00	4.88E-01	8.91E-01	
1	18	3.66	0.414	0.238	0.176	3.69E-02	0.3048	8.25E+00	5.28E-01	8.99E-01	
1	19	3.35	0.414	0.238	0.176	3.69E-02	0.3048	8.25E+00	5.67E-01	9.08E-01	
1	20	3.05	0.414	0.238	0.176	3.69E-02	0.3048	8.25E+00	6.07E-01	9.16E-01	
1	21	2.74	0.414	0.238	0.176	3.69E-02	0.3048	8.25E+00	6.46E-01	9.24E-01	
1	22	2.44	0.414	0.238	0.176	3.69E-02	0.3048	8.25E+00	6.85E-01	9.33E-01	
1	23	2.13	0.414	0.238	0.176	3.69E-02	0.3048	8.25E+00	7.25E-01	9.41E-01	
1	24	1.83	0.414	0.238	0.176	3.69E-02	0.3048	8.25E+00	7.64E-01	9.50E-01	
1	25	1.52	0.414	0.238	0.176	3.69E-02	0.3048	8.25E+00	8.03E-01	9.58E-01	
1	26	1.22	0.414	0.238	0.176	3.69E-02	0.3048	8.25E+00	8.43E-01	9.66E-01	
1	27	0.91	0.414	0.238	0.176	3.69E-02	0.3048	8.25E+00	8.82E-01	9.75E-01	
1	28	0.61	0.414	0.238	0.176	3.69E-02	0.3048	8.25E+00	9.21E-01	9.83E-01	
1	29	0.30	0.414	0.238	0.176	3.69E-02	0.1524	4.13E+00	9.61E-01	9.92E-01	
1	29.5	0.15	0.414	0.238	0.176	3.69E-02	0.1524	4.13E+00	9.80E-01	9.96E-01	
1	30	0.00	0.414	0.238	0.176				1.00E+00	1.00E+00	

Attachment F-1
Example DLM Spreadsheet Calculations

Dominant Layer Model Simulaiton
Residential Scenario. Shallow Source. Benzene

		Remark
λ	2.00E-03 hr-1	
	4.8E-02 day-1	
t1/2	3.47E+02 hr	
	1.44E+01 day	
L1	0.46 m	1.50 ft
L2	1.98 m	6.50 ft
L3	2.13 m	7.00 ft
Deff	5.45E-03 m ² /d	
D1eff	5.45E-03 m ² /d	
D2eff	5.45E-03 m ² /d	
D3eff	5.45E-03 m ² /d	
θ 2m	0.25 -	Region 2 Avg
η	5.57	API 4674 Eq. 15
α DLM	1.06E-06	Eq. 16 modified for high QsoilXLcrk/(DcrkxAcrk)
Bio atten factor	7.95E+01	(α JEM) / (α DLM)
β'	0.00E+00	Eq. 17 modified for high QsoilXLcrk/(DcrkxAcrk)
γ	-1.57E+02	Eq. 18
σ	-4.71E+02	Eq. 19
ψ	2.39E-03	Eq. 20
ϕ	-4.88E-03	Eq. 21
C1	1.00E+00	Csource - Set to 1 to show relative concentrations
C2	3.74E-01	Eq. 24
C3	1.04E-03	Eq. 23
C4 alternate	3.13E-05	Eq. 22 modified for high QsoilXLcrk/(DcrkxAcrk)

JEM Calcs		
Deff Ab/Qbldg/LT		8.72E-05
Qs Lc/Dc/Ac		3.51E+03
Qs/Qb		2.46E-03
a JEM		8.42E-05

									DLM Update	JEM
Region	Depth (ft)	z (m)	n	θ v	θ m	Deff (m ² /d)	L(i) (m)	L(i)/D(i) (d/m)	C/Csource	C/Csource
3	0.5	2.13	0.379	0.127	0.253	5.45E-03	0.03048	5.60E+00	3.13E-05	0.00E+00
3	0.6	2.10	0.379	0.127	0.253	5.45E-03	0.03048	5.60E+00	2.33E-04	1.43E-02
3	0.7	2.07	0.379	0.127	0.253	5.45E-03	0.01524	2.80E+00	4.36E-04	2.86E-02
3	0.75	2.06	0.379	0.127	0.253	5.45E-03	0.0762	1.40E+01	5.71E-04	3.57E-02
2	1	1.98	0.379	0.127	0.253	5.45E-03	0.0762	1.40E+01	1.04E-03	7.15E-02
2	1.25	1.91	0.379	0.127	0.253	5.45E-03	0.0762	1.40E+01	1.59E-03	1.07E-01
2	1.5	1.83	0.379	0.127	0.253	5.45E-03	0.0762	1.40E+01	2.27E-03	1.43E-01
2	1.75	1.75	0.379	0.127	0.253	5.45E-03	0.0762	1.40E+01	3.13E-03	1.79E-01
2	2	1.68	0.379	0.127	0.253	5.45E-03	0.0762	1.40E+01	4.22E-03	2.14E-01
2	2.25	1.60	0.379	0.127	0.253	5.45E-03	0.0762	1.40E+01	5.65E-03	2.50E-01
2	2.5	1.52	0.379	0.127	0.253	5.45E-03	0.0762	1.40E+01	7.52E-03	2.86E-01
2	2.75	1.45	0.379	0.127	0.253	5.45E-03	0.0762	1.40E+01	9.98E-03	3.21E-01
2	3	1.37	0.379	0.127	0.253	5.45E-03	0.0762	1.40E+01	1.32E-02	3.57E-01
2	3.25	1.30	0.379	0.127	0.253	5.45E-03	0.0762	1.40E+01	1.75E-02	3.93E-01
2	3.5	1.22	0.379	0.127	0.253	5.45E-03	0.0762	1.40E+01	2.31E-02	4.29E-01
2	3.75	1.14	0.379	0.127	0.253	5.45E-03	0.0762	1.40E+01	3.05E-02	4.64E-01
2	4	1.07	0.379	0.127	0.253	5.45E-03	0.0762	1.40E+01	4.03E-02	5.00E-01
2	4.25	0.99	0.379	0.127	0.253	5.45E-03	0.0762	1.40E+01	5.33E-02	5.36E-01
2	4.5	0.91	0.379	0.127	0.253	5.45E-03	0.0762	1.40E+01	7.04E-02	5.71E-01
2	4.75	0.84	0.379	0.127	0.253	5.45E-03	0.0762	1.40E+01	9.30E-02	6.07E-01
2	5	0.76	0.379	0.127	0.253	5.45E-03	0.0762	1.40E+01	1.23E-01	6.43E-01
2	5.25	0.69	0.379	0.127	0.253	5.45E-03	0.0762	1.40E+01	1.62E-01	6.79E-01
2	5.5	0.61	0.379	0.127	0.253	5.45E-03	0.0762	1.40E+01	2.15E-01	7.14E-01
2	5.75	0.53	0.379	0.127	0.253	5.45E-03	0.0762	1.40E+01	2.83E-01	7.50E-01
1	6	0.46	0.379	0.127	0.253	5.45E-03	0.0762	1.40E+01	3.74E-01	7.86E-01
1	6.25	0.38	0.379	0.127	0.253	5.45E-03	0.0762	1.40E+01	4.79E-01	8.21E-01
1	6.5	0.30	0.379	0.127	0.253	5.45E-03	0.0762	1.40E+01	5.83E-01	8.57E-01
1	6.75	0.23	0.379	0.127	0.253	5.45E-03	0.0762	1.40E+01	6.87E-01	8.93E-01
1	7	0.15	0.379	0.127	0.253	5.45E-03	0.06096	1.12E+01	7.91E-01	9.29E-01
1	7.2	0.09	0.379	0.127	0.253	5.45E-03	0.03048	5.60E+00	8.75E-01	9.57E-01
1	7.3	0.06	0.379	0.127	0.253	5.45E-03	0.06096	1.12E+01	9.17E-01	9.71E-01
1	7.5	0.00	0.379	0.127	0.253				1.00E+00	1.00E+00

ATTACHMENT F-2

COMMENTS AND RESPONSE TO COMMENTS ON DOMINANT LAYER MODEL

Shell Oil Company



March 12, 2001

Dante Rodriguez
U.S. Environmental Protection Agency, Region IX
Mail Stop SFD-7-1
75 Hawthorne Street
San Francisco, California 94105

Environmental Remediation

4482 Barranca Parkway
Suite 180-171
Irvine, CA 92604

949-654-1275
949-654-1303 (FAX)

cbpaineiii@shellus.com

Gloria Conti
Department of Toxic Substances Control
5796 Corporate Avenue
Cypress, California 90630

RE: Administrative Order on Consent (AOC): U.S. EPA Docket No. 92-13
Responses To Comments Received On:
Vapor Transport Modeling Report, Del Amo Study Area, Dated November 4, 1999

Dear Mr. Rodriguez and Ms. Conti:

Enclosed herewith are responses to the following written comments received from EPA and DTSC on the subject report:

- January 7, 2000 letter to C.B. Paine from Dante Rodriguez, and
- March 8, 2000 letter to Kathleen Salyer from Haissam Salloum, with 3 attachments:
 1. January 6, 2000 Memo to Gloria Conti from Marie McCrink,
 2. January 12, 2000 Memo to Gloria Conti from Joe Hwong, and
 3. February 23, 2000 Memo to Gloria Conti from Michael Schum.

Several copies of our responses are enclosed for you to distribute to those who provided the written comments on the draft report.

In responding to the comments we describe actions we have taken to modify the report, or provide additional information in response to statements or questions contained in the comments. Given the nature of many of the comments, we suggest that before we formally reissue the revised report, it would be desirable for us to schedule a conference call after the reviewers of the report have had opportunity to read over our responses. We anticipate that some additional discussion would be helpful in flushing out any remaining questions, and would help us in issuing a final report that is fully responsive to all the questions and comments.

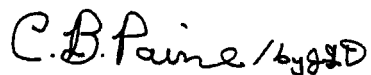
Additionally, in accordance with our schedule to submit a draft risk assessment report on or before March 30, 2001, we plan to proceed at this time with the vapor modeling work in support of the risk assessment. For the risk assessment, our approach for modeling vapor transport of

Dante Rodriguez
Gloria Conti
March 12, 2001
Page 2

chlorinated compounds from soil and contaminated groundwater to the surface will be to apply a simple single-layer Johnson and Ettinger model which does not account for any biodegradation that may be occurring and will provide a conservative estimate of the risk (see response to EPA comment #2, attached).

If questions arise during your review of our comment responses, we are available to meet or teleconference with you and/or any of the reviewers to address any further questions. Please contact John Dudley at (805) 964-6010, ext. 317 with any questions, or if you feel it is appropriate to meet or arrange for a teleconference.

Sincerely,

Handwritten signature of C.B. Paine in cursive script.

C.B. Paine
Project Coordinator For Respondents

RESPONSE TO EPA JANUARY 7, 2000 COMMENTS

1. *The modeling effort to date offers a reasonable approach for estimating a range of values for the intrusion rate of volatile compounds from groundwater emission sources or from emissions originating in subsurface soils. However, use of the fitted decay coefficients presumes that the degradation evaluated at the three experimental sites is ubiquitous and that similar coefficients can be used at other locations. Because there are no data on dissolved oxygen gradients in vadose zone soils, there is no way to ensure that aerobic degradation is occurring throughout the site. We recommend using confirmatory soil gas sampling at prospective locations. This sampling could consist of in situ measurements of vapor-phase total organics, one sample above the biodegradation interval and another below the interval. In the absence of shallow soil contamination, the soil gas concentration below the biodegradation interval at the groundwater interface can be calculated from the groundwater concentration. Use of a subsurface sampling device such as a Geoprobe can be used to attain the shallow soil gas concentrations. This sampling would confirm the existence of the concentration gradient across the hypothetical degradation interval and could also be used to calibrate the model to location-specific vapor concentrations. Use of this technique would depend on many factors, but in the end, would depend on the degree of certainty required. [Craig Mann]*

Response:

The Respondents agree that additional vertically distributed soil gas data for benzene and oxygen at a few on-site locations would be of value in confirming that the pattern of degradation in the vadose zone above contaminated groundwater noted at the three sites evaluated in the report is representative of the site as a whole. A comprehensive data gaps analysis is planned as part of the baseline risk assessment, currently in progress for the soil and NAPL operable unit. Additional soil gas profiling at selected locations may be included in a draft scope of work developed to address any additional data gaps revealed during the risk assessment.

2. *The analyses conducted thus far were for benzene, which is assumed to be biodegrading. If TCE is relatively resistant to biodegradation, as has been suggested, then we would expect to see a different soil profile for this chemical than that demonstrated for benzene. This additional information would provide greater assurance to the agencies that the interpretations of the soil profiles presented in the draft "Vapor Transport Modeling Report" are correct. If the soil profiles for the two different contaminants turn out to be similar, then this raises some additional interesting questions that would need to be flushed out before acceptance of the site-specific decay coefficients. [Stan Smucker]*

Response:

Modeling of TCE in the soil profile above contaminated groundwater at selected locations such as the Coca-Cola site within the Del Amo site may be performed, and if conducted, the output will be appended to the final report or submitted under separate cover. For the site-wide risk assessment, in accordance with our schedule to submit a draft risk assessment report on or before March 30, 2001, a more conservative approach will be adopted for TCE and other chlorinated compounds by using the simple Johnson and Ettinger (1991) model (JEM) which does not take credit for any biodegradation that may be occurring in the vadose zone.

**RESPONSE TO DTSC MARCH 8, 2000 COMMENTS
ON THE DRAFT VAPOR TRANSPORT MODELING REPORT,
DEL AMO STUDY AREA**

The Del Amo Respondents are pleased to present responses to the aforementioned comments on the Draft Vapor Transport Modeling Report, Del Amo Study Area (herein referred to as the Draft Report). The responses are provided for each DTSC reviewer in the following.

REVIEW COMMENTS OF MARIE T. MCCRINK DATED JANUARY 6, 2000

- 1. Section 4.0 Key Assumptions Used. The fourth bullet states that significant biodegradation of aromatic hydrocarbons takes place in the vadose zone. The GSU recommends that this key assumption be completely substantiated with field data, specific to the three modeled areas, before the methodology is applied to the rest of the Study Area as part of the FS. (a)*

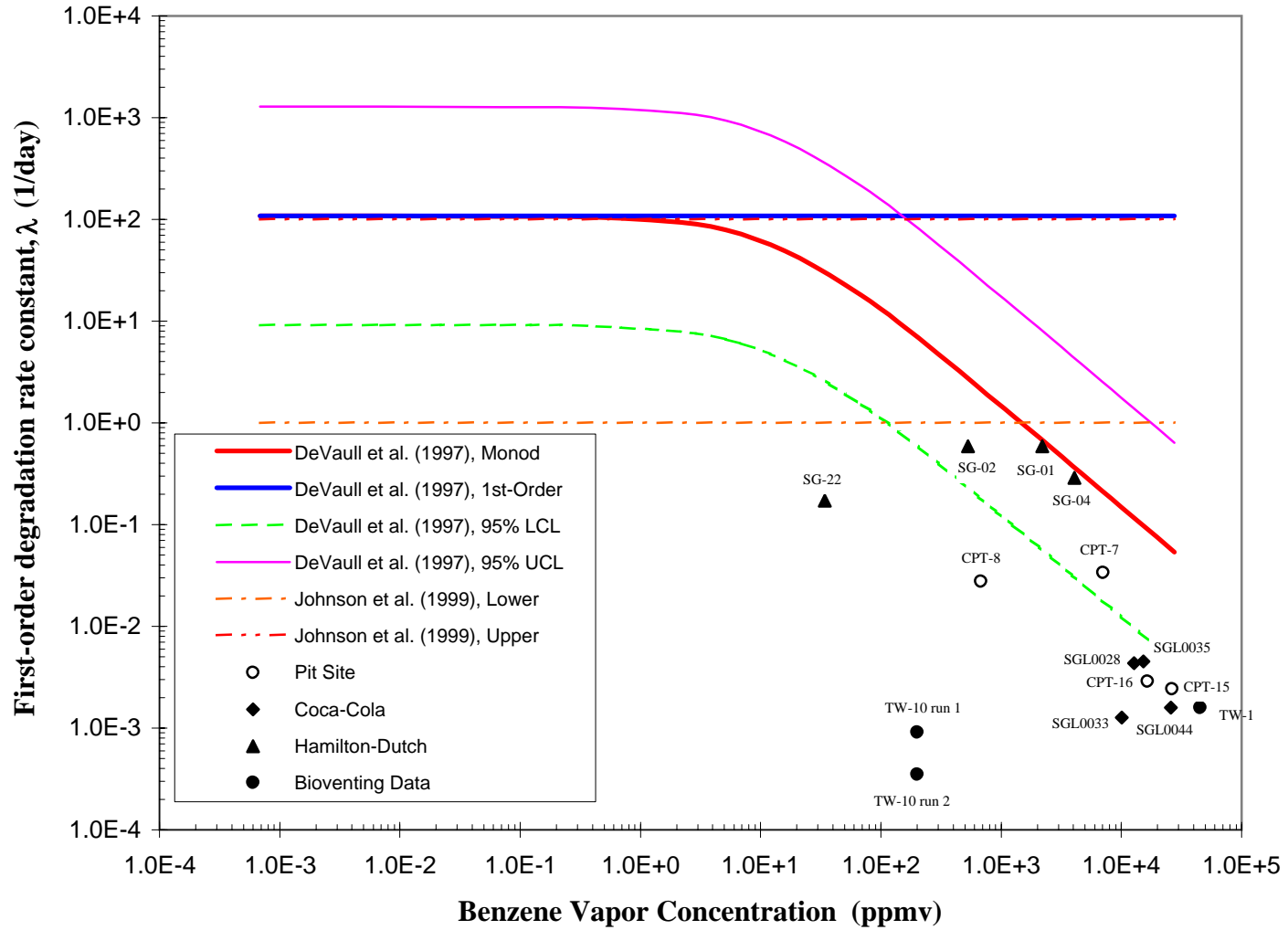
Response:

We would first like to point out that the investigations summarized in the Draft Report clearly demonstrate that biodegradation or other similar BTEX destruction mechanisms are taking place in the vadose zone at the Del Amo Site. This conclusion is also strongly supported by field tests previously and recently conducted in the Pit Site within the Study Area. Results of the field studies are summarized below.

I. Bioventing Test Results and Comparison to Site Vapor Transport Model Results and Other Empirical Data

A Pilot Treatability Test using the bioventing technology was performed in the Pit Site to estimate the degradation rates in the presence of air (oxygen) (Dames & Moore, 1993). Field bioventing tests were performed in SVE test well TW-1, immediately north of Pit-1C, and background SVE test well TW-10 in the northwest corner of the Pit Site. Field data indicate that first-order kinetics can describe the aerobic biodegradation of the aromatic petroleum hydrocarbon contaminants in the vadose zone. The oxygen consumption rate constants were measured to be $8.40 \times 10^{-3} \sim 3.79 \times 10^{-2} \text{ day}^{-1}$. The corresponding biodegradation rate constants of aromatic hydrocarbons following air (oxygen) injection into vadose zone soils range from 3.50×10^{-4} to $1.58 \times 10^{-3} \text{ day}^{-1}$, assuming the degradation is controlled by aerobic destruction of benzene (Dames & Moore, 1999, Eq. (27)). Note that TW-10 was a background well located in an area with low initial benzene concentration; the rate constants estimated for that location may not provide a true measure of the degradation and hence are not compared to other rate constants in Figure 1.

FIGURE 1
Comparison of Degradation Rate Constants



The biodegradation rate constant obtained from the bioventing test in TW-1 is plotted against initial average benzene vapor concentrations present in vadose zone at the time of testing, and compared to the model-estimated rate constants at three areas within the Del Amo Study Area, including the Pit Site area, the Coca-Cola area, and the Hamilton-Dutch area (Dames & Moore, 1999) in Figure 1, which also contains similar data from several investigators¹. Note that the vapor transport modeling was conducted independently from the Pilot Treatability Test. The figure shows that the treatability-test rate constant of TW-1 is near the 95% LCL established by DeVuall et al. (1997). This constant is also consistent with the range of rate constants derived by the vapor transport modeling. This good comparison between the modeled biodegradation rates and those derived from the bioventing tests in the Pit Site confirms that the model that incorporates biodegradation in the vadose zone is appropriate for assessing vapor transport under the specific site conditions, and provides independent support of the range of model-estimated aerobic degradation rates not only at the Pit Site, but also at two other widely spaced areas within the Del Amo Study Area.

II. Baseline O₂ and CO₂ Measurements

Vertical profiles of oxygen and carbon dioxide in vadose zone soils were recently measured at seven locations within the Pit Site (Table 1). Aerobic degradation of aromatic hydrocarbons is the dominant biodegradation process in vadose zone soils when available oxygen exceeds 1% to 4% by volume, and the soils contain suitable moisture and nutrient levels (McAllister and Chiang, 1994; Hinchee et al., 1995; Wiedemeier et al., 1998). All measured oxygen levels in vadose zone vapor samples are within or greater than this range. Secondly, O₂ levels generally show an inverse relationship to benzene vapor concentrations. This is consistent with increased utilization (consumption) of O₂ in the presence of higher levels of available fuel (benzene or other aromatic hydrocarbon) for aerobic microbes. Thirdly, CO₂ levels generally show an inverse relationship with O₂ levels and a direct relationship with benzene vapor concentrations. Again, these relationships are consistent with aerobic degradation of the aromatic hydrocarbons in the Pit Site vadose zone.

In summary, therefore, we concur with U.S. EPA (2000) on its review comment number 1 of the Draft Report that states: “The modeling effort to date offers a reasonable approach for estimating a range of values for the intrusion rate of volatile compounds from groundwater emission sources or from emissions originating in subsurface soils”.

¹ Note that TW-10 was a background well located in an area with very low initial benzene concentration; the rate constants estimated may not provide a true measure of the degradation and hence are not included in the figure.

TABLE 1
 OXYGEN AND CARBON DIOXIDE DATA IN VADOSE ZONE SOILS
 DEL AMO WASTE PITS AREA (1)

Well ID#	SAMPLE DEPTH (feet bgs)	ASTM D1946 CO ₂ %	ASTM D1946 O ₂ %
MW-B"-1	29.2	21	3.2
MW-B"-2	38.2	19	2.6
MW-B"-3	49.2	19	3.9
MW-C"-1	29	7.9	15
MW-C"-2	38	24	1.4
MW-C"-3	50	17	9.5
MW-F"-1	32.4	10	10
MW-F"-2	39.4	2.2	22
MW-F"-3	48.4	7.6	12
MW-H"-1	27.4	9.2	6.1
MW-H"-2	39.4	6.8	7.3
MW-H"-3	46.4	12	5.1
MW-J"-1	32.4	0.17	22
MW-J"-2	39.4	13	6.8
MW-J"-3	48.4	11	7.8
MW-L"-1	29.3	18	1.5
MW-L"-2	36.3	20	2.4
MW-L"-3	50.3	9.6	8.3
MW-M"-1	32.3	19	2.6
MW-M"-2	37.3	19	4.8
MW-M"-3	52.3	Non Recoverable sample	

(1) Source: C2REM and Dames & Moore (2000)

The GSU also recommends that the information on Biodegradation in Vadose Zone Soils presented at the October 26, 1999 Vapor Transport Modeling Workshop be included in this report. This discussion, in conjunction with area specific field data, will help provide evidence to support the occurrence of biodegradation in the vadose zone. (b)

Response:

The Respondents agree with this recommendation. The referenced information will be included as an appendix in the Vapor Transport Modeling Report.

The GSU concurs that there is good agreement presented in this report between observed soil gas concentrations and the results of the DLM, which automatically incorporates biodegradation in the vadose zone. However, the GSU can not recommend approval of a document that assumes biodegradation is occurring. This assumption should be supported by facts from existing data and/or by proposing an assessment of biodegradation in the vadose zone based on field parameters measured at each site. (c)

Response:

The Respondents would like to point out that active degradation taking place in the Study Area is supported not only by numerical modeling, but also by field observations. During the bioventing tests conducted as part of the Pilot Feasibility Test at the Pit Site, degradation has been demonstrated to be occurring at an oxygen consumption rate of 8.40×10^{-3} to 3.79×10^{-2} day⁻¹ and a benzene consumption rate constant of 3.50×10^{-4} to 1.58×10^{-3} day⁻¹. For further details, please see response to McCrink's comment 1a in the above.

Finally, as stated on page 4, the DLM predicts relatively higher vadose zone biodegradation rate constants than those estimated from groundwater studies (DeVaull et al., 1997). Therefore, the uncertainty of applying groundwater studies to the vadose zone further supports the need to establish the occurrence of biodegradation in the vadose zone based on field evidence. (d)

Response:

First, modeling presented in the Draft Report was not based on degradation rate constants estimated from groundwater studies. Rather, it was based on demonstrated vadose zone degradation, and measured rates of aerobic degradation in the vadose zone based on measured oxygen consumption during controlled respiration testing in the vadose zone (see the response to McCrink's comment 1a above).

Second, it is reported that vadose zone degradation rate constants estimated from the DLM are typically higher than those estimated from groundwater studies (Johnson et al., 1999,

p.416). Johnson et al. (1999) believe that there may be alternative mechanistic explanations for this behavior. They reported DLM-estimated vadose zone half-lives of roughly 22 day^{-1} compared to 0.001 to 0.01 day^{-1} from groundwater plume data fitting. These values are generally consistent with the DeVaul et al. (1997) study for aerobic degradation except for high vapor concentrations where the DeVaul et al. (1997) rate constants tend to be more conservative. The site-specific application of DLM to the three sites within the Del Amo Study Area yielded rate constants that range from 1.23×10^{-3} to $5.90 \times 10^{-1} \text{ day}^{-1}$, which are near or below the 95% LCL of DeVaul et al. (1997) (see Figure 1). It is the intention of the Respondents to apply the site-specific degradation rate constants in the sitewide risk assessment.

2. Section 4.0 Key Assumptions Used. The fifth bullet states that the influence of individual source areas have not overlapped laterally and the source can be considered separately by the vapor transport model. The GSU recommends a discussion be included that specifies the procedure to follow if overlapping source areas are encountered when this methodology is applied to other parts of the Study Area.

Response:

This recommendation will be considered and where appropriate, implemented in the sitewide risk assessment. In the Study Area, there may be cases in which more than one contamination source impacts the soil and soil vapor above the source areas. In that case, the risk will be assessed for the overlapping sources separately, and then be combined by the method of superposition. The development and application of such an approach will be included in the risk assessment.

3. Section 5.0 Results. The third paragraph discusses the chemical and geologic parameters input into the DLM.

- a. *K_v, Vertical Intrinsic Permeability: The text states that the value for soil in the vadose zone was assumed to be 10^{-12} m^2 , which is equivalent to a water saturated hydraulic conductivity of $9.8 \times 10^{-4} \text{ cm/sec}$. The GSU recommends that an explanation be provided about why an assumed value has been used rather than a field measured value, and how that value was estimated to be adequate. Also, a sensitivity analysis of this parameter should be included to indicate how a higher or lower value impacts the value of Q_{soil} , the flow rate of soil gas into the building.*

Response:

As documented on page 9 in the Draft Report, the vertical permeability used in the model was selected after considering the vertical permeability values obtained

through 1-D consolidation tests and saturated zone aquifer tests. The test data showed significant variations, as can be expected for this site with its heterogeneous soils. The value of 10^{-12} m^2 was selected to be within the range of test-derived data. In response to this comment, a sensitivity analysis on this parameter will be completed and discussed in the finalized report.

- b. ***Hydraulic Conductivity:*** *The text states that values for this parameter were estimated from pumping tests of the saturated Upper Bellflower zone. The GSU recommends that the test specify if this parameter represents horizontal or vertical hydraulic conductivity and how it is used in the DLM. Based on the context, this usually refers to horizontal conductivity. If this is the case, an explanation should be included about how a horizontal hydraulic conductivity value from the saturated zone can be justified for use in a vadose zone model in which vertical migration is the dominant transport path.*

Response:

The hydraulic conductivity discussed in the Draft Report were values obtained from the same hydrostratigraphic unit with similar soil composition to the vadose zone. Hydraulic conductivity derived from pumping tests are indeed more representative of flow in the horizontal direction in the saturated zone; however, 1-D consolidation tests showed similar and variable vertical and horizontal permeabilities. Therefore, the Respondents believe that it was appropriate to compare the hydraulic conductivity to the vertical permeability in the report to gain an understanding about their orders of magnitude.

- c. ***Q_{soil} flow rate of soil gas into the building:*** *This term is listed in Table 5-1, Input Parameters for Modeled Locations in the Pit Site Area, but is not discussed in this section. The GSU recommends that a complete discussion of Q_{soil} be included in the text. All parameters in the equation should be defined and all parameters affecting Q_{soil} should be defined and discussed. It is the GSU's understanding that this parameter will drive the equation for phase II of this modeling effort in which potential concentrations of VOC vapors in indoor air resulting from subsurface sources will be estimated for risk assessment purposes.*

Response:

Q_{soil} is simply calculated from the other input parameters using Eq. (24) in Johnson and Ettinger (1991). All the other input parameters are provided in Table 5-1 in the

Draft Report. The equation and parameters used for calculating Q_{soil} will be clarified in the final report.

- 4. Section 5.0 Results. In the last paragraph of this section on page 10, the text states that in most cases studied, the Johnson and Ettinger (1991) Model (JEM) without degradation over-estimates the shallow vapor concentration by about 3 orders of magnitude... The GSU recommends a discussion be added to this section about the significance of cases studied in which the JEM rather than the DLM appears to accurately estimate the shallow soil vapor concentration. This occurred at the Coca-Cola Area location SGL0034 and at the Hamilton-Dutch Area locations SG-05 and SG-06. Based on the modeling results of those locations, it appears that when the JEM is the better predictor of soil gas concentration, this is evidence of a shallow source area rather than the deep groundwater source.*

Response:

This recommendation will be incorporated into the text of the final report. A paragraph will be developed to summarize the modeling results for locations SGL0034, SG-05, and SG-06. However, it is important to note that in a preliminary assessment of the locations for which sufficient data existed, once a shallow source was simulated in the model, the results for the transport from that shallow depth to the ground surface still indicate that some degree of biodegradation was necessary to reproduce the observed soil vapor concentrations above that depth. The combined results, therefore, indicate that degradation is taking place whether the source is present in groundwater or in shallow soil.

- 5. Table 5-1, Input Parameters for Modeled Locations in the Pit Site Area. This table contains values for K_v and Q_{soil} that have been used for modeling the Pits Area. The GSU recommends that values specific to the Coca-Cola and Hamilton-Dutch Areas be calculated.*

Response:

The values have been calculated and will be provided in the revised report.

REVIEW COMMENTS OF JOE T. HWONG DATED JANUARY 12, 2000

- 1. Numerous parameters were used to develop the vapor transport model for benzene. Because each parameter may have a specific effect on the simulation results, each parameter should be explained in detail and a discussion provided regarding their effect on the modeling results. In addition, the ranges for each parameter should be provided along with a sensitivity analysis to support the selection of each parameter.*

Response:

Parameters associated with Eqs. (1) through (26) are all defined in the text of the Draft Report. The selection of key parameters is discussed on pages 9 through 15 of the Draft Report. As stated in response to Comment 3a of McCrink, a sensitivity analysis on the vertical permeability will be completed and provided in the final report. As for every other parameter, the Respondents do not think that this report should repeat the original development of JEM and DLM in addition to the brief summary as already provided; rather, the readers should refer to the original documents for further details of the JEM and DLM including sensitivity of input parameters. For reference, these documents (i.e., Johnson and Ettinger, 1991 and Johnson et al., 1999) are attached herein.

- 2. Page 16, Section 7.0 Summary of Findings – The paragraph states that “This suggests that the models are adequate for predicting near surface concentrations of aromatic hydrocarbon vapors from subsurface sources.” The depth of the near surface should be defined and that definition supported in the report.*

Response:

The terms “near surface” and “shallow depth” are used to describe shallow soil contamination as opposed to groundwater emission sources. It should be noted that there are some variations in ground surface elevations and depths to groundwater across the Study Area. The depth to groundwater measured on October 9-10, 1997 varied from approximately 49 ft at SBL0124 in the Hamilton-Dutch Area to approximately 61 ft at SBL0125 in the Coca-Cola Site. In the risk assessment, the near surface is defined as the vadose zone between 0 and 15 ft below ground surface.

- 3. Additional data should be collected to verify the modeling results for the benzene vapor concentration, especially, from the depths of 10 to 60 feet below ground surface. The additional data will help to verify the accuracy of the modeling results.*

Response:

Please see our response to McCrink’s comment 1a.

REVIEW COMMENTS OF MICHAEL SCHUM DATED FEBRUARY 23, 2000

HERD has also reviewed comments on the approach supplied by DTSC Geologic Services Unit Staff (memos from M. McCrink dated 1/6/2000 and J. Hwong dated 1/12/2000). We agree with their assessment particularly as it applies to attempting to apply the model to

areas outside of the study area where geologic conditions may not be the same as those used to estimate model parameters within the study area.

In the past few years HERD has had considerable involvement with several versions of the fate and transport model referred to as the “Johnson and Ettinger Model”. HERD has recently been recommending that the version of this model released by the USEPA in January 1999 as part of their CERCLA guidance be used to estimate potential indoor air risks if there is a potential for exposure from VOCs ...

1. Proposed model has not been adequately peer-reviewed. The second paragraph in Section 2.0 states that “vapor transport models using the newly released dominant-layer model (Johnson et al., 1999)” will be used. HERD has reviewed this citation and we do not concur that the article is sufficient to establish the model as a widely applied, rigorously peer-reviewed fate and transport model that should be routinely applied to health risk assessments for CalEPA. In fact, the article cites as the basis for the model development an unpublished manuscript by the same authors (Johnson and Kembrowski, 1998) implying that the model has not undergone a formal scientific peer review process. This is reinforced by the statement on pg. 409 of the cited article which notes that “Neither model has undergone rigorous comparison with extensive field data.” While the modeling studies and field data currently being conducted at Del Amo will help to provide this information, there still needs to be independent confirmation by scientists not so intimately involved with promulgating their own version of a biodegradation model.

Response:

It is shown in the Draft Report that the only vapor transport model that has been peer reviewed to the extent suggested (i.e., the Johnson and Ettinger model or JEM) does not adequately match the site data. Consequently, the improved Johnson et al. (1999) model (DLM) was used to better estimate the potential impact to indoor air at the site. The DLM is basically a modification of the JEM to account for biodegradation in the vadose zone, which was published in Johnson and Ettinger (1991). The theoretical development of DLM has been completed separately from the Johnson et al. (1999) paper that was published in the Journal of Soil Contamination. The DLM has been reviewed by U.S. EPA’s technical consultant, Mr. Craig Mann (1999). The Respondents will be pleased to meet with the DTSC technical staff to discuss the derivation of the equations used in the DLM.

2. Model is calibrated against itself Field data on soil gas measurements are used to generate biodegradation rate constants in lieu of measuring biodegradation rates specifically. While this approach is not without merit, it limits the application of the

fitted model to those areas with virtually identical soil geological profiles, soil moisture content, and dissolved oxygen profiles. We recommend independent confirmation of these rate constants which could be accomplished by suitably designed field experiments.

Response:

First, it is a commonly accepted practice to calibrate transport models such as this against field data collected from an area, and then to apply the calibrated model to evaluate transport in the same general area (ASTM, 1996). This was necessary because, to the best of our knowledge, no approach existed that would allow for direct field measurement of biodegradation rate constant in vadose zone under site conditions similar to Del Amo. In this study, biodegradation rate constants were adjusted to match field data collected from three different areas, the Pit Site, Coca-Cola, and Hamilton-Dutch, within the Del Amo Study Area, and then compared to published values to ensure results are consistent with observations elsewhere. The results obtained are therefore, to a large extent, field measurements.

Secondly, the bioventing tests conducted in the Pit Site confirmed that the degradation is taking place in the Study Area and that the degradation rate constants estimated by the model are consistent with the measured values (see Figure 1 and the response to McCrink's comment 1a). Therefore, additional field experiments are not necessary to determine the degradation rate constants for the site.

3. Conclusions based on circular reasoning. Related to the previous comment, Page 11, Section 5.1.3, first paragraph states that "the DLM model, which incorporates biodegradation, results in an excellent match with the observed soil gas concentrations. This demonstrates that biodegradation is occurring in the Pit Site Area". The DLM model is not a mechanism based model. It relies on fitting observed soil gas data to estimate an empirical biodegradation rate constant. As such, it is not surprising that the predicted results "fit" the original data used to generate the prediction. It is not proof that biodegradation is occurring.

Response:

The Respondents would first like to clarify that biodegradation incorporated in the DLM and subsequently used in this report includes those mechanisms or processes that result in reduction of the soil vapor concentrations that can be quantified by first-order kinetics. For practical purposes of estimating the vapor release at the ground surface and into buildings, it is more important to focus on the model's ability to simulate concentration profiles rather than discerning the exact contributing mechanism. It is in this regard that we conclude that

the good match between DLM predictions and the observed soil vapor concentrations is consistent with biodegradation occurring in the Pit Site.

In addition, contrary to some other models that may not provide unique calibration against a given set of observation data, our experience with the DLM suggests that the fitting set of parameters fall into a narrow range that are unique and physically consistent with our conceptual model. Therefore, the model fitting with the DLM provides a fairly unique way of reproducing the field conditions that will be adequate for the risk assessment purposes.

Finally, we would like to reiterate that bioventing tests that were separately conducted confirmed that vadose zone biodegradation is taking place in the Study Area, as discussed in detail in our response to McCrink's comment 1a. The good comparison of model-estimated rate constants and bioventing tests-derived values provides a strong validation to the degradation model developed for the Pit Site.

4. Conclusions not supported by the data. Page 17, second paragraph states that the estimated benzene biodegradation rate constants are “conservative compared to these published values” as shown in Figure 7-1. HERD does not agree with this conclusion. The estimated rate constants are lower than nearly all “published” comparisons. A first order rate constant, expressed as a fraction degraded per day (1/day), that is lower than another value is less conservative not more conservative.

Response:

The Respondents have to disagree with this comment. The first-order degradation incorporated into the DLM can be written as:

$$dC/dt = -\lambda C \tag{1}$$

where C is concentration, t is time, and λ is the rate constant. For a stagnant contaminant source with an initial concentration of C_0 at time 0, the remaining concentration at any given instant can be calculated as follows,

$$C(t) = C_0 \exp (-\lambda t) \tag{2}$$

It can be seen from this equation that the smaller the λ , the larger the C(t). Similarly, when using the DLM, lower values of λ will result in higher estimated indoor air concentrations which will lead to more conservative results as far as the health risk is concerned.

Summary

HERD always recommends that site-specific data be used to estimate human health risks when available. HERD also recommends that the most current USEPA recognized fate and transport model be used. Since the proposed changes to the USEPA model have not been adopted by the USEPA, we do not recommend that the revised model be used exclusively in any health risk assessment submitted to DTSC for review. We agree that there is evidence to suggest that biodegradation may be occurring and should be evaluated by the best available science, and we suggest that predicted results from both types of models be included in the ongoing site-wide risk assessment.

Response:

The Del Amo Respondents agree with DTSC on the need to use site-specific data to evaluate the health risk for the specific site conditions. As detailed in our response to McCrink's comment 1a, we also believe that both field data (including bioventing tests, baseline CO₂ and O₂ measurements) and modeling results (presented in the Draft Report and herein) clearly demonstrate significant biodegradation in the vadose zone in the Study Area. In addition, it should be noted that the modeling work presented in the Draft Report that extends the JEM to DLM has been extensively reviewed by the U.S. EPA including its technical consultant. The U.S. EPA technical consultant, Mr. Craig Mann, has reviewed the theoretical development of the equations, the modeling approach, as well as the application of the approach to the three sites studied (Mann, 1999). At the October 26, 1999 Vapor Transport Modeling Workshop, Mr. Mann has also concurred with the general approach proposed for conducting the site-wide risk assessment. Following this detailed review, both JEM and DLM have been used in the evaluation presented in the Draft Report. In its January 7, 2000 review comments, the U.S. EPA (2000) stated that "The modeling effort to date offers a reasonable approach for estimating a range of values for the intrusion rate of volatile compounds from groundwater emission sources or from emission originating in subsurface soils". The success of this exercise convinces us, as U.S. EPA concurred in their January 2000 review, that the DLM is an appropriate tool for the site-wide risk assessment.

REFERENCES

ASTM, 1996. STP 1288, Subsurface Fluid Flow (Ground-Water and Vadose Zone) Modeling.

C2REM and Dames & Moore, 2000. SVE Baseline Monitoring Results and Low Flow SVE Evaluation Report, Del Amo Waste Pits Operable Unit. May 2, 2000.

Dames & Moore, 1993. Phase I Treatability Study Evaluation Report, Del Amo Pit Site. April 5, 1993.

Dames & Moore, 1999. Draft Vadose Zone Transport Modeling Report. November 4, 1999.

DeVaull, G.E., R.A. Ettinger, J.P. Salanitro, and J.B. Gustafson, 1997. Benzene, Toluene, Ethylbenzene, and Xylenes [BTEX] Degradation in Vadose Zone Soils During Vapor Transport: First-Order Rate Constants, in Proceedings of the API/NGWA Petroleum Hydrocarbons and Organic Chemicals in Ground Water: Prevention, Detection, and Remediation Conference, Houston, Texas, November 12-14, 1997 (Ground Water Publishing Company, Westerville, Ohio), p. 365-379.

Johnson, P.C., and R.A. Ettinger, 1991. Heuristic model for predicting the intrusion of contaminated vapors into buildings. *Environmental Science and Technology*. 25(8), p.1445-1452.

Johnson, P.C., M.W. Kemblowski, and R.L. Johnson, Assessing the Significance of Subsurface Contaminant Vapor Migration to Enclosed Spaces: Site-Specific Alternatives to Generic Estimates, *Journal of Soil Contamination*, 8(3) 389-421, 1999.

Mann, C. (EQM, Inc.), 1999. Memoranda to D. Rodriguez (EPA) regarding Soil Gas Profile Modeling at the Del Amo Superfund Site. June 3, 1999 and August 30, 1999.

McAllister, P.M., and C.Y. Chaing, 1994. A Practical Approach to Evaluating Natural Attenuation of Contaminants in Ground Water, *GWMR, Spring 1994*, p161-173.

U.S. EPA, 2000. Letter from D. Rodriguez to C.B. Paine, Shell Oil Company. Jan. 7, 2000.

Wiedemeier, T.H., M.A. Swanson, D.E. Moutoux, E. K. Gordon, J.T. Wilson, B.H. Wilson, D.H. Kampbell, P.E. Haas, R.N. Miller, J. E. Hansen, and F.H. Chapbelle, 1998. Technical Protocol for Evaluating Natural Attenuation of Chlorinated Solvents in Ground Water, *EPA/600/R-98/128*.

ATTACHMENTS

Johnson, P.C., and R.A. Ettinger, 1991. Heuristic model for predicting the intrusion of contaminated vapors into buildings. *Environmental Science and Technology*. 25(8), p.1445-1452.

Johnson, P.C., M.W. Kemblowski, and R.L. Johnson, Assessing the Significance of Subsurface Contaminant Vapor Migration to Enclosed Spaces: Site-Specific Alternatives to Generic Estimates, *Journal of Soil Contamination*, 8(3) 389-421, 1999.

Assessing the Significance of Subsurface Contaminant Vapor Migration to Enclosed Spaces: Site-Specific Alternatives to Generic Estimates

Paul C. Johnson,¹ Mariush W. Kemblowski,² and Richard L. Johnson³

¹Dept. of Civil and Environmental Engineering, Arizona State University; ²Utah Water Research Laboratory, Utah State University; ³Dept. of Environmental Science and Engineering, Oregon Graduate Institute

The move toward more structured risk-based corrective action (RBCA) approaches has led to an increased awareness and interest in better understanding vapor migration to enclosed spaces. The significance of this pathway is currently the subject of intense debate, with many believing that existing non-site-specific (aka "Tier 1", or "generic") risk-based screening levels are too conservative. However, little data are available to justify alternate approaches, and so this pathway must be addressed further on a more site-specific basis at many sites. Unfortunately, little guidance exists for doing this. In answer to this need, options for addressing this pathway on a more site-specific basis are presented here. These include a more refined use of the existing screening algorithms for layered geologic settings, as well as use of recently updated algorithms that consider biodegradation. Each option has associated with it site-specific data collection and interpretation requirements, and these can vary in complexity of analysis and intensity of data requirements. Also, a vision for a much simpler pathway screening analysis is presented and accompanied by a discussion of the developments necessary to progress toward that goal. This improved approach would determine, based on site characteristics assessed during an initial site assessment (specifically moisture content or measured effective diffusion coefficient and source zone vapor concentration), whether the vapor intrusion pathway needs be addressed further at the site.

KEY WORDS: risk-based corrective action, vapor migration, generic estimates.

INTRODUCTION

When soils are impacted by leaks or spills, or wastes are placed in impoundments, there is the potential for contaminant vapor migration to enclosed spaces (buildings, conduits, etc.) and leachate migration to groundwater. Historically, regulations have considered the potential for leachate from contaminated soils and wastes to impact groundwater; however, the issue of vapor migration has only recently begun to be formally and quantitatively addressed. This has been brought about in large part by the move toward more structured risk-based corrective action (RBCA) approaches (e.g., ASTM 1995) and an increased awareness of this pathway.

The significance of the vapor intrusion pathway and natural attenuation of vapors in the vadose zone are currently the subject of intense debate. When common screening-level algorithms (e.g., Johnson and Ettinger, 1991; Little *et al.*, 1992) are combined with conservative soil properties, geometries, and exposure assumptions, then the resulting target risk-based screening levels (RBSLs) are very low. In fact, they are often one to three orders-of-magnitude lower than existing cleanup guidelines in many states. For example, the sample calculation shown in the ASTM RBCA Standard (ASTM, 1995) suggests that benzene concentrations in excess of 5 $\mu\text{g}/\text{kg}$ -soil could be of concern if one wishes to be protective to a 10^{-6} excess cancer risk level.

Many intuitively feel that the current generation of screening-level predictive models are too conservative and lead to unnecessarily low cleanup targets. Some point to the fact that the algorithms generally do not account for biodegradation and other possible vadose zone attenuation mechanisms. Based on the biodegradation literature, it is reasonable to expect that some chemicals of interest degrade as they migrate, especially those originating from petroleum spills (e.g., benzene). If this is true, then these chemicals should be found at concentrations much less than those predicted by the current generation of screening level algorithms. This hypothesis is supported to some degree by the Fitzpatrick and Fitzgerald (1997) Massachusetts indoor air survey, the data of Fischer *et al.* (1996), and others who have observed and reported on petroleum hydrocarbon biodegradation in the vadose zone under natural conditions (e.g., Ostendorf and Campbell, 1991).

Unfortunately, little data exist to refute or support existing algorithms, or to quantify the degree of overconservatism. This lack of data is a result of many factors, including the fact that interest in this pathway is relatively new. Johnson and Ettinger (1991) and Little *et al.* (1992) conclude that the screening algorithms should predict reasonable results when contaminants are present in soil gas immediately adjacent to a basement, based on a comparison of model predictions with published radon intrusion data (e.g., Nazaroff *et al.*, 1987). However, rigorous comparisons of model predictions and measurements for well-characterized sites where contaminant sources are located some distance away from a building have yet to be reported. Recently, Fitzpatrick and Fitzgerald (1997) presented their

conclusions from a study of sites in Massachusetts where indoor air samples were collected. Their goal was to review site characteristics and then identify specific trends and field conditions that most influence vapor migration and vapor intrusion into buildings. They also were interested in assessing the validity of generic state guidance derived from use of the Johnson and Ettinger (1991) algorithm. In summary, they noted that the generic Massachusetts guidelines overestimated vapor intrusion impacts for petroleum fuel hydrocarbon sites; however, they also found that the generic screening guidelines sometimes underpredicted indoor concentrations at sites where chlorinated organic vapors were present. Contrary to the popular belief that the models are overly conservative, the authors concluded that the generic Massachusetts guidelines were not conservative enough for site screening purposes, at least for chlorinated compound sites.

Given limited data and limited understanding, the potential for high sensitivity to site-specific conditions, and the tendency to lean toward conservativeness when developing regulations, it seems unlikely that technically defensible alternatives for developing generic screening levels will surface in the near-term. The inevitable consequence is that many sites containing volatile carcinogens are unlikely to satisfy generic RBSLs for this pathway. Thus, this pathway will need to be addressed on a more site-specific basis, and options are needed to ensure that this is done in a technically defensible manner. Some state-level regulatory agencies are already struggling with developing site-specific guidance for assessing this pathway.

In answer to this need, options for addressing the vapor migration pathway on a more site-specific basis are proposed here. These include a more refined use of existing screening algorithms for layered geologic settings, as well as the use of updated algorithms that consider biodegradation. These options stem from consideration of practically available data, existing algorithms, theoretical considerations, and empirical experience (Jury *et al.*, 1983; Kampbell *et al.*, 1987; Nazaroff *et al.*, 1987; Garbesi and Sextro, 1989; Jury *et al.*, 1990; Johnson *et al.*, 1990; Loureiro *et al.*, 1990; Ostendorf and Kampbell, 1990; Johnson and Ettinger, 1991; Johnson and Perrot, 1991; Hodgson *et al.*, 1992; Little *et al.*, 1992; Unlu *et al.*, 1992; Ostendorf, 1993; Jin, 1994; Acomb *et al.*, 1996; Auer *et al.*, 1996; Fischer *et al.*, 1996; Jeng *et al.*, 1996; Lahvis and Baeher, 1996; Smith *et al.*, 1996; Uchria, 1996; BP, 1997; DeVaul, 1997; DeVaul *et al.*, 1997; Li, 1997; Sextro, 1997; Stout, 1997). The data collection and data reduction activities can easily be arranged in a sequence of increasing complexity, increasing data requirements, and likely increasing cost. Whether this approach is reasonable and defensible can only be determined by application to actual field sites followed by a review of the results and experiences. It is recognized that with application, our knowledge will continue to grow, and opinions and recommended practices are likely to evolve and become refined over the next few years.

In order to provide insight to the technical challenges, the reader is first provided an introduction to current approaches for developing generic risk-based screening

levels and a discussion of other technical considerations important to the development of the options described here. This is followed by the proposed array of options for assessing the significance of the vapor intrusion pathway on a more site-specific basis. At the end of this report, a vision for a much simpler site-specific assessment is presented and accompanied by a discussion of the developments necessary to progress toward that goal.

CURRENT APPROACHES FOR DEVELOPMENT OF GENERIC RBSLS

For reference, Figure 1 presents a conceptual model of the situation of interest. The concern here is the potential for adverse impacts due to contaminant vapors emanating from vadose zone soils, impacted capillary fringe soils, or dissolved chemicals in groundwater.

Incidence of vapors in enclosed spaces fall into two major classes. In one class, enclosed-space vapors are found at concentrations near those that could cause immediate impacts (e.g., fire, explosion, acute health risks, etc.). This is most often due to a direct or highly permeable connection (e.g., electrical conduit, gasoline entering a sewer, etc.) between a flammable liquid/vapor and the enclosed space. This class of sites deserves immediate attention and response as required by most state and federal regulatory guidance. In the second class of sites, our concern is with diffusion and advection from the vapor source through a soil layer and into an enclosed space. This report focuses exclusively on this second class of sites, where the concern is for longer-term health effects and time is available to adequately address the problem on a more site-specific basis.

Screening level algorithms for the vapor intrusion pathway (Johnson and Ettinger, 1991; Little *et al.*, 1992; Johnson and Kemblowski, 1998) couple source zone partitioning, vadose zone transport, building foundation transport, and enclosed-space mixing algorithms. The resulting algorithms then depend on parameters related to soil, chemical, and building characteristics. ASTM (1995), USEPA (1996), and some state regulatory agencies have used the Johnson and Ettinger (1991) algorithm to relate the estimated indoor vapor concentration C_{indoor} [mg/m³] to the source zone vapor concentration C_{source} [mg/m³]:

$$\alpha = \frac{\left[\frac{D_T^{\text{eff}} A_B}{Q_B L_T} \right] \exp\left(\frac{Q_{\text{soil}} L_{\text{crack}}}{D_{\text{crack}}^{\text{eff}} \eta A_B} \right)}{\exp\left(\frac{Q_{\text{soil}} L_{\text{crack}}}{D_{\text{crack}}^{\text{eff}} \eta A_B} \right) + \left[\frac{D_T^{\text{eff}} A_B}{Q_B L_T} \right] + \left[\frac{D_T^{\text{eff}} A_B}{Q_{\text{soil}} L_T} \right] \left(\exp\left(\frac{Q_{\text{soil}} L_{\text{crack}}}{D_{\text{crack}}^{\text{eff}} \eta A_B} \right) - 1 \right)} \quad (1)$$

Here $\alpha = (C_{\text{indoor}}/C_{\text{source}})$ is the vapor attenuation coefficient, and A_B = surface area of enclosed space in contact with soil (m²); $D_{\text{crack}}^{\text{eff}}$ = effective overall vapor-phase

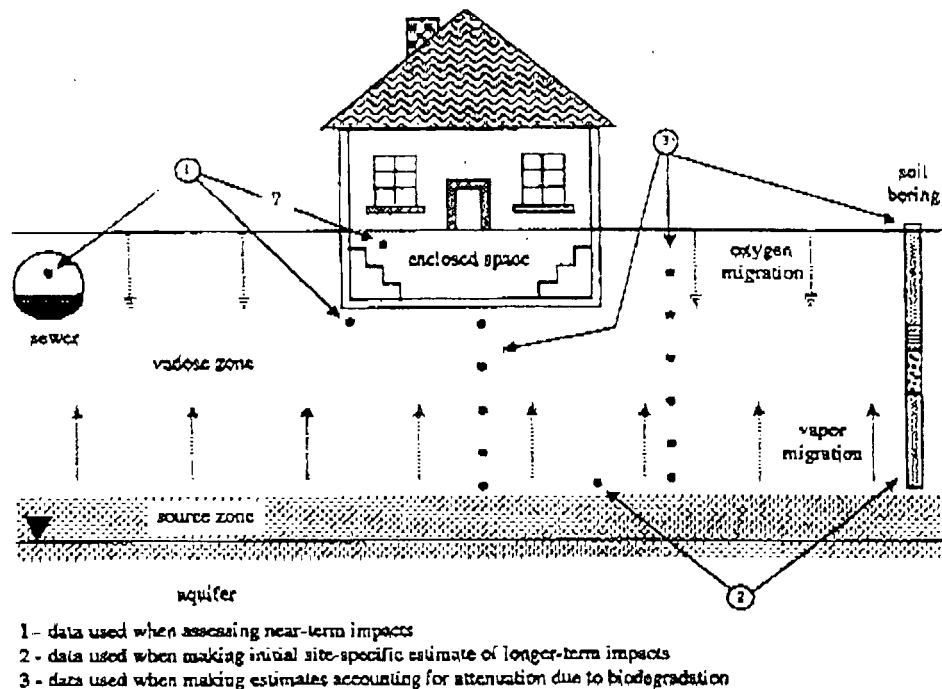


FIGURE 1

Schematic of vapor migration scenario and sampling options.

diffusion coefficient through the walls and foundation cracks [m^2/d]; D_i^{eff} = effective overall vapor-phase diffusion coefficient between the source and foundation [m^2/d]; L_{crack} = thickness of enclosed space walls and foundation [m]; L_T = source-foundation separation [m]; Q_a = enclosed space air exchange rate [m^3/d]; Q_{soil} = soil gas flow rate into enclosed space due to underpressurization [m^3/d]; η = fraction of enclosed space surface area open for vapor intrusion [m^2/m^2].

The effective porous media overall vapor-phase diffusion coefficients are generally determined from the Millington-Quirk formulation (Millington, 1959; Millington and Quirk, 1961; Millington and Shearer, 1971):

$$D^{eff} = D^{air} \frac{\theta_v^{3.33}}{\theta_T^2} + \left(\frac{D^{H_2O}}{H_i} \right) \frac{\theta_m^{3.33}}{\theta_T^2} \quad (2)$$

where: H_i = Henry's Law constant [$(mg/m^3\text{-vapor})/(mg/m^3\text{-}H_2O)$]; θ_m = volumetric moisture content [$m^3\text{-}H_2O/m^3\text{-soil}$]; θ_T = total porosity [$m^3\text{-voids}/m^3\text{-soil}$]; θ_v =

volumetric vapor content [$\text{m}^3\text{-vapor}/\text{m}^3\text{-soil}$]; D^{air} = molecular diffusion coefficient in air [m^2/d]; $D^{\text{H}_2\text{O}}$ = molecular diffusion coefficient in water [m^2/d].

For reference, molecular diffusion coefficients in air for most petroleum fuel compounds range from 0.05 to 0.10 cm^2/s (0.4 to 0.9 m^2/d), molecular diffusion coefficients in water are roughly 1/10000 of molecular diffusion coefficients in air. USEPA (1996) tabulates relevant chemical properties for many chemicals of interest. Total porosity varies roughly between 0.35 and 0.45 for most soil types; in many well-drained sandy soils, $\theta_m < \theta_T/5$, θ_m can approach $\theta_T/2$ in clayey soils, and θ_m approaches θ_T as one moves down through the capillary fringe to groundwater. More information on the parameterization of moisture levels through unsaturated soils and the capillary fringe in various soil types is presented in Guymon (1994).

In typical RBSL calculations, the source zone vapor concentration C_{source} [mg/m^3] is often assumed to be related to the source zone total soil concentration C_T [$\text{mg}/\text{kg}\text{-soil}$], assuming a single-component, linear-partitioning relationships, and three-phase equilibrium (vapor, sorbed, dissolved phases):

$$C_T = C_{\text{source}} \theta_v \left[1 + \frac{\theta_m}{\theta_v H_i} + \frac{\rho_b K_d}{\theta_v H_i} \right] / \rho_b = C_{\text{source}} \theta_v R_v / \rho_b \quad (3)$$

where: K_d = soil sorption coefficient [$(\text{mg}/\text{kg}\text{-soil})/(\text{mg}/\text{m}^3\text{-H}_2\text{O})$]; R_v = soil vapor retardation factor [unitless]; ρ_b = soil bulk density [$\text{kg}\text{-soil}/\text{m}^3\text{-soil}$].

While this expression is used frequently, it is not appropriate for cases where an immiscible phase is present (e.g., residual hydrocarbon source zones). In those cases the partitioning calculations are much more complex and generally nonlinear (Johnson *et al.*, 1990). At high residual soil concentration levels (typically >500 mg/kg total hydrocarbons for gasoline; see Johnson *et al.*, 1990), the partitioning is better approximated by Raoult's Law. Equation (3) may over- or underpredict the vapor concentration calculated using Raoult's Law.

As an example of the use of Eq. 1, Figure 2 presents α vs. D_T^{eff}/L_T for the following reasonable parameter values: $A_B = 50 \text{ m}^2$; $Q_B = 1200 \text{ m}^3/\text{d}$ (12 air changes per day in 100 m^3 enclosed space) $Q_{\text{soil}} = 1.5 \text{ m}^3/\text{d}$ (= 1 L/min); $L_{\text{crack}} = 0.15 \text{ m}$; $D_{\text{crack}} = 0.1 \text{ m}^2/\text{d}$ (cracks filled with well-drained sandy soil; note the results are not sensitive to reasonable changes in this parameter for these conditions) $\eta = 0.001 \text{ m}^2/\text{m}^2$ (note --- the results are not sensitive to reasonable changes in this parameter for these conditions).

This graph allows examination of changes in attenuation with changes in source-enclosed space separation (L_T) and effective diffusion coefficient (D_T^{eff}). For reference moving along the x-axis in the direction of increasing D_T^{eff}/L_T corresponds to moving a source closer to the enclosed space, or, alternatively, to increasing the effective diffusion coefficient (e.g., when decreasing the moisture content). As can be seen, no matter where the source is placed, or what the soil

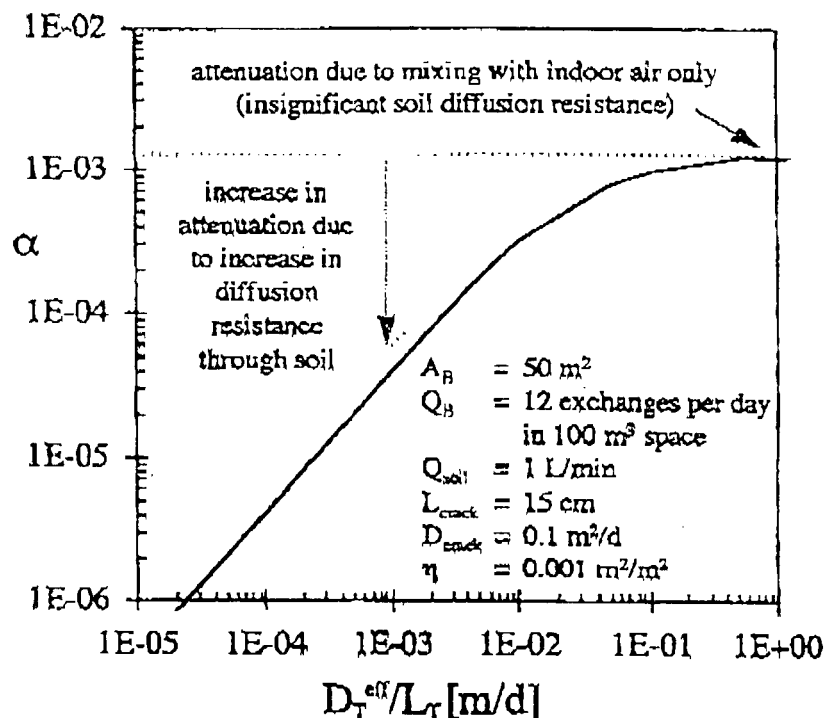


FIGURE 2

Johnson and Ettinger (1991) site-specific vapor attenuation coefficient $\alpha = (C_{\text{indoor}}/C_{\text{source}})$ estimate as a function of the overall effective vapor-phase porous media diffusion coefficient D_T^{eff} and distance between the source and foundation L_T .

properties are, $\alpha \leq 10^{-3}$. The upper asymptote of $\alpha = 10^{-3}$ corresponds to the case where sources are very close to buildings, transport is controlled by advection through the foundation, and attenuation is due solely to dilution by mixing within the enclosed space (e.g., radon intrusion). Below $D_T^{\text{eff}}/L_T = 0.1$ m/d, α is sensitive to changes in source-foundation separation and moisture content. For Q_{soil} values in this range, it can be shown that the results in Figure 2 are not sensitive to changes in η or $D_{\text{crack}}^{\text{eff}}$ within a reasonable range of η and $D_{\text{crack}}^{\text{eff}}$ values.

Due to this sensitivity to source-foundation separation and soil moisture content, and the potential for a wide range of conditions to be encountered in practice, generic calculations are often biased toward relatively close sources and well-drained sandy soils. Thus, α ranges from 10^{-4} to 10^{-3} in most generic RBSL developments.

These results also point toward a practical opportunity for improving the generic RBSL screening process so fewer sites need be addressed on a site-specific basis.

Rather than develop a single attenuation factor for the most conservative geometry and soil type, a table of α values or a contour plot could be developed for a range of possible source-foundation separations and soil types.

Johnson and Ettinger (1991) also show how to account for depleting sources, although this option has not been used often by those developing generic RBSLs. This may be attributed to the fact that users must also define a generic source zone thickness. The impact of considering depleting sources is more significant for carcinogenic compounds, because exposure to these compounds is averaged over a longer period of time (often 30 years) than for noncarcinogens (often 7 years or less).

KEY TECHNICAL CONSIDERATIONS

Factors not typically considered in generic RBSL development include a range of soil types, layered stratigraphies, biodegradation of contaminants, and depleting sources. Any or all of these can be considered when assessing the significance of the vapor intrusion pathway on a site-specific basis. Also, as shown in Figure 1, there are myriad site-specific sampling options. The following technical considerations play an important role in the selection of site-specific data collection and analysis options presented below:

- The options should utilize measurements that are easily integrated into typical site assessments; thus, there is an emphasis on using soil cores, soil moisture, and soil gas measurements.
- For reasons discussed above (see discussion associated with Eq. 3), methods that do not rely on soil vapor-soil contamination partitioning calculations are preferred; thus, the options below emphasize use of soil gas measurements.
- Given current site assessment practices and tools, it is difficult to define source zone geometries and source zone masses with any reasonable accuracy; thus, considering depleting sources on a site-specific basis is not typically a practicable option, although it could be considered in developing generic RBSLs as discussed above.
- The time required for vapors to reach near-steady concentrations at any point increases with the square of the distance from the source and also is affected by the chemical properties of the compound of interest. In addition, the presence or absence of surface barriers (pavement, buildings, etc.) can affect near surface vapor concentrations; thus, in making decisions involving potential future impacts, some options below emphasize the use of soil gas concentrations measured near the source rather than measurements near the surface or enclosed space.

Expanding on this last bullet item, an estimate of the time τ_{ss} [d] required to reach near-steady vapor concentrations and fluxes at any distance L [m] from a source is

$$\tau_{ss} \Rightarrow \frac{R_v \theta_v L^2}{D^{air}} \quad (4)$$

where all quantities are as defined above with R_v the vapor-phase retardation factor, given by Eq. 3. Equation 4 derives from solutions to transient diffusion problems (Crank, 1956) with step-change boundary conditions imposed at zero time. Figure 3 presents calculated τ_{ss}/R_v values for a range of soil moisture contents and: $D^{air} = 0.09 \text{ cm}^2/\text{d}$ ($= 0.78 \text{ m}^2/\text{d}$); $D^{H_2O} = 1 \times 10^{-5} \text{ cm}^2/\text{d}$ ($= 8.6 \times 10^{-5} \text{ m}^2/\text{d}$); $\theta_v = 0.35 \text{ m}^3\text{-voids}/\text{m}^3\text{-soil}$; $H_i = 0.2 \text{ (mg}/\text{m}^3\text{-vapor)}/(\text{mg}/\text{m}^3\text{-H}_2\text{O})$.

For reference, the chemicals most likely to cause exceedences of flammable levels ($C_{indoor} > 1\% \text{ v/v}$) at fuel release sites will have retardation factors close to unity (e.g., propanes, butanes, pentanes). Oxygen will move relatively unretarded

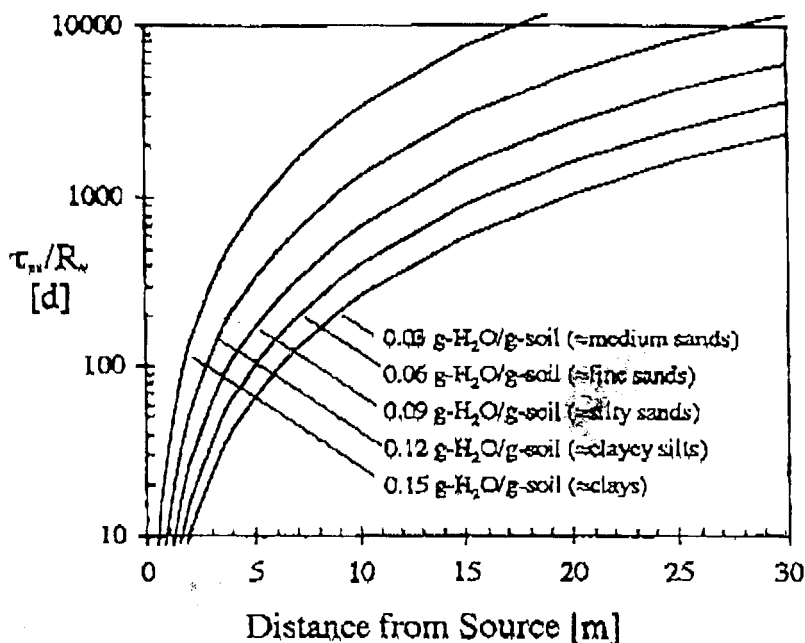


FIGURE 3

Estimated time for nonretarded chemicals to reach near steady vapor concentrations (τ_{ss}/R_v) at the distance L from a source. For retarded compounds multiply the (τ_{ss}/R_v) value by the retardation factor R_v defined in Eq. 4.

Copyright © 1999, CRC Press LLC — Files may be downloaded for personal use only. Reproduction of this material without the consent of the publisher is prohibited.

(high Henry's Law Constant and low sorption), and chemicals most often of concern from health considerations (e.g., monoaromatic hydrocarbons, MTBE) will have vapor-phase retardation factors on the order of $10 < R_v < 100$. Thus, different chemicals will approach near-steady concentrations at different times.

Figure 3 again emphasizes that soil gas hydrocarbon concentrations closer to the source zone reach near-steady values relatively quickly (hours, days); those several meters away may require years or decades to reach near-steady conditions as τ_{ds} increases with the square of the distance from the source. It should be noted that analyses that consider chemical reactions will show that near-steady conditions can be reached faster than shown in Figure 3 when significant degradation rates occur. Significant advection will also decrease the time to reach near steady conditions, as might be the case if pressure-driven vapor flow occurs along or within a permeable conduit.

The major conclusions here are that soil gas concentrations measured near a source will, in most cases, always be representative of near-steady conditions; meanwhile, near-surface, or soil gas concentrations measured several meters from a source may, or may not be representative of near-steady conditions. Thus, the reader is cautioned that site-specific assessment relying on indoor or near-surface and near-foundation or soil gas concentrations measured several meters from a source should only be used when one is confident that the time since the release exceeds the estimate of the time to reach near-steady conditions given by Eq. 4. Site-specific assessment using soil gas concentrations measured near the source is always an option, provided that the user has an understanding of the subsurface geology between the source and enclosed space (see later section).

SITE-SPECIFIC ASSESSMENT OF THE SIGNIFICANCE OF VAPOR MIGRATION TO ENCLOSED SPACES

It is assumed that situations requiring emergency response have been addressed, site conditions have already been compared against generic risk-based screening levels, and exceedences have been noted. Therefore, a more site-specific assessment of future and long-term impacts is desired.

As discussed above, generic RBSLs often assume a vadose zone that is homogeneous, sandy, and relatively dry. Furthermore, biodegradation is neglected and the vapor source is constant with time. Thus, on a site-specific basis, one might assess the potential for increased attenuation (relative to the generic RBSL case) due to: (1) layered strata, (2) higher moisture contents, (3) biodegradation in the vadose zone, and (4) source depletion with time. One might also elect to pursue direct measurement of enclosed-space concentrations or near-foundation soil gas measurements.

In the following, this range of options is discussed. Direct enclosed-space measurement is discussed in the next section and then near-foundation measurements are discussed in a subsequent section. Factors that decrease the potential for

vapor migration impacts, relative to typical regulatory generic base cases, are considered in two later sections. There, increased diffusion resistance is discussed in one of those sections, the use of soil gas concentrations with depth to guide refined analyses are discussed in another, and the incorporation of vadose zone biodegradation in the analysis is addressed in a later section. Source depletion is discussed briefly in the final section.

Table 1 summarizes the options and data collection requirements for each.

Direct Measurement of Enclosed-Space Vapor Concentrations

Whenever it is suspected that explosions, fires, or acute health impacts might occur, vapor samples are quickly collected from the enclosed space or building. Use of this same direct measurement approach for the more refined site-specific assessments of future and long-term impacts, however, is envisioned to be very limited for several practical and technical reasons.

First, obtaining vapor samples from enclosed spaces and interpreting the results involves a host of complex issues and sensitivities. For example, there may be alternate indoor vapor sources already within the enclosed space. Also, sampling occupied buildings or residences often causes unnecessary emotional stress to the occupants. Therefore, for these considerations alone, unless other data (odors, flammable subfoundation vapor concentrations, etc.) suggest a short-term threat, direct collection of indoor vapor samples is generally not preferred. Guidance on considerations for indoor air sampling is given in USEPA (1992). Some of the complications and interferences of indoor air sampling are covered in a series of Total Exposure Assessment Methodology (TEAM) studies undertaken by USEPA (1987).

Second, there is the issue discussed in the previous section concerning whether the current vapor concentrations are representative of long-term conditions. For example, enough time may not have passed to ensure near-steady conditions, or the concentrations may be affected by other dynamic processes (e.g., seasonal changes in soil conditions).

Third, many site-specific assessments will involve sites where a building or enclosed space does not currently exist, and the concern is for impacts under reasonable potential future scenarios.

Therefore, as stated above, this option is envisioned to be of limited use when making more refined site-specific assessments of potential impacts from vapor migration to enclosed spaces.

Use of Soil Gas Samples Collected Near Surface or Near the Foundation of the Enclosed Space

Near surface and subfoundation sampling is an option that is attractive for two primary reasons. First, obtaining samples is relatively straightforward and vapor

TABLE 1
Refinement Options and Associated Data Collection and Analysis Needs

Analysis step	Refinement relative to previous analysis	Description	Data needs relative to base list of needs*
Generic RBSL	None	Calculation of base case RBSLs using generic properties; user should ensure that generic inputs are conservative relative to actual site conditions, soil type and depth to contamination should be known	<ul style="list-style-type: none"> • None
Indoor sampling	Direct measure — no prediction	Vapor sample collected in enclosed space and compared with regulatory limits	<ul style="list-style-type: none"> • Indoor vapor samples at different times of the year • Surety of no other sources • Time since release
Near-foundation and near-surface sampling	Direct measure of current conditions in soil near enclosed-space and estimate of impact to enclosed space	Near-foundation measurement coupled with simple advective-driven vapor intrusion equation	<ul style="list-style-type: none"> • Near-foundation soil gas sample • Estimate of enclosed-space air exchange rate • Time since release
Site-specific: simple refined calculation	Site-specific estimates of effective porous media diffusion coefficients	Use of algorithms employed in Generic RBSL calculation, but input of site-specific effective diffusion coefficient estimate (or value measured <i>in situ</i>), and source zone vapor concentration	<ul style="list-style-type: none"> • Source zone soil vapor concentration • Moisture content vs. depth • Effective diffusion coefficients measured <i>in situ</i> (optional)
Site-specific: refined 1	Site-specific assessment of attenuation due to biodegradation	Use of modified screening-level algorithms, degradation fitting parameter determined from vertical soil gas profile and soil properties, and possibly effective diffusion coefficient measured <i>in situ</i>	<ul style="list-style-type: none"> • Source zone soil vapor concentration • Moisture content vs. depth • Estimate of time since release • Soil vapor concentrations with depth, including O₂ • Effective diffusion coefficients measured <i>in situ</i> (optional)
Site-specific: refined 2	Source zone depletion	Same as above, except model refinements account for source depletion	<ul style="list-style-type: none"> • Same as above, plus source zone dimensions and source mass

* Base case data needs include: subsurface lithology and depth to contamination.

sampling probes can often be driven to depth by hand or with hand-operated power tools. Second, analysis of the data generally does not require additional characterization of the subsurface, or does it rely on prediction of vapor transport through the subsurface between the source and enclosed-space foundation. For example, using Figure 2 one can estimate near-term indoor concentrations from subfoundation measurements:

$$C_{\text{indoor}} = \frac{C_{\text{soil gas}}}{1000} \quad (5)$$

where $C_{\text{soil gas}}$ [mg/m³] is the chemical concentration in soil gas immediately adjacent to the basement wall or foundation. This estimate is specific to the inputs defined previously above, but it is consistent with published data from field studies focused on the relationships between concentrations of radon in soil gas and indoor radon concentrations (Nazaroff, 1987). For enclosed spaces with less air circulation, the resulting indoor concentrations could be greater.

As in the case of direct indoor measurement, it should be noted that there are also serious limitations to this approach, mainly:

- Near-surface soil gas measurements are more prone to sampling errors (often short-circuiting down the sampling probes).
- The presence or absence of surface barriers (pavement, buildings, or lack thereof) can affect near-surface vapor concentrations. For example, near-surface measurements made at open surface sites are unlikely to be representative of near-surface soil gas concentrations under buildings (i.e., see BP, 1997). In contrast, vapor concentrations at depth near the source are not affected significantly by the surface conditions.
- It is possible that not enough time has passed since the release for near-steady soil gas concentrations to be achieved near the surface as discussed above. Meanwhile, near-steady-state vapor concentrations are achieved rapidly enough at depth near the source zone that knowledge of the release history is not critical.

Use of Site-Specific Diffusion Coefficients in the Generic RBSL Algorithms

In this simple refinement option, algorithms employed in generating generic RBSLs are used; however, generic effective diffusion coefficients, soil types, moisture contents, and source-receptor distances are replaced with values more representative of the site under consideration. In this case the data required for generating a conservative site-specific indoor air concentration estimate include:

Copyright © 1999, CRC Press LLC — Files may be downloaded for personal use only. Reproduction of this material without the consent of the publisher is prohibited.

- The source zone vapor concentration
- The location, thickness, and moisture content of all subsurface strata located between the source and enclosed space

Once the data are collected, the following analysis is performed:

1. A subsurface conceptual model is created in which the subsurface is divided into distinct strata, each having a thickness L_i [m]
2. Effective vapor-phase porous media diffusion coefficients (D_i^{eff}) are calculated for each layer using Eq. 2; alternatively, site-specific values can be measured using the method described by Johnson *et al.* (1998)
3. The overall effective diffusion coefficient for the region between the source and enclosed space D_T^{eff} [m^2/d] is calculated using:

$$\frac{D_T^{eff}}{L_T} = \frac{1}{\sum_{i=1}^n \left(\frac{L_i}{D_i^{eff}} \right)} \quad (6)$$

where $L_T (= \sum L_i)$ is the distance between the source and building.

4. Use the (D_T^{eff}/L_T) value calculated with Eq. 6 and Eq. 1 to calculate α , or read the attenuation factor value from Figure 2, if the inputs are reasonable for that site.
5. Use α and the measured source zone vapor concentration C_{source} to determine if expected indoor concentrations exceed target levels.

For example, consider the data shown below in Table 2 for a site that has been conceptualized as having five depth intervals as shown in Figure 4a (BP, 1997). There the moisture content decreases with depth, thereby causing the effective diffusion coefficient to increase with depth. From this table we see that $(D_T^{eff}/L_T) = 0.0042$ m/d. Using Figure 2, this yields $\alpha = 1.5 \times 10^{-4}$. For reference, using standard generic assumptions (ASTM, 1995; sandy soil at 1 m depth), the corresponding values would be $(D_T^{eff}/L_T) = 0.061$ m/d and $\alpha = 8.4 \times 10^{-4}$. Thus, by considering the site-specific soil moisture distribution, the generic enclosed-space concentration estimate was reduced by a factor of about six.

At this site, the source zone vapor concentrations are 94,000 mg/m³ (approx. 0.02% v/v) for total hydrocarbons and 120 ppm, for benzene. Using the site-specific estimate for α yields indoor concentration estimates of 14 mg/m³ (approx. 3 ppm) for total hydrocarbons and 20 ppb, (= 80 $\mu\text{g}/\text{m}^3$) for benzene.

The results of this analysis indicate that even though source zone concentrations exceed flammable levels, concentrations within the enclosed space should remain

TABLE 2
 Sample Use of Field Data
 (Data from BP 1997)
 to Determine Site-Specific Effective
 Vapor-Phase Diffusion Coefficients

Depth [ft BGS]	Type	θ_m [g-H ₂ O/ g-soil]	θ_m [m ³ -H ₂ O/ m ³ -soil] ^a	D_T^* [m ² /d] ^b	D_T^*/L [m/d]
0-4	Silty sand	0.11	0.19	0.016	0.013
4-7	Silty sand	0.12	0.20	0.010	0.011
7-10	Silty sand	0.10	0.16	0.023	0.025
10-13	Sand	0.056	0.10	0.067	0.073
13-16	Sand	0.059	0.10	0.062	0.068
				$D_T^*/L_T =$	0.0042

^a Assuming a bulk soil density of 1.7 g-soil/cm³-soil.

^b For $D_T^* = 0.09 \text{ cm}^2/\text{s} = 0.78 \text{ m}^2/\text{d}$.

well below flammable levels. In fact, this low level would not likely be detected on a portable field instrument, and the benzene concentration is at most an order of magnitude greater than typical urban background levels (Shaw and Singh, 1988). Consistent with this analysis, petroleum hydrocarbons and benzene were not detected above background levels in the building at this site.

Fischer *et al.* (1996) also present soil gas and indoor air concentrations at a petroleum spill site. From their SF₆ tracer gas study data, one can estimate $\alpha = 10^{-4}$ for nondegrading compounds located close to the building that they studied. This is in good agreement with the generic α plot given in Figure 2. The one order-of-magnitude difference ($\alpha = 10^{-3}$ in Figure 2 vs. 10^{-4} measured) is attributable to the high indoor air exchange rates in their study building. Using Figure 2 with the soil moisture and porosity data for that site produces $(D_T^*/L_T) = 0.035 \text{ m/d}$ and $\alpha = 7 \times 10^{-4}$. Using the measured soil gas and indoor air isopentane concentrations yields $\alpha = 7 \times 10^{-7}$. Thus, in this case indoor concentrations are three orders of magnitude lower than predicted by the conservative layered geology algorithm. The agreement would be to within two orders of magnitude, rather than three, if the site-specific building characteristics and exchange rates reported by the authors were considered.

Use and Interpretation of Soil Gas Data with Depth

While soil gas samples with depth are not required in the analysis above, these data can be used to corroborate and test assumptions built into the site conceptual model (e.g., soil moisture and geology assumptions). It is also useful for assessing if additional model refinements are warranted.

Copyright© 1999, CRC Press LLC — Files may be downloaded for personal use only. Reproduction of this material without the consent of the publisher is prohibited.

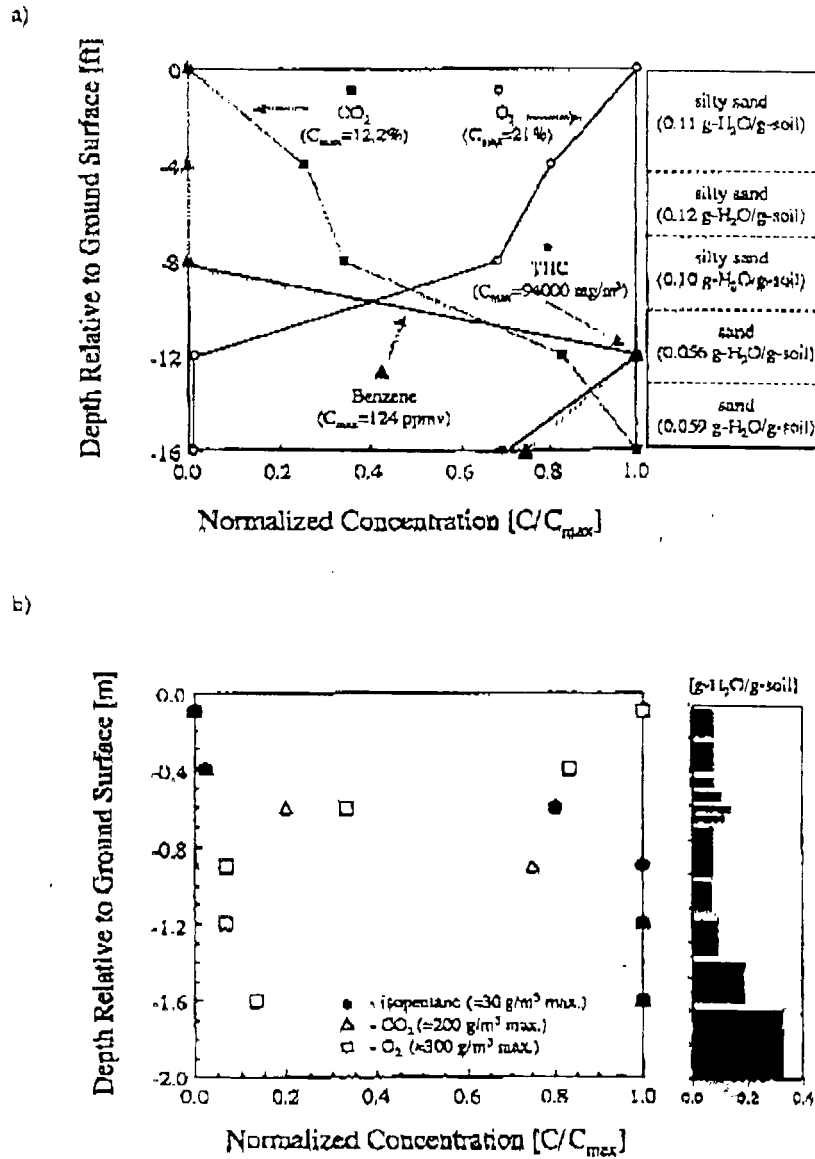


FIGURE 4

Sample presentation using data from (a) BP (1997) and (b) Fischer et al. (1996).

First, the data should only be used if enough time has passed for near steady conditions to have been reached at that sampling depth. The distance from the source, knowledge of the spill history, and Figure 3 can be used in making this decision.

Copyright© 1999, CRC Press LLC — Files may be downloaded for personal use only. Reproduction of this material without the consent of the publisher is prohibited.

Second, soil gas concentrations should be plotted vs. depth and then compared with the expected soil gas concentration profile for the soil moisture content and soil type data, or the measured site-specific effective diffusion coefficients (Johnson *et al.*, 1998).

Next, the data should be plotted and reviewed. Figures 4a and 4b show sample data presentations for data from BP (1997) and Fischer *et al.* (1996). The BP data represent soil gas samples obtained with depth adjacent to a building, while the Fischer *et al.* data represent soil gas samples collected from beneath a building. When plotting data, it is preferred that the soil gas concentrations be overlaid on, or plotted next to, a conceptual model of the subsurface. Available moisture content data should be presented as well. Once the data are plotted, regions across which concentration decrease or increase sharply should be identified.

To check data consistency with the initial refinement discussed above in, the measured vapor concentrations should be compared with the expected concentration profile for the conservative case where soil properties vary with depth, but there is no degradation. For a system composed of n layers, the concentration $C_j(z)$ in any layer j is expected to be:

$$C_j(z) = C(z=0) + [C(L_T) - C(z=0)] \frac{\sum_{i=1}^{j-1} \left(\frac{L_i}{D_i^{eff}} \right) + \frac{z}{D_j^{eff}}}{\sum_{i=1}^{j-1} \left(\frac{L_i}{D_i^{eff}} \right)} \quad (7)$$

where z [m] is measured up from the bottom of layer j , $C(L_T)$ is the concentration at the upper boundary (determined using Eq. 15 in Johnson and Ettinger (1991)), L_i [m] is the thickness of layer i having the effective diffusion coefficient D_i^{eff} [m^2/d]. In layered settings, larger concentration gradients are expected across regions with finer-grained soils and larger moisture contents. For example, Figures 5a and 5b present the predicted concentration profiles for the data presented in Figures 4a and 4b, respectively. For open surfaces, $C(L_T)$ is generally much less than $C(z=0)$ and can be neglected; however, this may not hold true for covered sites or below a building (Fischer *et al.*, 1996, BP 1997).

At this point, the predicted concentration distributions should be compared with the field data. If there is good agreement, then diffusion is likely the dominant transport attenuation mechanism, biodegradation is not playing a significant role, and the initial site-specific estimate of attenuation likely describes behavior adequately at the site. For example, consider Figures 5a and 5b. Here the concentration profiles are not well predicted, although the qualitative features are better predicted in Figure 5b than in 5a. Agreement would be better in Figure 5b, if it happened that the moisture content in the 0.48 to 0.58 m region BGS was closer to 0.15 g-H₂O/g-soil than to 0.10 g-H₂O/g-soil. The effect of this change on the predictions is shown in Figure 5b.

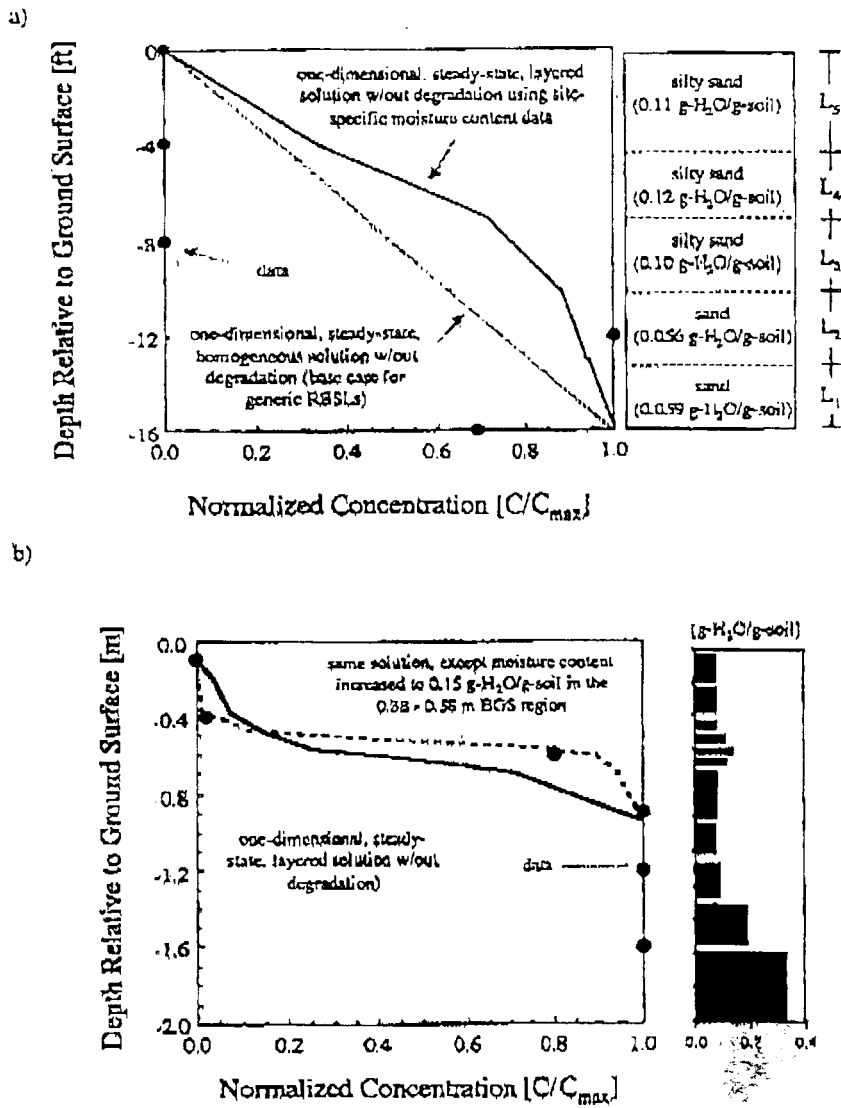


FIGURE 5

Vapor concentration data compared with predictions for one-dimensional transport through a layered system without degradation, using data from (a) BP (1997) and (b) Fischer et al. (1996).

As in Figure 5a, the sharp transitions observed in actual concentration profiles may not appear in the predicted concentration profiles, and deviations might not be easily attributable to reasonable errors in soil property measurements. One

Copyright © 1999, CRC Press LLC — Files may be downloaded for personal use only. Reproduction of this material without the consent of the publisher is prohibited.

possibility is that these sharp transitions could be the result of thin finer-grained soil layers not detected in the initial geologic assessment. To test this hypothesis at a site, the user can either collect additional continuous soils cores, or conduct *in situ* diffusion coefficient measurements in the region of the sharp transition. For example, given the data in Figure 4a, *in situ* diffusion coefficient measurements would be made in the 4 to 8 ft BGS, 8 to 12 ft BGS, and 12 to 16 ft BGS intervals. It should be noted that there may be more than one plausible hypothesis for a given data set. For example, Fischer *et al.* proposed that their observed sharp transition was the result of more highly transmissive near-surface soils and subsurface advective flow resulting from wind-induced pressure gradients.

Ideally, soil gas samples should be collected from each distinct soil strata identified by the geologic assessment at a site. Vadose zone sampling implants connected to ground surface with small diameter (1/8" OD) nonadsorbing tubing are the preferred method of data collection. It is recommended that the implants be left in place for future sampling, because often more than one sampling event is necessary. The implants can then also be used for performing *in situ* diffusion coefficient measurements. The intent here is not to provide detailed guidance for soil gas sampling; however, the two main concerns in soil gas sampling are the ability to collect discrete depth samples and to prevent atmospheric dilution. For this reason, readers should note that: (1) sample line and vapor sampler volumes should be minimized so that the purge volume is small, (2) the potential for atmospheric short-circuiting down the annulus between the soil and sampler should be minimized, and (3) sampling flow rates in the range of about 1 L/min or less are preferred.

Accounting for Attenuation Due to Biodegradation in Site-Specific Assessments

Incorporation of aerobic biodegradation into the site-specific assessment of potential vapor migration impacts is discussed here. As in previous sections, much of the following analysis is appropriate only for sites that have reached near-steady conditions. In the case that near-steady conditions are not likely to have been achieved, the user should review the discussion below in concerning site conditions that are likely more conducive for degradation, and to identify if such conditions exist at their site.

To assess if significant vapor migration attenuation due to biodegradation is occurring, it is necessary to characterize the vertical soil gas distribution and vapor transport properties of the unsaturated zone. Information needed includes:

- Total hydrocarbon soil gas concentration vs. depth.
- Specific chemicals soil gas concentrations of interest vs. depth (e.g., benzene)

- Oxygen soil gas concentrations vs. depth
- Site conceptual model (layers, soil types, depth to source, etc.)

When selecting specific analytes, it is useful to include at least one compound that is known to be recalcitrant to degradation and is relatively unretarded, even though it may not be of concern from a health risk perspective. As mentioned above, these data can be used to ensure that estimates of the diffusive properties of the soil are reasonable and that near-steady conditions exist.

In some cases, there will be large discrepancies between the measured concentrations and those predicted with Eq. 7 as is the case in Figure 5a and Figure 6 (Ostendorf and Kampbell, 1991). This may be an indication of significant biodegradation, but may also be due to either poor site characterization data or non-near-steady conditions. Thus, if it is hypothesized that biodegradation is playing an

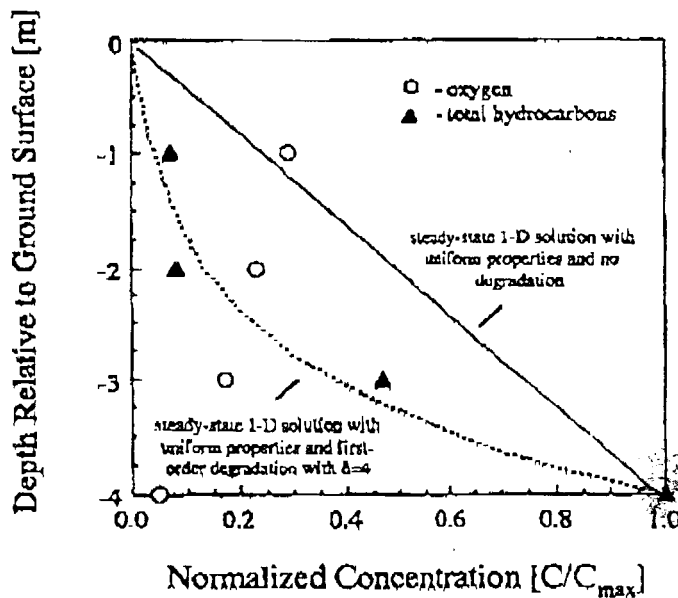


FIGURE 6

Normalized hydrocarbon and oxygen soil gas concentrations in a shallow near-homogeneous setting; data from Ostendorf and Kampbell (1991). Lines show expected concentration profiles in homogeneous settings at near steady conditions for no degradation, and first-order degradation.

Copyright © 1999, CRC Press LLC — Files may be downloaded for personal use only. Reproduction of this material without the consent of the publisher is prohibited.

important role, then it is important to look for other supporting evidence of biodegradation, including

- Decreasing oxygen concentrations with depth that are consistent with the contaminant vapor concentration profile (e.g., sharp transitions in same region) and substantially different from oxygen profiles with depth in background soils
- Elevated carbon dioxide levels consistent with oxygen profile
- Relatively stable soil gas concentrations with time

These are traditional indicators of aerobic biodegradation. If one simply desires only to demonstrate that natural attenuation is occurring in the vadose zone, then the data needs listed above are sufficient for this purpose at most sites. If, however, one wishes to be more quantitative and to incorporate bio-attenuation into the development of site-specific vapor intrusion pathway screening levels, additional analysis is necessary.

If the data suggest that biodegradation is playing a significant role, as is suggested in Figures 5b and 6, then the next challenge is to characterize this behavior sufficiently to be able to refine the assessment of the significance of the vapor migration pathway. At this point in time it is not clear how to best accomplish this in general, as available data have been limited and models are still being developed, tested, and refined. Below two possible screening-level model refinements (Johnson and Kemblowski, 1998) are presented. These are inspired by available field and laboratory soil column data. Neither model has undergone rigorous comparison with extensive field data. Both are capable of mimicking characteristics of the available data as shown below, and hence are adequate for fitting and extrapolation purposes. Both decouple oxygen and hydrocarbon vapor transport so that complete speciation of the hydrocarbon vapors is not required.

The first algorithm mimics data from shallow (<4 m BGS) and relatively homogeneous settings, such as those studied by Ostendorf and Kampbell (1991) in the field and DeVaul (1997) in the laboratory. Figure 6 presents a subset of the data from Ostendorf and Kampbell (1991) as an illustration. Generally in these settings the oxygen concentration in the soil gas remains high (>5% v/v), except perhaps in the vicinity of the source zone. The contaminant vapor concentrations appear to decrease exponentially with distance away from the source, and at any point are less than those that would be predicted by the one-dimensional steady-state model discussed in the previous section, assuming uniform properties and no degradation.

Here a screening model that assumes a first-order reaction in a homogeneous medium is used. In this case the equation describing the steady-state vapor concentration profile $C(Z)$ [mg/m^3] is

$$C(Z) = \frac{C(Z=1)[e^{-\delta z} - e^{\delta^2}] + C(Z=0)[e^{-\delta(1-z)} - e^{\delta(1-z)}]}{[e^{-\delta} - e^{\delta}]} \quad (8)$$

where L [m] is the depth interval of interest, $Z = z/L$ is the normalized height above the source zone, δ is given by:

$$\delta = \sqrt{\frac{\lambda_1 \theta_m L^2}{H_1 D^{eff}}} \quad (9)$$

where λ [d^{-1}] is a first-order decay coefficient for degradation that is assumed to occur in the soil moisture. The parameter η represents a ratio of degradation rate to diffusion rate; therefore, it is expected that attenuation will increase with increasing δ .

For reference, Figure 7 presents a family of type curves predicted by Eq. 8 for a range of δ values, assuming that $C(Z=1) \ll C(Z=0)$. Note that the curves in

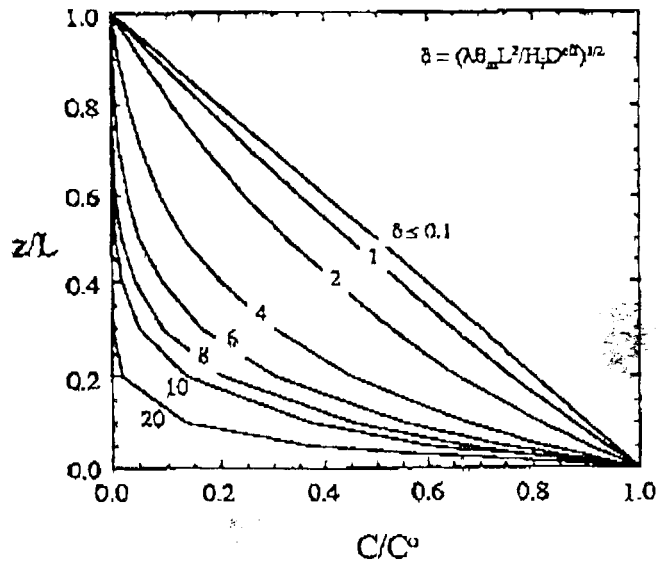


FIGURE 7

Predicted vapor concentration profiles for a homogeneous system at steady-state with a first-order reaction using Eq. 8.

Copyright© 1999, CRC Press LLC — Files may be downloaded for personal use only. Reproduction of this material without the consent of the publisher is prohibited.

Figure 7 suggest that degradation does not significantly impact the shape of the vapor concentration distribution unless $\eta > 1$.

Incorporating Eq. 8 into the development of Johnson and Ettinger (1991) yields the following refined equation for the attenuation factor (Johnson and Kemblowski 1998):

$$\alpha = \frac{C_{\text{indoor}}}{C_{\text{source}}} = \left\{ \frac{1-\beta}{\left[(1-\beta) \left(\frac{Q_B L}{D_{\text{eff}} A_B} \right) \left(\frac{e^\delta - e^{-\delta}}{2\delta} \right) + \beta \left(\frac{Q_R}{Q_{\text{soil}}} \right) \left(\frac{e^{-\delta} + e^\delta}{2} \right) + \left(\frac{e^{-\delta} + e^\delta}{2} \right) \right]} \right\} \quad (10)$$

where:

$$\beta = 1 - \exp\left(\frac{Q_{\text{soil}} L_{\text{crack}}}{D_{\text{crack}} A_{\text{crack}}} \right) \quad (11)$$

and all other parameters are as defined above for Eq. (1).

Figure 8 plots the attenuation factor α as a function of (D_{eff}/L) for a range of δ . All parameter values are the same as those used in Figure 2. Note that unless, $\delta > 1$ the impact of including degradation is negligible. In addition, α is very sensitive to small variations in δ when $\delta > 1$.

The procedure for using this refined model is as follows:

1. Compare field data with predictions given by Eq. 8 for a range of δ values (one simple approach would be to plot normalized data on top of Figure 7)
2. Assess whether Eq. 8 adequately describes the data, and if so, find the value of δ that best fits the field data
3. Then use this value of δ to obtain a value of α from Eqs. 10 and 11, or Figure 8
4. Use α and the measured source zone vapor concentration C_{source} to determine if expected indoor concentrations exceed target levels.

For example, as shown in Figure 6, the Ostendorf and Kampbell data can be reasonably fit with Eq. 8 using $\delta = 4$.

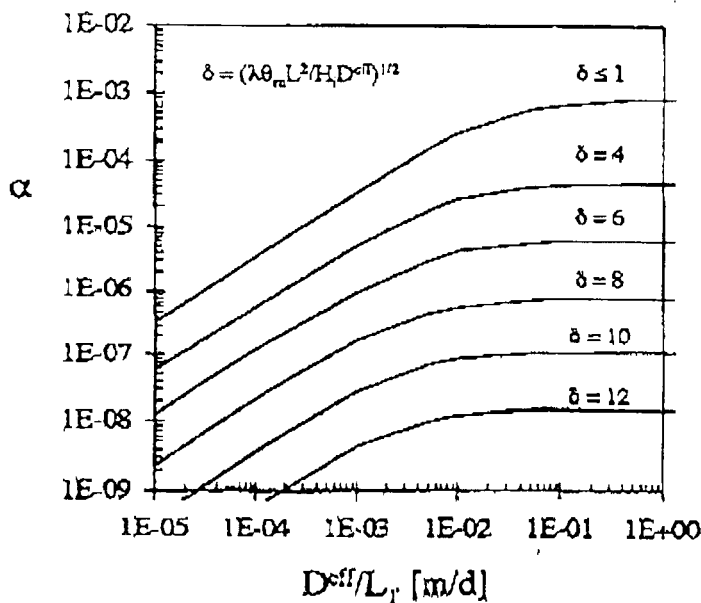


FIGURE 8

Attenuation coefficient predicted by Eq. 10 for the case of a homogeneous medium at steady-state with a first-order degradation reaction.

Given the sensitivity to small changes in δ when $\delta > 1$, it is recommended that δ be regarded simply as a site-specific fitting parameter. It is also recommended at this time that δ values derived for one site not be used at other sites. In addition, δ values may be specific only to the setting for which they are measured; for example, the data in Figures 4a and 6 are specific to two sites without ground cover. It is not yet known if it is appropriate to extrapolate that data to covered areas at those two sites.

If one is interested in developing a database of first-order degradation rate values (λ_{γ}) with an aim toward justifying conservative base-level generic degradation rates, then great care should be taken to also characterize the diffusive properties of the system at each site contributing to the database.

Data of the type shown previously in Figure 4 are not well fit by the simple first-order degradation model discussed above. These data sets are characterized by substantial changes in contaminant and oxygen concentrations across relatively thin vadose zone sections. Generally, these sections also correspond to regions of higher moisture content or decreased air-filled porosity. Thus, the processes occur-

ring in these sections dominate the overall observed behavior for a number of reasons, including higher diffusion resistances and increased residence times for reaction.

Data of this type might be reasonably fit by a "dominant layer" model (Johnson and Kemblowski, 1998). In this approach the vadose zone is conceptualized as having three zones as shown in Figure 9. A central zone in which the reaction takes place is bordered by two zones through which transport occurs without reaction. At near steady-state conditions the concentration profile for this scenario is given by (Johnson and Kemblowski, 1998):

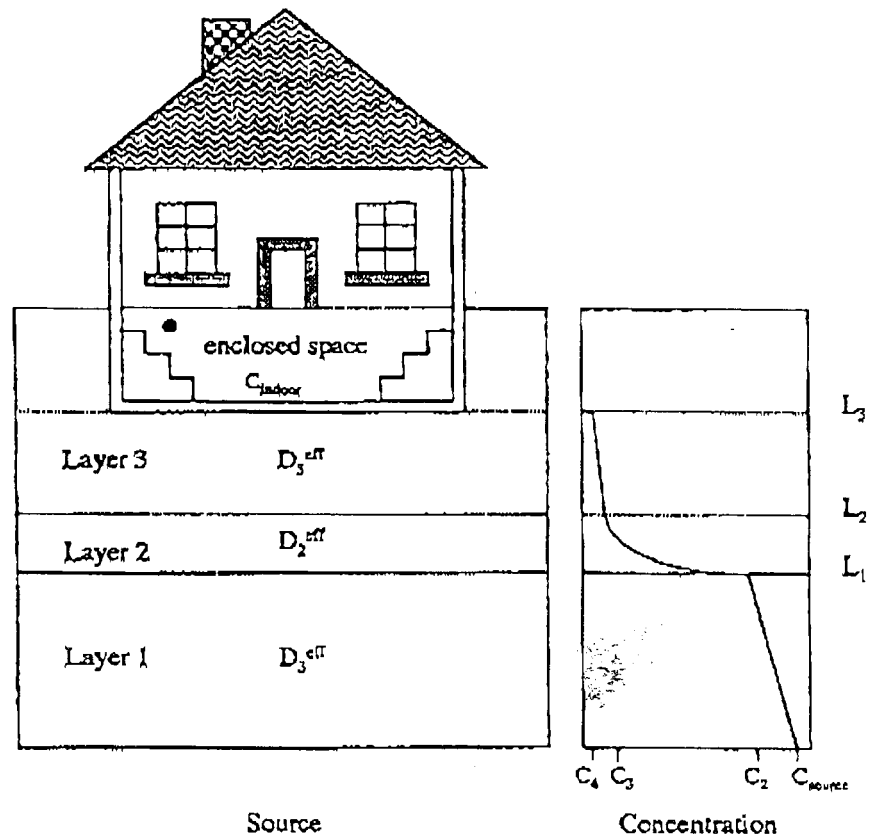


FIGURE 9

Schematic of dominant layer model bio-attenuation scenario.

Copyright© 1999, CRC Press LLC — Files may be downloaded for personal use only. Reproduction of this material without the consent of the publisher is prohibited.

$$C(z) = C_{\text{source}} - (C_{\text{source}} - C_2) \left(\frac{z}{L_1} \right) \quad \text{Region 1 } (0 < z < L_1) \quad (12)$$

$$C(z) = \frac{\left[C_3 e^{\delta \frac{(L_1-z)}{(L_2-L_1)}} - C_2 e^{\delta \frac{(L_2-z)}{(L_2-L_1)}} \right]}{[e^{-\delta} - e^{\delta}]} + \frac{\left[C_2 e^{-\delta \frac{(L_2-z)}{(L_2-L_1)}} - C_2 e^{-\delta \frac{(L_1-z)}{(L_2-L_1)}} \right]}{[e^{-\delta} - e^{\delta}]} \quad \text{Region 2 } (L_1 < z < L_2) \quad (13)$$

$$C(z) = C_3 - (C_3 - C_4) \left(\frac{z - L_2}{L_3 - L_2} \right) \quad \text{Region 3 } (L_2 < z < L_3) \quad (14)$$

where:

$$\delta = \sqrt{\frac{\lambda_i \theta_m (L_2 - L_1)^2}{H_i D^{eff}}} \quad (15)$$

Using the general development of Johnson and Ettinger (1991), the attenuation coefficient α for this approach becomes (Johnson and Kemblowski, 1998):

$$\alpha = \frac{C_{\text{indoor}}}{C_{\text{source}}} = \left\{ \frac{1 - \beta}{\left[(1 - \beta) \left(\frac{Q_B L}{2\phi\gamma\psi} \right) + \left(\beta \left(\frac{Q_B}{Q_{\text{soil}}} \right) - 1 \right) \left(\frac{1 + \gamma\psi - \phi\psi^2}{2\gamma\psi^2} \right) \right]} \right\} \quad (16)$$

where:

Copyright© 1999, CRC Press LLC — Files may be downloaded for personal use only. Reproduction of this material without the consent of the publisher is prohibited.

$$\beta = 1 - \exp\left(\frac{Q_{\text{soil}} L_{\text{crack}}}{D_{\text{crack}} A_{\text{crack}}}\right) \quad (17)$$

$$\gamma = \left(\frac{D_1^{\text{eff}}}{D_2^{\text{eff}}}\right) \frac{[e^{-\delta} - e^{\delta}]}{\delta} \frac{(L_2 - L_1)}{L_1} \quad (18)$$

$$\sigma = \left(\frac{D_1^{\text{eff}}}{D_2^{\text{eff}}}\right) \frac{[e^{-\delta} - e^{\delta}]}{\delta} \frac{(L_2 - L_1)}{(L_3 - L_2)} \quad (19)$$

$$\psi = \frac{1}{e^{-\delta} + e^{\delta} - \gamma} \quad (20)$$

$$\phi = \left(\frac{A_B D_3^{\text{eff}}}{L_3 - L_2}\right) \frac{1}{[\sigma - (1/\psi) - \gamma + 4\psi]} \quad (21)$$

To solve for the concentration profile, Eq. 16 is first solved to get α . Then each of the following relations is solved sequentially for C_4 , C_3 , and C_2 , in terms of C_{source} .

$$\frac{C_4}{C_{\text{source}}} = \frac{2\beta\gamma\psi\phi - \alpha Q_{\text{soil}}}{(\beta - 1)Q_{\text{soil}} - \frac{\beta\phi}{\psi} - \beta\gamma\phi + 4\beta\psi\phi} \quad (22)$$

$$\frac{C_3}{C_{\text{source}}} = \frac{2\gamma\psi + \sigma(C_4/C_{\text{source}})}{\sigma - \frac{1}{\psi} - \gamma + 4\psi} \quad (23)$$

$$\frac{C_2}{C_{\text{source}}} = 2\psi(C_3/C_{\text{source}}) - \gamma\psi \quad (24)$$

These equations are easily set up and solved within any standard spreadsheet. Figure 10 illustrates model predictions compared with the data from Fischer *et al.* (1996) for the case of the parameters defined in Table 3. No attempt has been made to find a best fit here, and it is clear that results are sensitive to small changes in δ . With $\delta = 6$ in Eq. 16, then $\alpha = 10^{-6}$, which is of the same order of magnitude as the empirical value based on measured soil gas and indoor isopentane concentrations. It is also roughly three orders of magnitude lower than the estimate generated in the previous section for the case of a layered system without degradation. Even though good agreement is achieved here, it should be cautioned that there may be other reasonable hypotheses consistent with this data set, as discussed

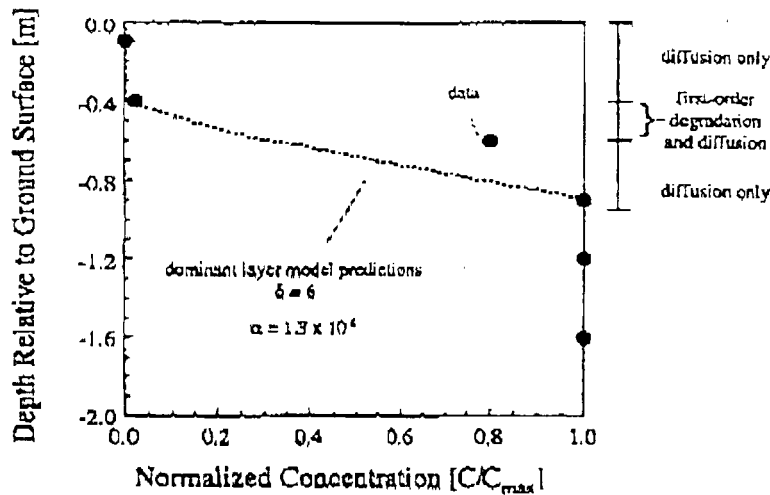


FIGURE 10

Comparison of dominant layer model with data from Fischer et al. (1996).

TABLE 3
Inputs Used in Generating
Figure 10 Using the Dominant Layer Model

Property	Layer		
	1	2	3
Thickness [m]	0.3	0.2	0.4
δ	0	6	0
D^{eff} [m ² /d]	0.07	0.02	0.05

above. This is especially true for this data set, especially because the first-order decay constant consistent with Eq. 15, $\delta = 6$, and the other site-specific data are about 1000 to 10,000 greater than typically reported first-order biodegradation rates (roughly $\lambda = 22 \text{ d}^{-1}$ vs. 0.001 to 0.01 d^{-1} based on dissolved groundwater plume data fitting). Here the data are used simply to demonstrate use of the equations as fitting and extrapolation tools, and it is recognized that there may be alternate mechanistic explanations for the behavior observed at this site.

Other Refinements

One can also consider source zone depletion when refining their assessment of potential vapor migration impacts. This requires knowledge of contaminant distri-

butions in soil and knowledge of contaminant partitioning properties and behavior. Johnson and Ettinger (1991) describe how to account for depleting sources using this information. It is not discussed further here, because it is unlikely that the necessary data will be known with any degree of accuracy greater than what would be assumed when generating generic RBSL estimates. It is also felt that the majority of sites can be adequately assessed on a site-specific basis using the guidance provided in previous sections. In addition, the issue of source longevity is one that has received little attention to date and is not well understood.

AN OPPORTUNITY FOR THE FUTURE

Figures 7 and 8 and the data from Fischer *et al.* (1996) and BP (1997) suggest that there is potential for a much simpler site-specific screening methodology to be developed. Collectively, this information suggests that there conditions might exist for which bio-attenuation is so significant that there would be no potential for adverse impacts at any possible source vapor concentration. If these critical conditions could be defined, then vertical soil gas profiling and determination of biological rate constants at each site would not be necessary. Instead, one would focus site assessment activities on identifying if the critical conditions were satisfied. As an added benefit, it would also not be as important to determine if vapor concentrations had reached near-steady conditions before reaching a conclusion regarding the significance of vapor migration.

One hypothesis is that these critical conditions include the following:

- No significant advective vapor flow ($uL/D_1^{eff} < 1$; μ = velocity)
- Sufficient oxygen for aerobic biodegradation ($>5\%$ v/v)
- Nonrecalcitrant, aerobically biodegradable compounds
- Slow enough diffusion rates and long enough distances for degradation to be significant

The first two can be reasonably quantified based on existing literature; for example, both the bioventing and groundwater biodegradation literature suggest that aerobic degradation slows significantly when oxygen concentrations are less than about 25% of air-saturated conditions (5% v/v or 2 mg/L-H₂O).

The last condition is the one for which future study is needed. To help show how it might be quantified, Figure 11 has been prepared. It presents the distance L_{ent} [m] over which the vapor concentration would be reduced by 99.9% as a function of soil moisture content for the range of first-order decay rates displayed. Figure 11 is derived from Eq. 8, which yields the condition for this case that:

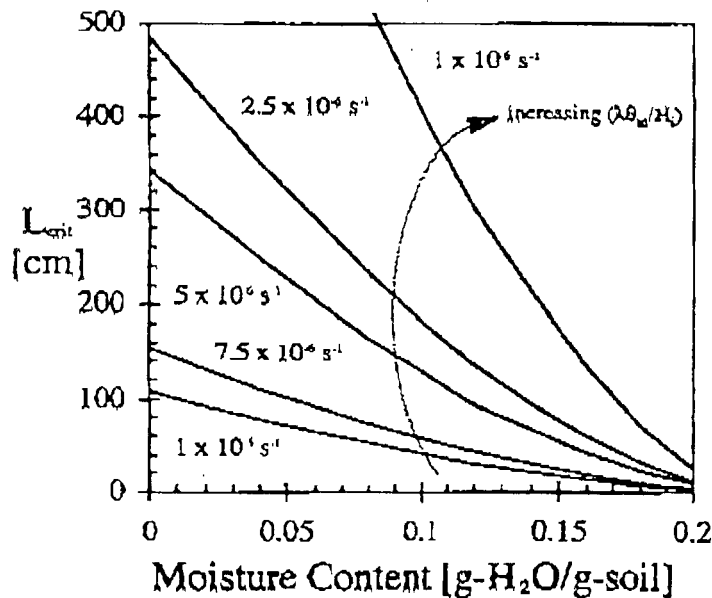


FIGURE 11

Hypothetical plot showing conditions necessary for significant bio-attenuation.

$$\frac{L_{crit}^2 \lambda \theta_w}{H_1 D^{eff}} = 6.9 \quad (25)$$

Figure 11 is presented for illustrative purposes only. It should be noted that at this time a range of reasonable first-order degradation rates has yet to be identified, and we do not even know if first-order expressions adequately describe the kinetics. The reader is referred to DeVaul *et al.* (1997) for more discussion on this issue.

However, for the sake of illustration, suppose that $10^{-6} < \lambda \theta_w / H_1 < 10^{-5} \text{ s}^{-1}$ is agreed to be a reasonable range and that a concentration reduction of 99.9% is sufficient to alleviate vapor migration concerns at service station spill sites. Then a graph of this type would define all the possible combinations of acceptable vadose zone thicknesses and moisture contents. Then, in the initial assessment, a user would simply collect and compare the site-specific moisture content distribution and source-receptor distance with a graph like this to ensure sufficient bio-attenuation. For example, soils with moisture contents $\approx 0.1 \text{ g-H}_2\text{O/g-soil}$ require soil thicknesses of $\approx 0.2\text{--}4.0 \text{ m}$ to assure a 99.9% reduction. Figure 11 shows that much thinner strata of higher moisture content would also achieve the same effect.

For a concept like this to progress, more well-documented data and fundamental research studies are needed to identify reasonable kinetic expressions and kinetic parameters and to verify the hypotheses presented above.

Copyright© 1999, CRC Press LLC — Files may be downloaded for personal use only. Reproduction of this material without the consent of the publisher is prohibited.

ACKNOWLEDGMENTS

The authors would like to acknowledge financial support provided by the American Petroleum Institute and the comments, suggestions, and encouragement provide by Roger Claff, George DeVaul, Harley Hopkins, Vic Kremesec, Tom Feargin, and Robert Ettinger.

REFERENCES

- Acomb, L., Rea, C., Simpkin, T., Hoffman, R., and Elder. 1996. Intrinsic Remediation of Shallow Vadose Zone Petroleum Hydrocarbons. The Proceedings of the APLINGWA Petroleum Hydrocarbons and Organic Chemicals in Groundwater: Prevention, Detection, and Remediation. Houston, TX, November 13-15, 367-382.
- ASTM. Standard Guide for Risk-Based Corrective Action Applied at Petroleum Release Sites. 1995. E1739-95; American Society for the Testing of Materials, 100 Barr Harbor Dr., West Conshohocken, PA 19428.
- Auer, L. H., Rosenberg, N. D., Birdsell, K. H., and Whitney, E. M. 1996. The effects of barometric pumping on contaminant transport. *J. Contamin. Hydrogeol.* 24, 145-166.
- British Petroleum. 1997. Summary of Field Activities Hydrocarbon Vapor Migration Research Project BP Oil Test Site Paulsboro, New Jersey. Prepared by Integrated Science and Technology, Inc. Cleveland, OH. February.
- Crank, J. 1956. *The Mathematics of Diffusion*. Oxford at the Clarendon Press.
- DeVaul, G. E. 1997. Biological and Other Loss Mechanisms Associated with Gasoline Volatilization from Soils. Presented at the Petroleum Environmental Research Forum (PERF) Workshop. Brea, CA. February 6 to 7.
- DeVaul, G. E., Etringer, R. A., Salanitro, J. P., and Gustafson, J. B. 1997. Benzene, Toluene, Ethylbenzene and Xylenes [BTEX] Degradation in Vadose Zone Soils During Vapor Transport: First-Order Rate Constants. The Proceedings of the APLINGWA Petroleum Hydrocarbons and Organic Chemicals in Groundwater: Prevention, Detection, and Remediation. Houston, TX. November.
- Fischer, D. and Uehrin, C. G. 1996. Laboratory simulation of VOC entry into residence basements from soil gas. *Environ. Sci. Technol.* 30(8), 2598-2603.
- Fischer, M. L., Bentley, A. J., Dunkin, K. A., Hodgson, A. T., Nazaroff, W. W., Sextro, R. G., and Daisey, J. M. 1996. Factors affecting indoor air concentrations of volatile organic compounds at a site of subsurface gasoline contamination. *Environ. Sci. Technol.* 30(10), 2948-2957.
- Fitzpatrick, N. A. and Fitzgerald, J. J. 1997. An Evaluation of Vapor Intrusion into Buildings through a Study of Field Data. Massachusetts Department of Environmental Protection.
- Garbesi, K. and R. G. Sextro. 1989. Modeling and field evidence of pressure-driven entry of soil gas into a house through permeable below-grade walls. *Environ. Sci. Technol.* 23(12), 1481-1487.
- Guymon, G. L. 1994. *Unsaturated Zone Hydrogeology*. Prentice Hall, New Jersey.
- Hodgson, A. T., Garbesi, K., Sextro, R. G., and Daisy, J. M. 1992. Soil-Gas Contamination and Entry of Volatile Organic Compounds into a House Near a Landfill. *J. Air Waste Manag. Assoc.* 42, 277-283.
- Jeng, C. Y., Kremesec, V. J., Jr., and Primack, H. S. 1996. Models of Hydrocarbon Vapor Diffusion Through Soil and Transport into Buildings. The Proceedings of the APLINGWA Petroleum Hydrocarbons and Organic Chemicals in Groundwater: Prevention, Detection, and Remediation. pp. 319-333. Houston, TX, November 13-15.

- Jin, Y. 1994. Transport and biodegradation of toluene in unsaturated soil. *J. Contamin. Hydrol.* 17, 111-127.
- Johnson, P. C., Bruce, C., Johnson, R. L., and Kemblowski, M. W. 1998. *In situ* measurement of effective vapor-phase porous media diffusion coefficients. Accepted for publication by *Environmental Science and Technology*.
- Johnson, P. C. and Ettinger, R. A. 1991. Heuristic model for predicting the intrusion of contaminant vapors into buildings. *Environ. Sci. Technol.* 25(8), 1445-1452.
- Johnson, P. C., Hertz, M. B., and Byers, D. L. 1990. Estimates for Hydrocarbon Vapor Emissions Resulting from Service Station Remediations and Buried Gasoline-Contaminated Soils. In *Petroleum Contaminated Soils*. pp. 295-326. Volume 3 (Kostecki, P. T. and Calabrese, E. J. Eds.). Lewis Publishers.
- Johnson, P. C. and Kemblowski, M. W. 1998. Refinements to the heuristic model for assessing impacts of vapor migration to enclosed spaces: bio-attenuation. In preparation.
- Johnson, R. L. and Perrott, M. 1991. Gasoline vapor transport through a high water content soil. *J. Contamin. Hydrol.* 8, 317-334.
- Jury, W. A., Spencer, W. F., and Farmer, W. J. 1983. Behavior assessment model for trace organics in soil. I. Model description. *J. Environ. Qual.* 12, 558-564.
- Jury, W. A., Russo, D., Streile, G., and El Abd, H. 1990. Evaluation of volatilization of organic chemicals residing below the soil surface. *Water Res. Res.* 26 (1), 13-20.
- Kampbell, D. H., Wilson, J. T., Read, H. W., and Stocksdale, T. T. 1987. Removal of Volatile Aliphatic Hydrocarbons in a Soil Bioreactor. *J. Air Pollut. Control Assoc.* 37, 1236-1240.
- Lahvis, M. A. and Bachr, A. L. 1996. Estimation of Rates of Aerobic Hydrocarbon Biodegradation by Simulation of Gas Transport in the Unsaturated Zone. *Water Res. Res.* 32 (7), 2231-2249.
- Li, D. X. 1997. Diurnal Changes in Subsurface Vapor Transport. Presented at the Petroleum Environmental Research Forum (PERF) Workshop. Brca, CA. February 6-7.
- Little, J. C., Daisey, J. M., and Nazaroff, W. W. 1992. Transport of Subsurface Contaminants into Buildings. *Environ. Sci. Technol.* 26(11), 2058-2066.
- Loureiro, C.O., Abriola, L. M., Mardin, J. E., and Sextro, R. G. 1990. Three-dimensional simulation of radon transport into houses with basements under constant negative pressure. *Environ. Sci. Technol.* 24(9), 1338-1348.
- Millington, R. J., 1959. Gas diffusion in porous media, *Science*, 130, 100-102.
- Millington, R. J. and Quirk, J. P., 1961. Permeability of Porous Solids. *Trans. Faraday Soc.* 57, 1200-1207.
- Millington, R. J. and Shearer, R. C., 1971. Diffusion in aggregated porous media, *Soil Sci.* 111, 372-378.
- Moore, A., Revell, S., and Norland, B. 1997. Calibration of Models of Vapor Transport into Buildings. The Proceedings of the API/NGWA Petroleum Hydrocarbons and Organic Chemicals in Groundwater: Prevention, Detection, and Remediation. Houston, TX. November 13-15.
- Moyer, E. E., Ostendorf, D. W., Richards, R. J., and Goodwin, S. 1994. Determination of petroleum hydrocarbon bioventing kinetics in an intact unsaturated zone soil core. Submitted to Water Resources Research.
- Nazaroff, W. W., Lewis, S. R., Doyle, S. M., Moed, B. A., and Nero, A. V. 1987. Experiments on pollutant transport from soil into residential basements by pressure-driven airflow. *Environ. Sci. Technol.* 21(5), 459-466.
- Ostendorf, D. 1993. Hydrocarbon vapor diffusion in intact core sleeves. *Ground Water Monitoring and Remediation*. Winter, 139-150.
- Ostendorf, D. W. and Kampbell, D. H. 1990. Bioremediated soil venting of light hydrocarbons. *Hazardous Waste and Hazardous Materials*. 7(4), 319-334.
- Ostendorf, D. W. and Kampbell, D. H. 1991. Biodegradation of hydrocarbon vapors in the unsaturated zone. *Water Resour. Res.* 27, 453-462.

- Sextro, R. 1997. Factors Controlling Entry of Soil Gas Contaminants into Buildings. Presented at the Petroleum Environmental Research Forum (PERF) Workshop. Brea, CA. February 6-7.
- Shah, J. T. and Singh, H. B. 1988. Distribution of volatile organic chemicals in outdoor and indoor air. *Environ. Sci. Technol.* 22(12), 1381-1386.
- Smith, J. A., Tisdale, A. K., and Cho, J. H. 1996. Quantification of natural vapor fluxes of trichloroethylene in the unsaturated zone at the picatinny arsenal, New Jersey. *Environ. Sci. Technol.* 30, 2243-2250.
- Stout, S. 1997. Field Case Studies Chlorinated Hydrocarbon Vapors. Presented at the Petroleum Environmental Research Forum (PERF) Workshop. Brea, CA. February 6-7.
- Unlu, K., Kemblowski, M. W., Parker, J. C., Stevens, D. K., Chong, P. K., and Kamil, I. 1992. A screening model for effects of land-disposed wastes on groundwater quality, *J. Contamin. Hydrol.* (11), pp. 27-49.
- United States Environmental Protection Agency, 1987. Total Exposure Assessment Methodology TEAM Study, Vols. 1-4. Office of Acid Deposition.
- United States Environmental Protection Agency. 1992. Assessing Potential Indoor Air Impacts for Superfund Sites. Office of Solid Waste and Emergency Response. EPA/540/R-95/128. PB96-963502. May.
- United States Environmental Protection Agency, 1996. Soil Screening Guidance: Technical Background Document. Office of Solid Waste and Emergency Response. EPA/540/R-95/128. PB96-963502. May.

Heuristic Model for Predicting the Intrusion Rate of Contaminant Vapors into Buildings

Paul C. Johnson* and Robert A. Ettlinger

Shell Development, Westhollow Research Center, Houston, Texas 77251

■ The intrusion into and subsequent accumulation of contaminant vapors in buildings and family dwellings is of concern for health and safety reasons. When preparing environmental and health risk assessments, one must be able to quantify this exposure pathway in order to decide if site-specific conditions correspond to unacceptable indoor contaminant vapor concentrations. For cases in which contaminated-site soil cleanup levels can be negotiated based on site-specific conditions, a related problem is the determination of residual contaminant levels below which associated adverse health effect risks are deemed negligible. Unfortunately, there are currently no accepted models for predicting vapor intrusion rates, and there is considerable debate over which transport mechanisms govern the process. This paper presents a heuristic model for screening-level calculations. It incorporates both convective and diffusive mechanisms, as well as contaminant soil, and building foundation properties. Sample calculations are presented for a range of parameter values to illustrate use of the model and the relative contributions of individual transport mechanisms.

Introduction

The intrusion and subsequent accumulation of radon vapors in commercial buildings and family dwellings has received considerable attention in the last decade. Of growing interest is the related problem of vapor transport from contaminated soils into buildings and dwellings. When preparing health and environmental risk assessments, regulators may require one to determine a residual contaminant level below which the associated adverse health effect risk is deemed negligible. To accomplish this, however, predictive transport models are required. Despite the attention focused on radon intrusion, no such validated models are available.

The current level of understanding is that both diffusion and convection contribute to vapor intrusion, and specific site characteristics will determine the significance of each. Nazaroff et al. (1) attempted to correlate radon concentrations in basements with building ambient pressure differences, wind speed, temperature differences, soil radon activity, and indoor air-exchange rates. In summary, for the three dwellings studied, typical building underpressurizations (ambient basement pressure drop) ranged between 1 and 50 Pa, and radon intrusion rates increased with increasing building underpressurization. Through the use of a tracer gas and controlled building underpressurization, Nazaroff et al. (2) studied the coupling between building underpressurization, induced soil depressurization, and flow of soil gas to a building. In another field study, Hodgson et al. (3) studied the transport of vapors from a landfill to a residential basement; they concluded that convective transport was negligible for the conditions at that site. By building a scale model of a building, Arnold (4) attempted to correlate building underpressurization, wind speed, soil type, soil gas intrusion rates, and pressure distributions in surrounding soils.

Attempts to model radon intrusion have produced both semianalytical solutions and detailed numerical codes. Landman (5), who considered only vapor-phase diffusion,

modeled radon transport through cracks in slabs and predicted that a slab with 1% open cracks by area will reduce the radon flux by 75% relative to the case of a bare dirt floor. Landman and Cohen (6) later tried to simplify this analysis and incorporate convective transport. Other authors, such as Zapalac (7), have attempted to model and measure radon fluxes through intact (i.e., no macroscopic cracks) concrete barriers.

Recently, numerical models have been employed by Garbesi and Sextro (8) and Loureiro et al. (9). The former model soil gas entry through "permeable" walls, rather than through cracks and openings, and predict reasonable soil gas entry rates for the cases studied. The latter couple soil gas flow field solutions with a contaminant transport model to predict radon intrusion rates through cracks and openings in basement floors and walls. It should be noted that one must be careful when extending results and conclusions from radon intrusion studies to the problem addressed in this study. In the case of radon intrusion, vapors are typically generated within the soil matrix adjacent to the foundation, while contaminant vapors of the type discussed in this report must migrate from a source located a distance from the building.

The goal of this work is similar to those of Nazaroff (10) and Nazaroff and Sextro (11); we want to develop a less computationally complex screening-level model for estimating contaminant vapor intrusion rates. Nazaroff (10) outlined a semianalytical approach for predicting indoor radon concentrations in the limit of convective-dominated transport, while Nazaroff and Sextro (11) described a more empirical technique based on a site-specific in situ measurement. Here we utilize the results and observations of these authors to formulate a heuristic model for predicting the intrusion rate of contaminant vapors into buildings through foundations in a more general scenario: contaminant vapors originating an arbitrary distance away from a building. This model can be used as a risk assessment screening-level tool; it can be used to identify sites, or contaminant levels, for which contaminant exposures through a vapor inhalation pathway may cause adverse health effects. It can also be used as a tool to help identify sites where more detailed numerical simulations or field sampling are appropriate. Below, the basis for the model is discussed, model equations are derived, and sample calculations are presented that illustrate the use of the model.

Heuristic Model Basis

While the formal development of the heuristic model is presented below, it is necessary to identify relevant phenomena that govern contaminant vapor transport into dwellings. In the following section, a dimensional analysis is conducted to assess the relative importance of each phenomenon. The transport of contaminants through soil matrices is often modeled by solving the following transport equation:

$$\frac{\partial \sum_i \epsilon_i C_i}{\partial t} + \sum_i \mathbf{u}_i \cdot \nabla C_i = \sum_i \nabla \cdot D_i^{\text{eff}} \nabla C_i + \sum_i R_i \quad (1)$$

where i is a subscript that specifies the phase (i.e., v = vapor, s = sorbed, f = free phase or precipitate, and m = soil moisture), t is time (s), ϵ_i is the volume fraction of phase i (volume of phase i /volume of soil, dimensionless), C_i is the concentration of contaminant in phase i (mass/volume of phase i , g/cm^3), u_i is the Darcy velocity vector associated with phase i (cm/s), ∇ is the del operator ($1/cm$), D_i^{eff} is the effective porous medium diffusion coefficient of contaminant in phase i (cm^2/s), and R_i is the formation rate of contaminant in phase i ($g/cm^3 \cdot s$).

For the special case where residual contaminant levels are low enough that no contaminant free-liquid/precipitate phase is present in the soil pores, under equilibrium conditions contaminant levels in the vapor, sorbed, and soil moisture phases are often assumed to be proportional to each other and the total contaminant level [Johnson et al. (12)]. Equation 1 can then be written in terms of a single phase concentration. One can assume, without any loss of generality, that contaminant levels in the soil moisture and vapor phases are related by a Henry's law constant, H (cm^3 of H_2O/cm^3 of vapor):

$$C_v = HC_m \quad (2)$$

A similar equation can be written for the relationship between sorbed and soil moisture phases, except that H is replaced by a sorption coefficient. If one assumes that diffusive transport is significant only in the vapor and soil moisture phases, then it follows from eq 2 that

$$\sum_i \nabla \cdot D_i^{eff} \nabla C_i = \nabla \cdot (D_v^{eff} + D_m^{eff}/H) \nabla C_v = \nabla \cdot D^{eff} \nabla C_v \quad (3)$$

where D^{eff} , defined by eq 3, is the "effective porous medium diffusion coefficient based on vapor-phase concentrations". The effective porous medium diffusion coefficients (D_m^{eff} and D_v^{eff}) are related to the pure component molecular diffusivities in water and air, D^{H_2O} and D^{air} , total soil porosity, $\epsilon_T = (\epsilon_v + \epsilon_m)$, vapor-filled porosity, ϵ_v , and moisture-filled porosity, ϵ_m , by the Millington-Quirk [Bruell and Hoag (13)] expression:

$$D_m^{eff} = D^{H_2O} \epsilon_m^{3.33} / \epsilon_T^2 \quad (4)$$

and

$$D_v^{eff} = D^{air} \epsilon_v^{3.33} / \epsilon_T^2 \quad (5)$$

where ϵ_m and ϵ_v are related to ϵ_T , the moisture content θ_m (cm^3 of H_2O/g of soil), and the bulk soil density ρ_b (g/cm^3):

$$\epsilon_m = \theta_m \rho_b \quad (6)$$

and

$$\epsilon_v = \epsilon_T - \theta_m \rho_b \quad (7)$$

For most compounds (except those with very small Henry's law constants), the contribution due to diffusion through the soil moisture will be insignificant in comparison with vapor-phase diffusion.

For the purpose of this analysis, we also assume that significant convective transport occurs only in the vapor phase, and vapor flow is described by Darcy's law:

$$u_v = -\frac{k_v}{\mu} \nabla P \quad (8)$$

where k_v is the soil permeability to vapor flow (cm^2), μ is the vapor viscosity ($g/cm \cdot s$), P is the pressure in the vapor phase ($g/cm \cdot s^2$), and u_v is the vapor-phase mass-average velocity (cm/s).

Table I. Dependence of Pe on Soil Type^a

soil type	permeability, k_v (darcy or $10^{-8} cm^2$)	Pe
silt	0.01-0.1	0.08-0.08
silty sand	0.1-1	0.08-0.8
fine sand	1-10	0.8-8
medium sand	10-100	8-80

^a $Pe = (k_v \Delta P_r L_D / D^{eff} \mu L_P)$, where $\Delta P_r = 10 Pa = 100 g/cm \cdot s^2 = 10^{-4} atm$, $D^{air} = 0.087 cm^2/s$ (benzene at 20 °C); $D^{H_2O} = 1.0 \times 10^{-5} cm^2/s$; $H = 0.18 cm^3$ of H_2O/cm^3 of vapor (benzene at 20 °C); $\epsilon_T = 0.38$; $\theta_m = 0.07 g$ of H_2O/g of soil (sandy soil at field capacity moisture content); $\rho_b = 1.7 g/cm^3$ of soil; $\mu = 1.8 \times 10^{-4} g/cm \cdot s$; $L_D = L_P$; $D^{eff} \approx D_v^{eff} = 0.087 cm^2/s \times (0.26^{3.33}/0.38^2) = 6.8 \times 10^{-3} cm^2/s$.

Inserting eqs 3 and 8 into eq 1 and nondimensionalizing the resulting equation yields

$$\frac{\partial \sum_i \epsilon_i C_i^*}{\partial t^*} - \left(\frac{L_P}{L_D} \right) (\nabla^* P^*) \cdot (\nabla^* C_v^*) = \nabla^* \cdot \left[\frac{D^{eff} \mu L_P}{k_v \Delta P_r L_D} \right] \nabla^* C_v^* + \sum_i R_i^* \quad (9)$$

where ΔP_r is the reference or characteristic indoor-outdoor pressure difference and * denotes nondimensional variables:

$$C_i^* = C_i / C_r \quad \nabla^* = L_D \nabla \quad P^* = P / \Delta P_r \\ t^* = t (k_v \Delta P_r / L_P L_D \mu) \quad R_i^* = R_i L_P L_D \mu / C_r k_v \Delta P_r$$

where C_r , L_D , and L_P are characteristic concentration, diffusion pathway length, and convection pathway length values, respectively, chosen to give the dependent concentration variable and derivatives of C_i^* and P^* magnitudes of order unity. Then the dimensionless group

$$[k_v \Delta P_r L_D / D^{eff} \mu L_P] = Pe \quad (10)$$

determines the relative significance of convective and diffusive transport mechanisms. Here Pe is the Peclet number, expressed in terms of the driving pressure ΔP_r . If $Pe \gg 1$, convective transport dominates; if $Pe \ll 1$, diffusive transport dominates. Note that the Peclet number defined by eq 10 contains two length scales L_D and L_P . This is appropriate for the problem of contaminant vapor intrusion into buildings, where the characteristic length scales for diffusion and convection may be quite different. Logical choices for L_D and L_P are the contaminant source-basement separation and the distance between ground surface and the basement floor, respectively.

It is useful to examine the magnitude of Pe before formulating any simpler vapor intrusion models. Based on the Nazaroff et al. (1, 2) studies, typical values of ΔP_r are 1-10 Pa (10-100 $g/cm \cdot s^2$), so we will choose the following representative parameter values: $\Delta P_r = 10 Pa = 100 g/cm \cdot s^2 = 10^{-4} atm$; $D^{air} = 0.087 cm^2/s$ (benzene at 20 °C); $D^{H_2O} = 1.0 \times 10^{-5} cm^2/s$; $H = 0.18 cm^3$ of H_2O/cm^3 of vapor (benzene at 20 °C); $\epsilon_T = 0.38$; $\theta_m = 0.07 g$ of H_2O/g of soil (sandy soil at field capacity moisture content); $\rho_b = 1.7 g/cm^3$ of soil; $\mu = 1.8 \times 10^{-4} g/cm \cdot s$; $L_D = L_P$. Table I presents values for Pe for different soil types. While θ_m , ϵ_T , ρ_b , and hence D^{eff} will vary with soil type, it has been assumed that all soils listed in Table I have similar total porosities, soil moisture contents, and bulk densities (an assumption that would not be valid for comparing sandy and clayey soils). The diffusion coefficients in water and air are also compound-specific; however, compounds whose molecular weights range from 70 to 300 have diffusion coefficients that differ by only a factor of ~ 2 [Lyman et al. (14)]. Of the parameters appearing in eq 10, the soil

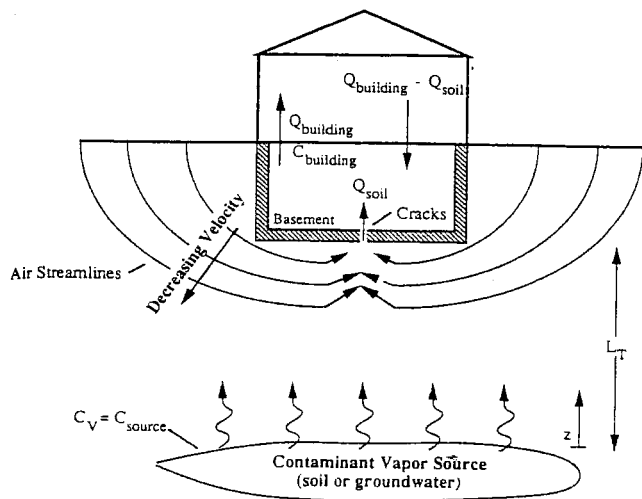


Figure 1. Vapor intrusion scenario.

permeability, k_v , is the most variable at any given site; it is not unusual for k_v to vary by 3 orders of magnitude across a site the size of a typical residential lot. As can be seen in Table I, Pe ranges between 0.01 and 100 for the soil types listed there. The significance of this observation is that any vapor intrusion model based only on either convective or diffusive transport mechanisms cannot reasonably describe the relevant phenomena over the typical range of soil types. Any proposed model, therefore, must include both transport mechanisms.

Formulation of the Heuristic Model

This discussion will be limited to problems in which chemical or biological transformations are not significant (i.e., $R_i = 0$). Recall that the goal of this development is to produce a predictive model suitable for screening-level calculations. Given that biological transformations in the unsaturated zone are presently not very well understood, it is not appropriate to attempt to incorporate them into this level of modeling. The reader should understand, however, that degradation due to microorganisms does occur; any model that includes them will predict lower intrusion rates than the model presented here (unless the contaminant of concern is produced by the biological transformation).

At this point we will restrict the analysis to steady-state (nondiminishing source) problems, although it will be shown later how one might adapt the results to diminishing source problems. Figure 1 presents a simplified sketch of the problem under consideration, in which a contaminant vapor source of concentration C_{source} is located some distance L_T below the floor of a basement or building slab. We want to predict the intrusion rate of vapors into the building. To accomplish this, the following assumptions are made:

(i) Contaminant vapors enter structures primarily through cracks and openings in the walls and foundation (electrical outlets, wall-floor seams, sump drains, etc.).

(ii) Convective transport is likely to be most significant in the region very close to a basement, or foundation, and vapor velocities decrease rapidly with increasing distance from a structure.

(iii) Vapor-phase diffusion is the dominant mechanism for transporting contaminant vapors from contaminant sources located away from the foundation to the soil region near the foundation.

(iv) All contaminant vapors originating from directly below the basement will enter the basement, unless the

floor and walls are perfect vapor barriers.

Assumption i reflects the current thinking that vapor intrusion is mainly due to cracks, seams, and openings in basement floors and walls, while ii and iii are based on the analysis presented above, the Peclet numbers appearing in Table I, and analogy to known solutions of fluid mechanics problems. In this simplistic model, contaminants volatilize from the source and diffuse toward the foundation. When convection is significant, they are "swept" into the building through cracks; otherwise, the contaminant vapors diffuse through the cracks and openings. Assumption iv restricts contaminant vapors from leaking around a building to ground surface and, therefore, adds a level of conservation to the model. Vapor leakage to the surface will be significant whenever the resistance to transport into a building is much greater than the resistance to transport to ground surface, such as buildings built on relatively intact slab foundations. It should be noted that the final results will not be limited by the validity of assumption i; if one follows the analysis below for the case where vapors are transported through intact porous walls, the final equations are identical in form with the results presented below (this will be shown later).

In addition to assumptions i-iv listed above, there are also assumptions inherent in the simplistic mathematical models described below. One-dimensional transport models form the basis for the heuristic model; therefore, it is assumed that the soil is homogeneous within any horizontal plane with respect to effective diffusion coefficients (heterogeneity in the vertical direction is accounted for). Also, it is assumed that convective vapor flow in the region near the foundation is uniform. This assumption, however, does not preclude application of the model to scenarios where there is a uniform layer of gravel adjacent to the foundation; in fact, the idealization described in assumption ii accurately represents this scenario, and one only needs to be sure to predict the soil gas entry rate based on properties of this region (and not the permeability of surrounding soils).

In the following, the heuristic vapor intrusion model is formulated by combining approximate mathematical descriptions of the relevant transport phenomena:

(a) **Diffusive Transport from the Source to a Region near the Structure.** As described above, it is assumed that contaminant vapors are transported from the contaminant source to a region near the structure, primarily by a molecular diffusion through pore vapor and soil moisture phases. The rate can be approximated by the expression

$$E_1 = A_B (C_{source} - C_{soil}) D_T^{eff} / L_T \quad (11)$$

where E_1 is the mass-transport rate toward the structure (g/s), A_B is the cross-sectional area through which vapors pass (cm^2), C_{source} is the vapor concentration at the contaminant source (g/cm^3), C_{soil} is the vapor concentration in the region near the structure (g/cm^3), L_T is the distance from contaminant source to foundation (cm), and D_T^{eff} is the "overall" effective porous media diffusion coefficient based on vapor-phase concentrations for the region between the source and foundation (cm^2/s).

The cross-sectional area, A_B , can be approximated by the total basement area (floor and walls). Assuming that convection, when significant, is only dominant in a region very near the foundation allows us to approximate the total diffusion length, L_T , as the distance between the source and foundation. The soil permeability to vapor flow, building underpressurization, and physical setting will determine the actual thickness of the convection-dominated region, which will increase with increasing permea-

bility to vapor flow and increased building underpresurization. In general, the unsaturated soil zone may be composed of several soil types with varying moisture contents and porosities, and the effective overall diffusion coefficient for a region between $z = 0$ and $z = L_T$ is

$$D_T^{eff}/L_T = \left[\int_0^{L_T} dz/D^{eff}(z) \right]^{-1} \quad (12)$$

where $D^{eff}(z)$ is the effective porous media diffusion coefficient at z , which is a function of the contaminant type and soil characteristics as defined by eqs 3-7.

For systems composed of n distinct soil layers defined by thicknesses L_i and uniform effective overall porous media diffusion coefficients D_i^{eff} , eq 12 reduces to

$$D_T^{eff}/L_T = \left[\sum_{i=0}^n L_i/D_i^{eff} \right]^{-1} \quad (13)$$

(b) Transport from Soil Gas into Building. The transport of contaminants from soil gas adjacent to a foundation is assumed to occur by a combination of convective and diffusive transport mechanisms. As a first approximation, the steady-state, one-dimensional solution to eq 9 for vapor transport through a crack (or porous medium) with a constant uniform convective velocity (Q_{soil}/A_{crack}) is used to predict the total rate of contaminant intrusion into a building:

$$E = Q_{soil} C_{soil} - \frac{Q_{soil}(C_{soil} - C_{building})}{[1 - \exp(Q_{soil}L_{crack}/D_{crack}A_{crack})]} \quad (14)$$

where E is the entry rate of contaminant into the building (g/s), Q_{soil} is the volumetric flow rate of soil gas into the building (cm^3/s), D_{crack} is the effective vapor-pressure diffusion coefficient through the crack (cm^2/s), L_{crack} is the thickness of the foundation (cm), $C_{building}$ is the contaminant vapor concentration in the building (g/cm^3), and A_{crack} is the area of cracks/openings through which contaminant vapors enter the building (cm^2).

The only "unknown" in eqs 11 and 14 is the soil gas contaminant concentration, C_{soil} , which can be obtained by requiring that the rates E_1 and E be equal at steady state. The result

$$C_{soil} = \left[C_{source} \left[\frac{D_T^{eff} A_B}{Q_{soil} L_T} \right] \left[\exp\left(\frac{Q_{soil} L_{crack}}{D_{crack} A_{crack}}\right) - 1 \right] + C_{building} \right] / \left[\left[\frac{D_T^{eff} A_B}{Q_{soil} L_T} \right] \left[\exp\left(\frac{Q_{soil} L_{crack}}{D_{crack} A_{crack}}\right) - 1 \right] + \exp\left(\frac{Q_{soil} L_{crack}}{D_{crack} A_{crack}}\right) \right] \quad (15)$$

can be substituted into eq 14 to obtain E , the rate of contaminant entry into a building through the foundation:

$$E = \left[\frac{D_T^{eff} A_B C_{source}}{L_T} \right] \left[\exp\left(\frac{Q_{soil} L_{crack}}{D_{crack} A_{crack}}\right) - \left[\frac{C_{building}}{C_{source}} \right] \right] / \left[\left[\frac{D_T^{eff} A_B}{Q_{soil} L_T} \right] \left[\exp\left(\frac{Q_{soil} L_{crack}}{D_{crack} A_{crack}}\right) - 1 \right] + \exp\left(\frac{Q_{soil} L_{crack}}{D_{crack} A_{crack}}\right) \right] \quad (16)$$

When eq 16 is written this way, E is the product of the steady-state diffusive rate of contaminant transport from a source to a bare dirt floor foundation (first term on

right-hand side) and a factor containing a number of dimensionless groups whose significance will be discussed below.

Indoor Air Quality. Equation 16 can be incorporated into a steady-state mass balance for a basement (or building) to produce an explicit expression for the indoor contaminant vapor. Assuming no other contaminant sources or sinks (i.e., sorption to walls or furniture) and a well-mixed building, this expression can be written

$$Q_{building} C_{building} = E \quad (17)$$

where $Q_{building}$ denotes the basement (or building) ventilation rate, expressed as a volumetric flow rate. Often, this term is expressed as the product of an "air-exchange rate" and a basement (or building) volume; however, here these terms are combined into $Q_{building}$. Substituting eq 16 into eq 17 and rearranging yields

$$C_{building} = \left[C_{building}^* \times \exp\left(\frac{Q_{soil} L_{crack}}{D_{crack} A_{crack}}\right) \right] / \left[\exp\left(\frac{Q_{soil} L_{crack}}{D_{crack} A_{crack}}\right) + \left[\frac{D_T^{eff} A_B}{Q_{building} L_T} \right] + \left[\frac{D_T^{eff} A_B}{Q_{soil} L_T} \right] \left[\exp\left(\frac{Q_{soil} L_{crack}}{D_{crack} A_{crack}}\right) - 1 \right] \right] \quad (18)$$

where

$$C_{building}^* = \left[\frac{D_T^{eff} A_B C_{source}}{Q_{building} L_T} \right] \quad (19)$$

In eqs 18 and 19, $C_{building}^*$ represents the indoor vapor concentration corresponding to the case where vapors diffuse from the source to a bare soil foundation. As will be derived later, this is the limiting case in which Q_{soil} becomes very small and the diffusional resistance through the basement floors/walls is significantly less than the diffusional resistance through the soil zone between the contaminant vapor source and building. Equation 18 can also be arranged to produce the "attenuation coefficient" α :

$$\alpha = C_{building}/C_{source} \quad (20)$$

or equivalently

$$\alpha = \left[\left[\frac{D_T^{eff} A_B}{Q_{building} L_T} \right] \times \exp\left(\frac{Q_{soil} L_{crack}}{D_{crack} A_{crack}}\right) \right] / \left[\exp\left(\frac{Q_{soil} L_{crack}}{D_{crack} A_{crack}}\right) + \left[\frac{D_T^{eff} A_B}{Q_{building} L_T} \right] + \left[\frac{D_T^{eff} A_B}{Q_{soil} L_T} \right] \left[\exp\left(\frac{Q_{soil} L_{crack}}{D_{crack} A_{crack}}\right) - 1 \right] \right] \quad (21)$$

Both eqs 18 and 21 depend on three dimensionless groups:

$$\frac{Q_{soil} L_{crack}}{D_{crack} A_{crack}} \quad \frac{D_T^{eff} A_B}{Q_{building} L_T} \quad \frac{Q_{soil}}{Q_{building}}$$

The first represents the equivalent Peclet number for transport through the foundation, the second is the attenuation coefficient (as defined in eq 20) for diffusion-dominated transport from a constant source to a bare dirt floor, and the third is the attenuation coefficient for con-

dis- vective transport from a source located adjacent to the building.

At this point it is useful to examine the behavior predicted by eq 21 in certain limiting situations, in order to verify that the mathematics represents the phenomena incorporated into their derivation and that the results fall within appropriate bounds:

(a) $(Q_{soil} L_{crack} / D_{crack} A_{crack}) \rightarrow \infty$. In this limit convection is the dominant transport mechanism through the basement (building) floor and walls. Equation 21 becomes

$$\lim_{\frac{Q_{soil} L_{crack}}{D_{crack} A_{crack}} \rightarrow \infty} \alpha \rightarrow \frac{\left[\frac{D_T^{eff} A_B}{Q_{building} L_T} \right]}{\left[\frac{D_T^{eff} A_B}{Q_{soil} L_T} \right] + 1} \quad (22)$$

If the source lies directly beneath the foundation ($L_T \rightarrow 0$), then $\alpha \rightarrow Q_{soil} / Q_{building}$, which is the proper result for convection-dominated transport of a vapor stream with concentration C_{source} . If the source is "far" from the basement (i.e., $D_T^{eff} A_B / Q_{soil} L_T \rightarrow 0$), then transport is limited by diffusion from the source to foundation, and $\alpha \rightarrow D_T^{eff} A_B / Q_{building} L_T$. Note that in the limit $Q_{soil} L_{crack} / D_{crack} A_{crack} \rightarrow \infty$ the results are independent of the cracked area of the floor and walls. This is because contaminant vapors are swept into the building as fast as they are transported to the soil adjacent to the floor and walls.

(b) $(Q_{soil} L_{crack} / D_{crack} A_{crack}) \rightarrow 0$. In this limit diffusion is the dominant transport mechanism through the basement floor and walls, and eq 21 reduces to

$$\lim_{\frac{Q_{soil} L_{crack}}{D_{crack} A_{crack}} \rightarrow 0} \alpha \rightarrow \frac{\left[\frac{D_T^{eff} A_B}{Q_{building} L_T} \right]}{1 + \left[\frac{D_T^{eff} A_B}{Q_{building} L_T} \right] + \left[\frac{D_T^{eff} A_B L_{crack}}{D_{crack} A_{crack} L_T} \right]} \quad (23)$$

Equation 23 contains two dimensionless groups. As discussed above, $D_T^{eff} A_B / Q_{building} L_T$ represents the attenuation coefficient for diffusive transport to a bare dirt floor. The second dimensionless group, $D_T^{eff} A_B L_{crack} / D_{crack} A_{crack} L_T$, is a measure of the diffusion rates through the soil relative to those through the floor and walls. If $D_T^{eff} A_B L_{crack} / D_{crack} A_{crack} L_T \ll 1$, then $\alpha \rightarrow D_T^{eff} A_B / Q_{building} L_T$ because $D_T^{eff} A_B / Q_{building} L_T$ will typically be much less than unity unless $Q_{building} \rightarrow 0$. If $D_T^{eff} A_B L_{crack} / D_{crack} A_{crack} L_T \gg 1$, then $\alpha \rightarrow D_{crack} A_{crack} / Q_{building} L_{crack}$, which is the appropriate attenuation coefficient for transport from a source located adjacent to the floor and walls. When $D_T^{eff} A_B L_{crack} / D_{crack} A_{crack} L_T \gg 1$, then diffusion through the floor and walls is the rate limiting mechanism, and there is a vapor concentration "buildup" below the building or basement.

(c) $Q_{building} \rightarrow 0$. This limit corresponds to a perfectly sealed basement, Q_{soil} must also approach zero, and the model predicts that $\alpha \rightarrow 1$; that is, the indoor contaminant vapor concentration approaches the contaminant vapor concentration in the soil gas.

Sample Calculations

On the basis of the analysis above, it appears that model predictions fall correctly within the appropriate bounds for all limiting cases examined. These results, however,

Table II. Parameter Values Used To Generate Figures 2-5

$A_B = 7 \text{ m} \times 10 \text{ m} + 2(2 \text{ m} \times 7 \text{ m}) + 2(2 \text{ m} \times 10 \text{ m}) = 138 \text{ m}^2 = 138 \times 10^4 \text{ cm}^2$
$L_{crack} = 6 \text{ in.} = 15 \text{ cm}$
$Q_{building} = 7 \text{ m} \times 10 \text{ m} \times 3 \text{ m} \times 0.5 \text{ volume exchanges/h} = 105 \text{ m}^3/\text{h} = 2.9 \times 10^4 \text{ cm}^3/\text{s}$
$D_{air} = 0.087 \text{ cm}^2/\text{s}$ (benzene)
$D_{H_2O} = 1.0 \times 10^{-5} \text{ cm}^2/\text{s}$
$H = 0.18 \text{ cm}^3$ of H_2O/cm^3 of air (benzene)
$\theta_m = 0.07 \text{ g}$ of H_2O/g of soil
$\epsilon_T = 0.38 \text{ cm}^3/\text{cm}^3$ of soil
$\rho_b = 1.7 \text{ g}/\text{cm}^3$
$\Delta P = 1.0 \text{ Pa} = 10 \text{ g}/\text{cm}\cdot\text{s}^2$

give no indication of what "typical" values of these dimensionless groups might be. It is useful at this point, therefore, to examine model predictions for a sample case. Consider a $10 \text{ m} \times 7 \text{ m} \times 3 \text{ m}$ (length \times width \times height) basement whose floor lies 2 m below grade. It is assumed that the floor/wall cracks and openings are filled with dust and dirt characterized by a density, porosity, and moisture content similar to that of the underlying soil. Model parameters A_B , L_{crack} , $Q_{building}$, D_{air} , D_{H_2O} , H , θ_m , ϵ_T , and ρ_b are given in Table II. The remaining unspecified parameters are the convective flow rate from the soil into the basement, Q_{soil} , the area of cracks, A_{crack} , and the distance between the contaminant source and the foundation, L_T . The soil gas flow rate, Q_{soil} , is likely to be dependent on the basement crack area, A_{crack} , soil type and stratigraphy, building underpressurization, and basement geometry. For simplicity, however, we will estimate Q_{soil} as suggested by Nazaroff (10):

$$Q_{soil} = \frac{2\pi \Delta P k_v X_{crack}}{\mu \ln [2Z_{crack}/r_{crack}]} \frac{r_{crack}}{Z_{crack}} \ll 1 \quad (24)$$

Equation 24 is an analytical solution for flow to a cylinder of length X_{crack} and radius r_{crack} located a depth Z_{crack} below ground surface; this is an idealized model for soil gas flow to cracks located at floor/wall seams. Here ΔP , k_v , and μ are as defined above. For this sample problem, $Z_{crack} = 2 \text{ m}$ (as stated above), X_{crack} is taken to be the total floor/wall seam perimeter distance (34 m), and for consistency r_{crack} is given by

$$r_{crack} = \eta A_B / X_{crack} \quad (25)$$

where the ratio $\eta = A_{crack} / A_B$, so that $0 \leq \eta \leq 1$. For reference, $\eta = 0.01$ corresponds to $r_{crack} = 4.1 \text{ cm}$ for the values of A_B and X_{crack} given above; $r_{crack} = 1 \text{ cm}$ corresponds to $\eta = 0.0025$.

In the Nazaroff et al. studies (1, 2), estimates for Q_{soil} are in the $280\text{--}2800 \text{ cm}^3/\text{s}$ ($1\text{--}10 \text{ m}^3/\text{h}$) range, for induced building underpressurizations of $5\text{--}30 \text{ Pa}$ and very permeable soils ($k_v > 10^{-8} \text{ cm}^2$). Note that $1 \text{ m}^3/\text{h}$ corresponds to $\sim 1\%$ of the assumed total basement air exchange rate ($0.5/\text{h}$). For the purpose of this sample calculation we choose $\Delta P = 1 \text{ Pa}$ ($10 \text{ g}/\text{cm}\cdot\text{s}^2$), which is probably a reasonable long-term average value for screening calculations.

Figure 2 presents soil gas flow rates predicted by eq 24 for $\eta = 0.01$ and $\eta = 0.001$. This figure illustrates the strong dependence of Q_{soil} on soil type, and a weaker dependence on crack size (as reflected in the value of η). For very permeable soils ($k_v \geq 10^{-6} \text{ cm}^2$), the predicted Q_{soil} values are of the same order of magnitude as the values observed by Nazaroff (1, 2). For example, $Q_{soil} = 260 \text{ cm}^3/\text{s}$ for $\eta = 0.01$ and $k_v = 1 \times 10^{-6} \text{ cm}^2$. For reference, medium sandy soils correspond to $10^{-7} < k_v < 10^{-6} \text{ cm}^2$.

Figures 3-5 present predicted attenuation coefficients α , for $\eta = 0.01$, and $\eta = 0.001$, as a function of k_v , for L_T

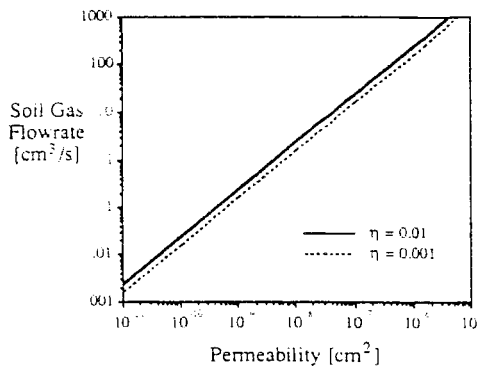


Figure 2. Dependence of soil gas entry flow rates, Q_{soil} , on soil permeability, k_v , as predicted by eq 24 for the parameters listed in Table II.

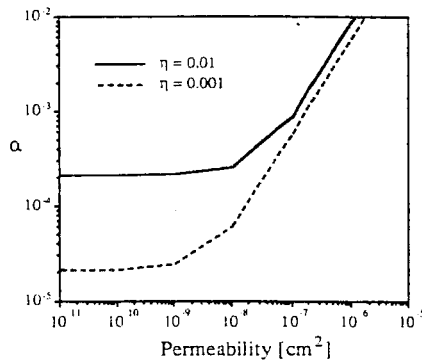


Figure 3. Dependence of attenuation coefficient, α , on soil permeability, k_v , as predicted by eq 21 for the parameters listed in Table II and $L_T = 0$.

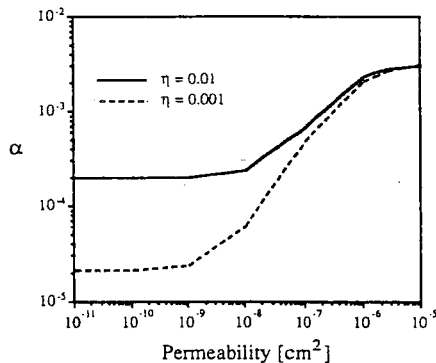


Figure 4. Dependence of attenuation coefficient, α , on soil permeability, k_v , as predicted by eq 21 for the parameters listed in Table II and $L_T = 100$ cm.

$= 0, 100, \text{ and } 1000$ cm. Recall that $\alpha = C_{\text{building}}/C_{\text{source}}$ and it is a measure of both the indoor contaminant vapor concentration and contaminant vapor intrusion rate. The results are plotted in this way to facilitate comparison with numerical modeling results presented by Loureiro et al. (9). Figure 3 corresponds to the case where the contaminant vapor source lies adjacent to the building foundation ($L_T = 0$) and is roughly equivalent to the radon intrusion scenario modeled by these authors. The screening model predicts results that are in good qualitative and quantitative agreement with the detailed numerical modeling results [i.e., see Loureiro et al. (9), Figure 11]; both predict that α (and hence the intrusion rate) is independent of k_v for "small" values of k_v and becomes proportional to k_v at "large" values of k_v . The transition between these two regimes occurs near $k_v = 10^{-8}$ cm². For $k_v < 10^{-8}$ cm², the

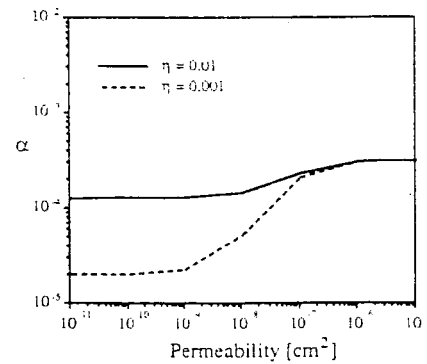


Figure 5. Dependence of attenuation coefficient, α , on soil permeability, k_v , as predicted by eq 21 for the parameters listed in Table II and $L_T = 1000$ cm.

soil gas flow rate through the cracks becomes so low that diffusion is the dominant transport mechanism and α is therefore independent of k_v . For $k_v > 10^{-8}$ cm², on the other hand, containment vapors are swept into the building primarily by convection. In this limit, $\alpha \rightarrow Q_{\text{soil}}/Q_{\text{building}}$ and becomes proportional to the resistance to flow (as measured by k_v). In this case the proposed screening model predicts $0.001 < \alpha < 0.01$ for $10^{-7} < k_v < 10^{-6}$ cm², which happens to fall in the range of values typically reported for radon intrusion studies. Figure 3 also indicates that the screening model predicts a dependence of intrusion rate and attenuation on the size of the crack, with the effect being more pronounced at lower permeabilities. As the crack size decreases, resistance to both diffusive transport and soil gas flow increases; thus, α is always predicted to be less for $\eta = 0.001$ than for $\eta = 0.01$. The decrease in flow rate predicted by eq 24 is apparently not as significant, however, as the increased resistance to diffusion through foundation cracks. Thus, for practical purposes, it can be concluded that the effect of crack size on contaminant vapor intrusion rates will be relatively insignificant in the limit of convective-dominated transport.

Figures 4 and 5 present model predictions for cases where the contaminant vapor source is located some distance L_T away from the foundation. In each figure the dependence of α on k_v is a sigmoidal-shaped curve, where α becomes independent of k_v in the limits of "large" and "small" soil permeabilities. In the limit of less permeable soils, soil gas flow rates are so low that vapor intrusion is governed entirely by the relative rates of diffusion through the soil and foundation. As the soil becomes more permeable, the "sweeping" of contaminant vapors into the building by soil gas flow increases the intrusion rate. At some point, however, diffusion from the containment vapor source to the region of soil gas flow limits the rate of contaminant vapor transport. For highly permeable soils, therefore, α becomes independent of k_v and only weakly dependent on foundation properties. The transition between Figures 4 and 5 also illustrates that α and the intrusion rate become less dependent on foundation properties as L_T increases. This is evidenced by the convergence of the "low" and "high" k_v asymptotes, and the $\eta = 0.001$ and $\eta = 0.01$ predictions as L_T increases; in the limit $L_T \rightarrow \infty$, diffusion through soil becomes the limiting transport mechanism.

Figures 3–5 illustrate the necessity of developing models that incorporate both convective and diffusive transport mechanisms. Single transport process based models cannot predict the wide range of behavior exhibited in these figures, nor can they explain the difference in the obser-

vati
of P
vap
lust
on t
pen
mec
por
tion
pre
cha
cati
It is
how
a re
effe
dict
and
for
corr
0.01
of b
It
prec
dim
The
corr
Ext.
Fou
In
vap
wall
On
proc
equi
 $\alpha =$
+
whic
D_{crac}
thro
is re;
4-7
and
resu
crac
unif
ther
lowe
this
foun
that
= D
Ext
Ec
vapp
of th
reaso
and
for l
wher

vations of Nazaroff (1, 2) for radon intrusion, and those of Hodgson et al. (3) for vapor transport of contaminant vapors from a landfill. The sample calculations also illustrate that the soil type can have a significant impact on the indoor vapor concentration, since Q_{soil} will be dependent on the soil permeability, and the effective porous media diffusion coefficient is sensitive to changes in soil porosity and moisture content. Being an analytical solution, eq 21 is easily used to study the sensitivity of model predictions over a range of reasonable soil and building characteristics. The major limitation to practical applications of the model is the lack of site-specific η values. It is not likely that such values can be easily measured; however, one can use the model to examine predictions for a realistic range of such values in order to determine the effect of this parameter at any given site. Clearly, predictions are insensitive to η in the limit of "permeable" soils and large source-foundation separations. A realistic range for η can be proposed by considering physical realizations corresponding to specific values of η . For example, $\eta = 0.01$ corresponds to a 1-cm-wide crack running the length of basement floor/walls every 100 cm.

It should be noted that Figures 2-5 contain model predictions for specific soil characteristics and building dimensions and are presented for illustrative purposes. The results should not be extrapolated to other sites not corresponding to the chosen parameters.

Extension of Theory to Relatively Permeable Foundation Walls

In the work of Garbesi and Sextro (8) it is assumed that vapor intrusion occurs through permeable below-grade walls, rather than through foundation cracks and openings. On the basis of this assumption, one can follow the approach used to derive eq 21 to obtain the following equivalent expression:

$$\alpha = \left[\frac{D_T^{eff} A_B}{Q_{building} L_T} \exp\left(\frac{Q_{soil} L_F}{D^F A_B}\right) \right] / \left[\exp\left(\frac{Q_{soil} L_F}{D^F A_B}\right) + \frac{D_T^{eff} A_B}{Q_{building} L_T} + \frac{D_T^{eff} A_B}{Q_{soil} L_T} \left[\exp\left(\frac{Q_{soil} L_F}{D^F A_B}\right) - 1 \right] \right] \quad (26)$$

which is similar to eq 21, except A_{crack} is replaced by A_B , D_{crack} is replaced by D^F , the effective diffusion coefficient through the porous foundation floor and walls, and L_{crack} is replaced by the foundation/wall thickness L_F . Equations 4-7 and 12 should be used to calculate D^F . While eqs 26 and 21 appear similar, they can predict quite different results. Equation 26 is independent of the area of cracks/openings because intrusion is assumed to occur uniformly over the floor/wall area. For a given Q_{soil} , therefore, the soil gas velocity through the floor/walls is lower for the permeable floor/wall case. The impact of this is that eq 26 may predict that transport through the foundation is diffusion dominated, while eq 21 predicts that it is convection dominated, for a given Q_{soil} and $D_{crack} = D^F$.

Extension of the Theory to Transient Problems

Equation 21 provides a screening estimate of indoor vapor concentrations, but does not account for depletion of the contaminant vapor source. This assumption is reasonable when short-term exposures are being estimated and does provide a conservative (upper bound) estimate for long-term exposures. There are situations, however, when more realistic long-term exposure estimates are de-

sired and it is unlikely that the source will remain constant for a long period of time (usually ~ 70 years for most exposure estimates). Many processes can contribute to an unsteady source, including the depletion due to transport away from the source, biodegradation, and chemical reaction. Of the three processes, the depletion due to transport is most often modeled, due to the current uncertain quantification of the other two. A first-order estimate of whether or not significant changes will occur over a given time period τ is obtained by calculating the mass of contaminant emitted from the source over that time period (τE) and comparing it with the initial residual contaminant mass in the soil directly below the building ($\rho_b C_R \Delta H_c A_B$):

$$\tau E \stackrel{?}{=} \rho_b C_R \Delta H_c A_B \quad (27)$$

where C_R and ΔH_c denote the average residual contaminant level in the soil (g/g of soil) and the thickness of the vertical interval (cm) over which the contaminant is distributed, respectively, and E is given by eq 16. If the left-hand side of eq 27 is greater than the initial mass of contaminant right-hand side, then it is possible that the contaminant lying beneath (or adjacent to) the building will eventually volatilize and enter the building. The validity of this assumption will depend on site characteristics.

The simplest extension of the model is derived by invoking the quasi-steady-state assumption used by Thibodeaux and Hwang (15) for single-component contaminants or mixtures of compounds having similar vapor pressures and molecular weights. In this approach it is recognized that the source-building separation increases with time due to depletion; however, it is assumed that the rate at which a steady-state vapor concentration profile is established is much greater than the rate at which depletion occurs. At any time, therefore, the emission rate is given by eq 16 with L_T replaced by the source-building separation at that time. Implicit in this approach is the assumption that depletion occurs first from the layers of contaminant closest to the building floor and walls, and a hypothetical "depletion zone" grows with time. In a sense, the mass of contaminant incorporated in the soil "dries up", beginning at the edge closest to the building. This is a reasonable assumption for diffusion-dominated transport to the building-soil interface, but not valid for convection-dominated transport from contaminated soil adjacent to a building floor. With this limitation in mind, eq 16 combined with a mass balance provides a mathematical expression of the quasi-steady-state assumption:

$$\rho_b C_R A_B \frac{d\delta}{dt} = \left[\frac{D_T^{eff} A_B C_{source}}{(L_T^0 + \delta)} \right] \left[\exp\left(\frac{Q_{soil} L_{crack}}{D_{crack} A_{crack}}\right) - \frac{\left[\frac{C_{building}}{C_{source}} \right]}{\left[\frac{D_T^{eff} A_B}{Q_{soil} (L_T^0 + \delta)} \right]} \times \left[\exp\left(\frac{Q_{soil} L_{crack}}{D_{crack} A_{crack}}\right) - 1 \right] + \exp\left(\frac{Q_{soil} L_{crack}}{D_{crack} C_{crack}}\right) \right] \quad (28)$$

where δ , t , and L_T^0 denote the "depletion zone" thickness ($\delta = 0$ at $t = 0$) (cm), time (s), and initial contaminant-building floor separation (cm), respectively. Equation 28 can be rearranged and rewritten in the form

$$d\delta^*/dt = \psi / (\beta + \delta^*) \quad (29)$$

where

$$\delta^* = \delta / L_T^0 \quad (30)$$

$$\psi = D_T^{\text{eff}} C_{\text{source}} / (L_T^0)^2 \rho_b C_R \quad (31)$$

$$\beta = \left(\frac{D_T^{\text{eff}} A_B}{L_T^0 Q_{\text{soil}}} \right) \left[1 - \exp \left(- \frac{Q_{\text{soil}} L_{\text{crack}}}{D_{\text{crack}} A_{\text{crack}}} \right) \right] + 1 \quad (32)$$

In this analysis it is assumed that the residual contaminant level in soil C_R is uniform, D^{eff} is constant as δ increases, and the ratio $C_{\text{building}}/C_{\text{source}} \ll 1$. Equation 29 can be solved to obtain

$$\delta^* = -\beta + \sqrt{\beta^2 + 2\psi t} \quad (33)$$

The time τ_D required to deplete a contaminated zone of thickness ΔH_c can be obtained from eq 33, by setting $\delta^* = \Delta H_c / L_T^0$

$$\tau_D = \frac{[\Delta H_c / L_T^0 + \beta]^2 - \beta^2}{2\psi} \quad (34)$$

Equation 34 predicts that τ_D increases with increasing L_T^0 and C_R ; increasing L_T^0 decreases the initial diffusive driving force, while increasing C_R increases the contaminant capacity of the contaminated soil zone. If $\tau \geq \tau_D$, the average emission rate into the basement (E) over the time period τ_D is obtained by a simple mass balance:

$$\langle E \rangle = \rho_b C_R \Delta H_c A_B / \tau \quad (35)$$

For time periods $\leq \tau_D$, the average emission rate is given by

$$\langle E \rangle = \frac{\rho_b C_R \Delta H_c A_B}{\tau} \left(\frac{L_T^0}{\Delta H_c} \right) [(\beta^2 + 2\psi\tau)^{1/2} - \beta] \quad (36)$$

which can be derived by substituting eq 33 for δ^* (δ/L_T^0) into the right-hand side of eq 28 and then averaging the resulting expression over the time period τ . As expected, eq 36 predicts a decrease in $\langle E \rangle$ with increasing τ . The corresponding long-term average attenuation coefficient (α) is then

$$\langle \alpha \rangle = \frac{\rho_b C_R \Delta H_c A_B}{Q_{\text{building}} C_{\text{source}} \tau} \left(\frac{L_T^0}{\Delta H_c} \right) [(\beta^2 + 2\psi\tau)^{1/2} - \beta] \quad (37)$$

While eqs 28-37 form a more sophisticated model than eq 21, one must be aware that increasing the level of sophistication usually increases the amount of site-specific information required. More sophisticated screening models are usually also based on additional assumptions, and one must be careful to ensure that these assumptions are valid for specific site characteristics.

Vapor Equilibrium Models

The models presented above require an estimate of the source vapor concentration, C_{source} . Two main approaches are used in vapor transport modeling; in the first C_{source} is assumed to be proportional to the residual level in the soil, and in the second C_{source} is independent of the residual level, but is a function of composition. The former is applicable in the limit of "low" residual levels where compounds are sorbed to the soil, dissolved in the soil moisture, and present in the vapor space; the latter is applicable for "high" residual levels where free-phase liquid or precipitate is trapped in the soil interstices. A more detailed description of this topic can be found in Johnson et al. (12), and it is not appropriate to repeat the discussion here. It is important to note, however, that if one chooses an incorrect model for predicting C_{source} , then it is possible to

over- or underpredict the actual C_{source} value by orders of magnitude.

Conclusions

We have derived and illustrated the use of a heuristic model of the intrusion rate of subsurface contaminant vapors into buildings through basement, or foundation, floors and walls. The model provides an exposure assessment screening-level tool; it can be used to identify sites, or contaminant levels, where contaminant exposures through a vapor inhalation pathway may cause adverse health effects. It can also be used to help identify sites where more detailed numerical simulation, or field sampling, is appropriate. The model was used to make predictions of basement vapor concentrations over a range of realistic parameters. It is clear from the wide range of results that field data will only be correlated by models such as this that incorporate both convective and diffusive transport mechanisms.

Currently, there are few reported experimental studies that are sufficiently detailed to compare with model predictions. However, the range of behavior, dependence on relevant parameters, and limiting bounds of the model are in qualitative agreement with published case histories. At this point, more detailed field studies and numerical simulations are needed to help validate this screening-level model.

Acknowledgments

We thank James D. Colthart for his thoughtful review and contributions to the presentation and technical content of this article.

Registry No. Radon, 10043-92-2.

Literature Cited

- (1) Nazaroff, W. W.; Feustel, H.; Nero, A. V.; Revzan, K. L.; Grimsrud, D. T.; Essling, M. A.; Toohey, R. E. *Atmos. Environ.* 1985, 19, 31-46.
- (2) Nazaroff, W. W.; Lewis, S. R.; Doyle, S. M.; Moed, B. A.; Nero, A. V. *Environ. Sci. Technol.* 1987, 21, 459-466.
- (3) Hodgson, A. T.; Garbesi, K.; Sextro, R. G.; Daisy, J. M. Presented at 81st Annual Meeting of APCA, June 19-24, 1988, Dallas, TX, 88-95B.1.
- (4) Arnold, L. J. Ph.D. Dissertation, Rutgers, The State University of New Jersey, 1988.
- (5) Landman, K. A. *Health Phys.* 1982, 43, 65-71.
- (6) Landman, K. A.; Cohen, D. S. *Health Phys.* 1987, 44, 249-257.
- (7) Zapalac, G. H. *Health Phys.* 1982, 43, 65-71.
- (8) Garbesi, K.; Sextro, R. G. *Environ. Sci. Technol.* 1989, 23, 1481-1487.
- (9) Loureiro, C. O.; Abriola, L. M.; Martin, J. E.; Sextro, R. G. *Environ. Sci. Technol.* 1990, 24, 1338-1348.
- (10) Nazaroff, W. W. *Radiat. Prot. Dosim.* 1988, 24, 199-202.
- (11) Nazaroff, W. W.; Sextro, R. G. *Environ. Sci. Technol.* 1989, 23, 451-457.
- (12) Johnson, P. C.; Hertz, M. B.; Byers, D. L. In *Petroleum Contaminated Soils*; Kostecki, P. T., Calabrese, E. J., Eds.; Lewis Publishers: Chelsea, MI, 1990; Vol. III, pp 295-326.
- (13) Bruell, C. J.; Hoag, G. E. In Proceedings of the NWWA/API Conference on Petroleum Hydrocarbons and Organic Chemicals in Groundwater: Prevention, Detection, and Restoration, November 12-14, 1986, Houston, TX.
- (14) Lyman, W. J.; Reehl, W. F.; Rosenblatt, D. H. *Handbook of Chemical Property Estimation Methods*; McGraw-Hill: New York, 1982.
- (15) Thibodeaux, L. J.; Hwang, S. T. *Environ. Prog.* 1982, 1, 42-46.

Received for review August 14, 1990. Revised manuscript received February 21, 1991. Accepted April 1, 1991.